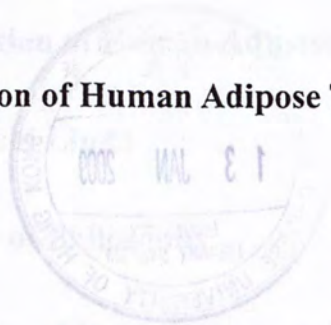


Abstract of thesis entitled:

Molecular Characterization of Human Adipose Tissue-derived Stem Cells



Submitted by Ng Wing Chi

for the degree of Master of Philosophy

at The Chinese University of Hong Kong in July 2007

**NG, Wing Chi Linda**

**A Thesis Submitted in Partial Fulfillment  
of the Requirement for the Degree of  
Master of Philosophy  
in  
Obstetrics and Gynaecology**

**© The Chinese University of Hong Kong  
September 2007**

**The Chinese University of Hong Kong holds the copyright of this thesis. Any person(s) intending to use a part or whole of the materials in the thesis in a proposed publication must seek copyright release from the Dean of the Graduate School.**



THE CHINESE UNIVERSITY OF HONG KONG

A Thesis Submitted in Partial Fulfillment  
of the Requirement for the Degree of  
Master of Philosophy  
in  
Obstetrics and Gynaecology

The Chinese University of Hong Kong  
Department of Obstetrics and Gynaecology

The Chinese University of Hong Kong holds the copyright of this thesis. Any  
person(s) intending to use a part or whole of the materials in the thesis for  
proposed publication must seek copyright clearance from the Dean of the  
Graduate School.

**Abstract of thesis entitled**

**Molecular Characterization of Human Adipose Tissue-derived Stem Cells**

**Submitted by Ng Wing-chi Linda**

**for the degree of Master of Philosophy**

**at The Chinese University of Hong Kong in July 2007**

### **ABSTRACT**

Adipose Tissue-Derived Stem Cells (ATSCs) have multipotency and plasticity to be induced into mesenchymal (chondrogenic) and non-mesenchymal (neural) lineages. The excellent abundance, better proliferation power and comparable differentiation potential make ATSCs an excellent stem cell for cell therapy and tissue engineering. The aims of this project were to define the effect of donor's reproductive status on the proliferation and differentiation potential of ATSCs and then to determine if microRNA plays a role during the differentiation of ATSCs, using chondrogenic lineage as a model. We isolated ATSCs from abdominal adipose tissues of women from different reproductive groups and induced towards chondrogenic and neural lineages. Although the differentiation capacity was unaffected by the donor's reproductive status, the proliferation rate of ATSCs from pregnant women was significantly higher than that of pre-menopausal and menopausal women. Real-time quantitative PCR examined the expression of 157 miRNAs between differentiated and undifferentiated ATSCs. Cluster



analysis identified a unique miRNA profile in ATSCs. Comparing to undifferentiated ATSCs, miR-199 family was consistently and significantly up-regulated in chondrogenic-induced ATSCs. Knockdown of miR-199a during chondrogenic induction decreased the expression of chondrogenic markers, suggesting a positive role of miR-199a in chondrogenesis. Microarray gene expression data with and without *in vitro* knockdown and over-expression of miR-199a revealed that the most significantly and consistently altered mRNAs were mainly restricted to genes involved in the TGF- $\beta$  signaling pathway including TGFB1, SMAD2/3 and BMP2/6. This suggests that miR-199a could be a novel miRNA promoting chondrogenesis through the TGF- $\beta$  signaling pathway. Our study identified miR-199a as a novel regulator in ATSC differentiation.



## 摘要

脂肪幹細胞( ATSCs )具有能夠被誘導成間質細胞 (如成軟骨細胞) 和非間質細胞 (如神經細胞) 的特性。因為其來源豐富, 以及具有較好的生長能力和分化潛力, 使得脂肪幹細胞作為一種非常優越的幹細胞有效地應用於細胞療法以及組織工程中。本課題的目的在於研究脂肪幹細胞供者生殖狀態對脂肪幹細胞生長及分化潛力的影響, 並且以在脂肪幹細胞分化成成軟骨細胞為模型來檢測 microRNA (miRNA) 是否在其分化過程中起作用。我們從不同生育階段女性的腹部脂肪中成功地分離出脂肪幹細胞並將其誘導成成軟骨細胞和神經細胞。儘管脂肪幹細胞的分化能力不受其供者生殖狀態的影響, 但妊娠期婦女脂肪幹細胞的生長能力卻顯著高於停經前和停經期後的女性。通過即時定量多聚酶鏈式反應 (Real-time quantitative PCR), 我們在脂肪幹細胞在分化前後分別檢測了 157 個 miRNA 的表達水準。通過群集分析法 (Clustering analysis), 我們鑒定了脂肪幹細胞帶有獨特的 miRNA 表達圖譜。並且發現在由脂肪幹細胞誘導成的成軟骨細胞中, miR-199 家族的表達水準顯著比未分化的成軟骨細胞高。在對由脂肪幹細胞誘導成成軟骨細胞過程的 miR-199a 基因表達抑制 (Knockdown) 實驗中, miR-199a 表達的降低導致了成軟骨細胞表達標誌物的降低, 說明 miR-199a 在軟骨形成過程中起到了積極的作用。在 miR-199a 的體外基因表達抑制或過表達的實驗前後, 我們用基因晶片分別檢測了其 mRNA 的表達水準, 結果顯示異常變化的 mRNA 主要集中在轉化生長因子  $\beta$  信號途徑中, 其中包括轉化生長因子 B1 (TGFB1)、轉化生長因子胞內信號蛋白 SMAD2/3 以及骨形態發生蛋白 2/6 (BMP2/6) 等等, 說明 miR-199a 可以通過轉化生長因子  $\beta$  信號途徑來促進軟骨形成。我們的研究在世界上首次闡述了 miR-199a 在脂肪幹細胞分化過程中具有調控作用。

## ACKNOWLEDGEMENTS

I would like to express my greatest gratitude to my supervisors, Professor S.K. Yip and Dr. Richard KW Choy, for their encouragement, patience and skillful guidance, especially Professor Yip for his great efforts in specimen collection, throughout the two years of my studies. It is indeed a fruitful and joyful experience for me to learn in the Department of Obstetrics and Gynaecology.

I would like to express great thanks to my laboratory colleagues, Tao Tang, Dawn W.T. Lui and Wandy Y.M. Liu for their advice and technical support in everything, Kenneth H.K. Wong for sacrificing his valuable time helping me in the microarray analysis and immunohistochemical analysis, Ronald C.C. Wang for his fruitful discussion and his help in specimen collection, as well as other colleagues for their help in the tedious lab works when I am running out of time.

I would also like to thank Professor Tony K.H. Chung for his care and encouragement, especially during my hard time at the beginning of my studies.

Sincere thanks are due to all the staff in the Lee Hysan Clinical Research Laboratory for technical supports.

Last but not least, I would like to express my deepest love to my parents and my sister for their encouragement, care and patience.



## Publications

- 1 Ng WC, Choy K W, Yip S K. Unique MicroRNA Expression Profile during Chondrogenic Differentiation of Human Adipose Tissue-derived Stem Cells. *Faculty Research Day 2006*, Faculty of Medicine, The Chinese University of Hong Kong, 19 August, 2006. (Poster)
- 2 Ng WC, Yip S K, Wang C C, Lui WT, Liu YM, Choy K W. Studying the MicroRNA Expression Profile during Chondrogenic Differentiation of Human Adipose Tissue-derived Stem Cells. *5th International Society for Stem Cell Research Annual Meeting*, Cairns, Australia, 17-20 June, 2007. (Poster)
- 3 Choy KW, Ng WC, Wang CC, Lui WT, Liu YM, Yip S K. The Proliferation and Differentiation Capacity of Human Adipose Tissue-derived Stem Cells among Different Individuals. *5th International Society for Stem Cell Research Annual Meeting*, Cairns, Australia, 17-20 June, 2007. (Poster)



## Abbreviations

APC	Antigen Presenting Cell
ATSC	Adipose Tissue-derived Stem Cell
BDNF	Brain-derived Neurotrophic Factor
bFGF	Fibroblast Growth Factor-basic
BMP	Bone Morphogenetic Protein
BMSC	Bone Marrow-derived Stem Cell
cDNA	Complementary Deoxyribonucleic Acid
CFU-F	Fibroblast Colony Forming Units
COL10A1	Collagen Type X, alpha 1
COL2A1	Collagen Type II, alpha 1
C <sub>T</sub>	Threshold Cycle
DNA	Deoxyribonucleic Acid
E2	17 $\beta$ - estradiol
ECM	Extracellular Matrix
ER	Estrogen Receptor
ESC	Embryonic Stem Cell
GAPDH	Glyseraldehyde-3-phosphate Dehydrogenase
GFAP	Anti-glial Fibrillary Acidic Protein
GO	Gene Ontology
HLA	Human Leukocyte Antigens
Ig	Immunoglobulin
MAP2	Microtubule-associated Protein 2
miRNA	MicroRNA
mRNA	Messenger RNA
MSC	Mesenchymal Stem Cell

NEF3	Neurofilament Triplet M Protein
NGF	Nerve Growth Factor
NSE	Neuron-Specific Enolase
Pre-miRNA	Precursor MicroRNA
Pri-miRNA	Primary MicroRNA
qRT-PCR	Quantitative Reverse Transcription - Polymerase Chain Reaction
RISC	RNA-induced Silencing Complex
RNAi	RNA Interference
RT-PCR	Reverse Transcription - Polymerase Chain Reaction
Sox9	Sex-determining Region Y-box 9
SVF	Stromal Vascular Fraction
TAH	Total Abdominal Hysterectomy
TGF $\beta$	Transforming Growth Factor Beta
TUBB3	Beta Tubulin III
VH	Vaginal Hysterectomy

# **TABLE OF CONTENTS**

	Page
<b>Abstract</b>	i
<b>Acknowledgement</b>	iv
<b>Publications</b>	v
<b>Abbreviations</b>	vi
<b>Table of Contents</b>	viii
<b>List of Tables</b>	xiii
<b>List of Figures</b>	xiv
<b>CHAPTER 1 INTRODUCTION</b>	1
<b>1.1 Stem Cells</b>	1
1.1.1 Definition of Stem Cells	1
1.1.2 Different Origins of Stem Cells	2
1.1.3 Challenges and Importance of Stem Cell Research	5
<b>1.2 Adult Mesenchymal Stem Cells</b>	7
1.2.1 Characteristics of Adult Mesenchymal Stem Cells	7
1.2.2 Adipose Tissue as an Alternate Source of MSCs	8
1.2.3 Adipose Tissue Versus Bone Marrow as a Source of MSCs	10
<b>1.3 Adipose Tissue-derived Stem Cells (ATSCs)</b>	11
1.3.1 Cell Surface Marker Characteristic of ATSCs	11
1.3.2 Global Gene Expression Profile of ATSCs	14
1.3.3 Immunomodulatory Effect of ATSCs	15
1.3.4 Proliferation Capacity of ATSCs	17
1.3.5 Multilineage Differentiation of ATSCs	18
	viii



1.3.5.1 Differentiation Capability of ATSCs : Adipogenesis	18
1.3.5.2 Osteogenesis	19
1.3.5.3 Skeletal and Smooth Muscle Myogenesis	21
1.3.5.4 Cardiomyogenesis	23
1.3.5.5 Chondrogenesis	24
1.3.5.6 Neurogenesis	27
<b>1.4 Signaling Pathways in Stem Cells</b>	<b>31</b>
1.4.1 Wnt Signaling	31
1.4.2 Notch Signaling	33
1.4.3 Signaling Pathway of the TGF- $\beta$ Superfamily	34
<b>1.5 Pathways Controlling Chondrogenesis</b>	<b>36</b>
<b>1.6 MicroRNA</b>	<b>39</b>
1.6.1 MicroRNA – A Novel Gene Regulator	39
1.6.2 Biogenesis of MicroRNAs	40
1.6.3 Post-transcriptional Repression by MicroRNAs	43
1.6.4 Role of MicroRNAs in Development	45
1.6.5 MicroRNAs in Stem Cell Differentiation	46
1.6.5.1 MicroRNA Expression Profile in ESCs	46
1.6.5.2 Lineage Differentiation	47
<b>1.7 Project Aims</b>	<b>52</b>
<b>1.8 Significance of Study</b>	<b>53</b>
<b>Chapter 2 Materials and Methods</b>	<b>54</b>
<b>2.1 Sample Collection</b>	<b>54</b>
<b>2.2 Isolation and Culture of ATSCs</b>	<b>54</b>
<b>2.3 Measurement of Cell Growth</b>	<b>55</b>

<b>2.4 Effect of Estrogen Treatment on ATSC Proliferation</b>	55
<b>2.5 Multilineage Differentiation of ATSCs</b>	55
2.5.1 Chondrogenic Differentiation	56
2.5.2 Neural Differentiation	56
<b>2.6 Immunocytochemical Analysis of Surface Markers and Lineage Specific</b>	57
<b>Markers</b>	
<b>2.7 Alcian Blue Staining</b>	58
<b>2.8 RNA Extraction</b>	58
<b>2.9 Reverse Transcription</b>	59
<b>2.10 Quantitative Real-time Polymerase Chain Reaction</b>	59
<b>2.11 Statistical Analysis of Real-time PCR Data</b>	61
<b>2.12 MicroRNA Profiling</b>	61
2.12.1 Reverse Transcription	62
2.12.2 Quantitative Real-time Polymerase Chain Reaction	62
<b>2.13 mRNA Target Prediction of MicroRNA</b>	63
<b>2.14 MicroRNA Knockdown Assay</b>	63
<b>2.15 MicroRNA Over-expression Assay</b>	64
2.15.1 Vector Amplification	64
2.15.1.1 Transformation	64
2.15.1.2 Purification of Plasmid DNA	65
2.15.1.3 Confirmation of Construct Insertion	66
2.15.2 Transfection of Plasmid and Establishment of MicroRNA Precursor	66
Expressing Cell Lines	
<b>2.16 Gene Expression Microarray</b>	67
2.16.1 Preparation of Amplification and Labeling Reaction	67
2.16.2 Purification of the Labeled/Amplified RNA	68

2.16.3 RNA Fragmentation	68
2.16.4 Hybridization	69
2.16.5 Array Washing and Scanning	69
2.16.6 Statistical Analysis of Microarray Data	69
<b>CHAPTER 3 RESULTS</b>	<b>71</b>
<b>3.1 Isolation and Characterization of ATSCs</b>	<b>71</b>
<b>3.2 ATSCs Exhibited Multilineage Differentiation</b>	<b>75</b>
3.2.1 Chondrogenic Differentiation	75
3.2.2 Expression of Chondrogenic Markers	76
3.2.3 Neural Differentiation	80
3.2.4 Expression of Neural Markers	83
<b>3.3 Effect of Donor's Reproductive Status on the Proliferation and         Differentiation Capacity of ATSCs</b>	<b>83</b>
3.3.1 Expression of Stem Cell Markers	86
3.3.2 Cell Proliferation Assay	86
3.3.3 Differentiation Capacity of ATSCs	89
<b>3.4 Effect of E2 Treatment on the Proliferation Rate of ATSCs</b>	<b>89</b>
<b>3.5 MicroRNA</b>	<b>91</b>
3.5.1 MicroRNA Expression Profile of Undifferentiated and Chondrogenic Differentiated ATSCs	91
3.5.2 Clustering Analysis Identified MicroRNAs Segregate with ATSCs	91
3.5.3 Identification of Differentially Expressed MicroRNAs in Chondrogenic-induced ATSCs	95
3.5.4 mRNA Target Prediction for miR-199a	97



<b>3.6 Correlating MicroRNA Expression and mRNA Levels: Clues to MicroRNA Function</b>	97
3.6.1 Effect of miR-199a RNAi in Phenotypic Changes of Chondrogenic-induced ATSCs	97
3.6.2 Identification of Potential Target Genes by Microarray Analysis of ATSCs with miR-199a Over-expression and Knockdown	102
<b>CHAPTER 4 DISCUSSION</b>	104
<b>CHAPTER 5 CONCLUSIONS</b>	115
<b>APPENDICES</b>	117
<b>REFERENCES</b>	120

## List of Tables

		Page
1	The cell surface marker expression of ATSCs	13
2	Comparison of cell surface phenotype between ATSCs and BMSCs	14
3	Primer sequences for lineage marker genes	60
4	Summary of adipose tissue samples collected from three groups of individuals	72
5	Table summarized the growth rate, CD90 expression intensity and morphology of ATSCs derived from three reproductive groups	87
6	Comparison of the chondrogenic differentiation capacity of ATSCs from three reproductive groups	90

## List of Figures

		Page
1	Biogenesis of MicroRNA	42
2	Lentiviral vector containing the miR-199a-1 precursor	64
3	Morphology of ATSCs derived from human adipose tissue	73
4	Immunostaining of mesenchymal stem cell markers of ATSCs	74
5	Morphology of spheroids formed in micromass culture	77
6	Immunostaining of spheroids in control and chondrogenic medium against chondrogenic markers	78
7	mRNA Expression of chondrogenic markers	79
8	Alcian blue staining of spheroids	81
9	Morphology of neurally induced ATSCs	82
10	Immunostaining of ATSCs in control and chondrogenic medium against neural markers	84
11	Real-time PCR results of neural markers in neurally induced ATSCs compared to control	85
12	Boxplot comparing the growth rates of ATSCs derived from the three reproductive groups	88
13	Expression profile of 157 miRNAs in undifferentiated and chondrogenic differentiated ATSCs	93
14	Hierarchical clustering comparing 157 miRNA expression profile of ATSCs with other tissues	94
15	Average fold change and expression level of 11 aberrantly expressed miRNAs in ATSCs after chondrogenic induction	96
16	Change in miR-199a expression after miR-199a knockdown.	99





# CHAPTER 1 INTRODUCTION

## 1.1 Stem Cells

The stem cell is the origin of life. Understanding how to control the differentiation and maintain pluripotency of a stem cell is not only the key to discover molecular mechanisms important for cell replacement therapy for many genetic, metabolic, and degenerative diseases but also control cancer development.

### 1.1.1 Definition of Stem Cells

Stem cells are unspecialized cells that are capable of self-renewal for indefinite period. Stem cells normally remain uncommitted in the body. However, under proper condition(s) with specific signals, stem cells can differentiate into many different types of specialized cells. Their capacity to renew themselves and to give rise to multiple specialized cells makes stem cells unique. (Bongso, et al 2005, Department of Health and Human Services 2001, Marshak, et al 2001, Sell 2004)

Stem cells can be classified by their differentiation power:

**Totipotent stem cells** can differentiate into all cell types of the three germ layers (Ectoderm, Mesoderm and Endoderm) in the body including the placenta. A fertilized egg is a type of totipotent stem cell. Cells produced in the first few divisions of the fertilized egg are also totipotent.

**Pluripotent stem cells** are descendants of the totipotent stem cells. They are

cells which develop about four days after fertilization. They can differentiate into all cell types of the three germ layers except totipotent stem cells and the cells of the placenta.

**Multipotent stem cells** are descendants of pluripotent stem cells. They retain the power to differentiate into different kinds of cell but not cells of all the three germ layers. Hematopoietic stem cells and neural stem cells are examples of multipotent stem cells.

**Unipotent stem cells** (or progenitor cells) can only produce one type of specialized cells. For example, erythroid progenitor cells differentiate into only red blood cells. These specialized cells produced are terminally differentiated, which are permanently committed to specific functions throughout the life time.

Division of stem cells can be symmetric or asymmetric. A symmetric division yields two identical daughter stem cells. An asymmetric division yields a daughter stem cell and a terminally differentiated daughter cell which has lost its differentiation capacity. Symmetric divisions occur in early embryonic development while asymmetric divisions occur during normal tissue renewal in adult.

### **1.1.2 Different Origins of Stem Cells**

Stem cells are commonly classified into three broad categories by their

origins. They are embryonic stem cells, fetal stem cells and adult stem cells.

### ***Embryonic stem cells (ESCs)***

Embryonic stem cells are derived from the inner cell mass of a blastocyst, which is an early embryo of 4 to 5 days. ESCs have the capability of long-term self-renewal that can undergo an unlimited number of symmetrical divisions without differentiating. They are pluripotent cells that have the ability to give rise to tissues of all three embryonic germ layers (mesoderm, endoderm, and ectoderm). Due to their pluripotency, ESCs can be widely applied in scientific researches and therapeutic uses.

However, the controversy over the moral status of the embryos used has raised sensitive ethical and religious arguments which greatly limit the development of human ESCs. At this stage, any therapeutic use of human ESCs is still hypothetical and highly experimental.

### ***Fetal stem cells***

Fetal stem cells can be isolated from fetal tissues such as brain, liver, kidney, blood, bone marrow as well as umbilical cord blood, amniotic fluid and placenta. Fetal stem cells are multipotent cells that can give rise to tissues of their own origins.



Although embryonic stem cells have a higher differentiation potential, their ethical constraints have encouraged the search of alternate stem cell sources. Fetal stem cells, which are mainly obtained from terminated fetuses, are less ethically contentious and therefore may be a possible alternative to ESCs. Moreover, as they are biologically closer to embryonic stem cells, they appear to be more primitive with greater differentiation capacity than adult stem cells. A recent report showed that stem cells from fetal tissues are more plastic, grow faster and have longer telomeres than adult stem cells (Guillot, et al 2007). Therefore, fetal stem cells also act as a powerful tool for cell therapy (Guillot, et al 2006, O'Donoghue, et al 2004). However, fetal tissues are difficult to obtain and this greatly limits their therapeutic uses.

### ***Adult stem cells***

Adult stem cells can be derived from adult tissues of all three germ layers such as brain, bone marrow, fat and liver. Adult stem cells are multipotent cells which can differentiate into cell type of their tissue origin. Recently, the discovery of adult stem cell's plasticity suggests that they can transdifferentiate into cell types of other germ layers. Examples of adult stem cells are neural stem cells, hematopoietic stem cells, mesenchymal stem cells, and endodermal stem cells.

### 1.1.3 Challenges and Importance of Stem Cell Research

Research has been done on stem cells since the discovery of the fertilized egg in the eighteenth century and great progress has been made in understanding the biological properties of stem cells. However, difficulties do exist in stem cell research that greatly limit its development. This is not limited to the numerous technical challenges needed to be overcome, such as the heterogeneity of the isolated stem cells, lack of specific markers for identification of different kinds of stem cells and long-term maintenance of stem cells in tissue culture, but also to the discovery and understanding the molecular mechanisms controlling the stem cell differentiation *in vitro* and *in vivo*.

The ultimate goal of stem cell research is to cure disease by cell regeneration and tissue engineering in the human body. However, new challenges come when the cells are implanted into our body. What are the homing mechanisms guiding stem cells to a site of injury after transplantation? How can we ensure that the implanted cell is completely integrated into the patient's own tissues and fully functional? How can we prevent transplantation rejection? Will there be a risk of cancer derived from the implanted stem cells? However, there are two major questions which need to be addressed before we can achieve our goal for cell therapy: (1) Does the physiological status of the stem cell donor affect the differentiation and proliferation of stem cells?

(2) What are the molecular mechanisms guiding stem cells to differentiation? .

Nonetheless, due to the characteristics of self-renewal and multilineage differentiation, stem cells offer a wide range of applications in both basic scientific research as well as clinical and therapeutic uses. Stem cells allow the study of various biological processes which are usually done in animal models. By acting as a powerful research tool, stem cells help identify genes, chemicals and small molecules involved in biological functions such as cell division and lineage differentiation. Moreover, drug tests are made possible on human cells which were previously not accessible. For example, new drugs for heart diseases, which are generally tested only in animal models due to absence of human heart cell lines, can now be tested on human cells using cardiocytes derived from human stem cells (Bremer, et al 2004).

Most importantly, human stem cells could provide an unlimited amount of tissue for cell therapies and tissue engineering for the treatment of a wide range of degenerative diseases such as Parkinson's disease, diabetes, traumatic spinal cord injury, Purkinje cell degeneration, Duchenne's muscular dystrophy, heart failure, and osteogenesis imperfecta. By replacing the dead or injured cells with differentiated stem cells, these incurable disorders may have a chance to be resolved in the future. In addition, stem cells, by acting as vehicles for gene transfer, can eliminate diseased genes and restore the normal functions of the defective genes.



## 1.2 Adult Mesenchymal Stem Cells

### 1.2.1 Characteristics of Adult Mesenchymal Stem Cells

Adult mesenchymal stem cells (MSCs) are multipotent cells which produce progeny that can differentiate into a variety of mesenchymal cell types. As a kind of adult stem cell, their main role in our body is to maintain homeostasis by replenishing dying cells due to injury or disease and regenerating damaged tissues (Holtzer 1978). Like all stem cells, adults MSCs possess the two main characteristics of typical stem cells: self-renewal and multi-lineage differentiation. However, so far, little is known about the biology of endogenous stem cell populations in adults and their precise role in tissue repair and regeneration.

MSCs were first identified and isolated from rat bone marrow by Friedenstein and colleagues in 1966. It was found that these cells have the capacity to differentiate into cells of connective tissue lineages, including bone, fat, cartilage and muscle. In bone marrow, they also act as stromal cells to support haematopoietic stem cells (Friedenstein, et al 1966). Later they were identified in many other tissues such as skeletal muscle, adipose tissue, synovium and periosteum (Cao, et al 2003, De Bari, et al 2001, Fukumoto, et al 2003a, Rodriguez, et al 2005a).

Adult MSCs may not have the pluripotency of embryonic stem cells, however, they still arouse great interest from scientists. One of the reasons is their plasticity,

which is the capability of adult stem cells to differentiate into tissues other than their tissue of origin, even crossing germ layers. The discovery of stem cell plasticity has overthrown the concept of lineage restriction and greatly widened their application in cell therapy and tissue engineering. Furthermore, unlike embryonic stem cells, adult MSCs do not face any ethical problems. This allows the collection of adult stem cells take place at any place at any time. Both pre-clinical and clinical studies showed successful examples in cell therapy that illustrate the therapeutic value of MSCs (Barry FP 2004; Schaffler A 2007).

However, stem cells are rare in adult tissues. For example, in bone marrow, MSCs only represent a very small fraction of 0.001-0.01% of total nucleated cell population (Pittenger, et al 1999). It will be difficult to obtain an amount of MSCs enough for therapeutic uses. Luckily, the recent discovery of MSCs in adipose tissue has introduced an excellent source of adult stem cells. As adipose tissues can be extracted in large volume with limited morbidity, they are an exciting alternative stem cell source (Zuk PA 2002; Schaffler A 2007).

### **1.2.2 Adipose Tissue as an Alternate Source of MSCs**

Adipose tissue is a highly complex tissue. It consists of many kinds of cells including mature adipocytes, preadipocytes, fibroblasts, vascular smooth muscle

cells, endothelial cells, resident macrophages and lymphocytes (Caspar-Bauguil, et al 2005, Weisberg, et al 2003, Zuk, et al 2001). Stromal vascular fraction (SVF) of the adipose tissue, is classically used as the source of preadipocytes. Adipose tissue has a remarkable ability to dynamically expand and shrink during the lifespan of an adult. Fat mass in human body can range from 2 to 3% of body weight in extremely well conditioned athletes to 60 to 70% of body weight in massively obese individuals. A small change in adipose tissue volume can be accommodated by changing the lipid stored in adipocytes. Therefore, larger changes must be achieved by the generation of new adipocytes by the pool of stem and progenitor cells from the vascular and nonvascular cells (Hausman, et al 2001, Rupnick, et al 2002). Recent studies have shown that cells from SVF display a large spectrum of differentiation, which suggests the presence of multipotent stem cells inside this tissue compartment (Zuk, et al 2002). There are many terms used in the literature describing these multipotent stem cells from adipose tissue, such as processed lipoaspirate (PLA) cells, adipose tissue-derived stromal cells (ADSCs), preadipocytes, and adipose stroma vascular cell fraction. In this thesis, the term adipose tissue-derived stem cells (ATSCs) will be used.



### **1.2.3 Adipose Tissue Versus Bone Marrow as a Source of MSCs**

MSCs were first identified in bone marrow, and most of the studies have focused on the MSCs found within the bone marrow stroma. However, the discovery of MSCs in adipose tissue has introduced a novel stem cell source which is believed to be more well-suited as a source of MSCs than bone marrow. Although bone marrow stem cells (BMSCs) have demonstrated great therapeutic potential, the procurement procedures for BMSCs are painful and frequently require general or spinal anesthesia. BMSCs cause donor site morbidity that limits the amount of marrow can be obtained, resulting in low yield of MSCs. On the other hand, adipose tissue is readily accessible. Using typical harvesting procedures like liposuction under local anesthesia, adipose tissue can be extracted in a large volume with limited morbidity. A higher yield upon tissue harvest therefore minimizes the time in culture required to generate a therapeutic cell dose (Strem, et al 2005a). Most importantly, ATSCs exhibit phenotypes, gene expression profiles as well as differentiation capabilities which are very similar to BMSCs (Lee, et al 2004). These all suggest that adipose tissue could be an exciting alternative stem cell source to bone marrow and a better candidate for cell therapy and tissue engineering.

### **1.3 Adipose Tissue-derived Stem Cells (ATSCs)**

#### **1.3.1 Cell Surface Marker Characteristic of ATSCs**

The cell surface marker characterization of ATSCs has been well studied (Gronthos, et al 2001, Klyushnenkova, et al 2005, Lee, et al 2004, Mitchell, et al 2006, Sakaguchi, et al 2005, Schaffler, et al 2007, Strem, et al 2005a) (Table 1). The cell surface phenotype of ATSCs is very similar to that of other MSCs, e.g. BMSCs (Strem, et al 2005a) (Table 2). ATSCs express CD73, CD90 and CD105 which matches the minimal criteria for human MSCs proposed by the Mesenchymal and Tissue Stem Cell Committee of the International Society for Cellular Therapy (Dominici M. 2006). In addition, they express a larger number of adhesion molecules like CD44 (hyaluronate receptor), CD54 (ICAM-1) and CD166 (ALCAM), as well as growth factors (CD117, stem cell factor) and integrins like CD29 (beta-1 integrin), CD49d (alpha-4 integrin) and CD49e (alpha-5 integrin). On the other hand, ATSCs lack the expression of known hematopoietic and endothelial markers such as CD3, CD4, CD11b, CD11c, CD14, CD16, CD19, CD31, CD34, CD45, CD79 $\alpha$ , CD104, CD133, CD144 and c-kit. The absence of expression of these markers indicates that ATSCs are not derived from circulating bone marrow hematopoietic stem cells.

However, STRO-1 which is a marker commonly used in the isolation of multipotent BMSCs (Dennis, et al 2002, Gronthos, et al 1994), is negatively or only

weakly detected in ATSCs (Gronthos, et al 2001, Schaffler, et al 2007). ATSCs also lack the expression of HLA-DR, a class II antigen of human leukocyte antigens (HLA) which is commonly associated with the acute rejection after transplantation. Lacking the HLA-DR expression allows ATSCs to escape from the immune system, suggesting their potential for heterologous transplantations.

In fact, the surface protein phenotype of ATSCs changes throughout the culture period. A study has compared the immunophenotype of freshly isolated human ATSCs to serial-passaged ATSCs (Mitchell, et al 2006). They found that the immunophenotype of ATSCs changed progressively with adherence and passage. Stromal cell-associated markers like CD13, CD29, CD44, CD63, CD73, CD90, CD166 were initially low in freshly isolated ATSCs but significantly increased with passages. On the other hand, Antigen presenting cell (APC)-associated markers such as CD45, CD11a, CD14, CD86 and HLA-DR initially expressed in freshly isolated SVF population and ATSCs at passage 0, which were found to be immunogenic in a mixed lymphocyte reaction. However, in passage 1 to passage 4 populations, cells did not express these APC-associated markers and were not immunogenic. These observations may be explained by the fact that heterogeneous populations exist in freshly isolated ATSCs, which may contain a significant percentage of immunogenic hematopoietic-derived APCs. Eventually, with progressive passage and expansion



of the adherent ATSCs, the number of these APCs decreases leaving the majority of ATSCs which are immunosuppressive.

<b>Surface Marker Expression in ATSCs</b>	
<b>Positively expressed</b>	<b>Negatively expressed</b>
CD9	CD3
CD10	CD4
CD13	CD11b
CD29	CD11c
CD44	CD14
CD49d	CD19
CD49e	CD31
CD54	CD34
CD55	CD40
CD59	CD45
CD73	CD79 $\alpha$
CD90	CD80
CD105	CD86
CD117	CD104
CD146	CD133
CD166	CD144
HLA-A/B/C	STRO-1
	HLA-DR
	c-kit

**Table 1 The cell surface marker expression of ATSCs.**

Markers	ATSCs	BMSCs
CD29	+	+
CD44	+	+
CD90	+	+
CD105	+	+
CD49d	+	-
CD49e	+	+
CD106	-	+
CD14	-	-
CD34	-	-
HLA-A/B/C	+	+
HLA-DR	-	-
c-kit	-	-
STRO-1	+-	+

**Table 2 Comparison of cell surface phenotype between ATSCs and BMSCs**  
(+ positively express ; +- weakly express ; - negatively express)

### 1.3.2 Global Gene Expression Profile of ATSCs

The global gene expression of ATSCs was recently characterized by Wagner et al. (Wagner, et al 2005). In this study the expression profiles of 51,144 genes in human were compared in MSCs derived from adipose tissue, umbilical cord blood, and bone marrow to terminally differentiated human fibroblasts. Only twenty-five genes were identified to be overlapping and upregulated in MSCs prepared from all three sources when compared to fibroblasts. These genes, including *fibronectin*, *ECM2*, *glypican-4*, *ID1*, *NF1B*, *HOXA5* and *HOXB6*, were involved in extracellular

matrix, morphogenesis, and development. On the other hand, several inhibitors of the Wnt pathway including *DKK1*, *DKK3*, *SFRP1* were down-regulated in all different MSCs compared to fibroblasts. When the gene expression profiles of MSCs from the three sources were compared, significant differences were found between genes expressed in MSCs from different sources, including genes involved in mesodermal differentiation and cell division. However, using a panel of 22 surface antigen markers, no phenotypic differences were found among the three MSC populations derived from different tissues. In another study by Lee and colleagues (Lee, et al 2004), gene expression profiles were compared between human MSCs derived from adipose tissue and bone marrow. They found that the gene expression profiles of the two MSC populations are highly similar. Less than 1% of the genes were differentially expressed between them. However, these studies only provide limited and undefined insights for deciphering exactly how "stemness" and "regulated differentiation" is maintained in ATSCs. Further work is required for elucidation of the transcriptional programming and molecular mechanisms which direct self-renewal and differentiation in ATSCs.

### **1.3.3 Immunomodulatory Effect of ATSCs**

As ATSCs do not express major histocompatibility complex (MHC) class II

(HLA-DR) or co-stimulatory molecules like CD80 (B7-1), CD86 (B7-2) and CD40 (Klyushnenkova, et al 2005), they can escape from the immune system easily without inducing allospecific T cell proliferative responses. The *in vitro* and *in vivo* immunosuppressive properties of ATSCs have been extensively studied (McIntosh, et al 2006, Puissant, et al 2005, Yanez, et al 2006). Mixed Lymphocyte Reaction (MLR) assay was commonly performed to assess the immunogenicity of ATSCs. When co-cultured with allogeneic lymphocytes e.g. peripheral blood mononuclear cells, ATSCs do not elicit a lymphocyte proliferative response. Interestingly, ATSCs even induce an *in vitro* immunosuppressive effect on allogeneic lymphocytes. The phytohemagglutinin (PHA)-mediated stimulation of T cells was significantly decreased with increasing proportion of ATSCs in the culture. Studies also proved that the direct cellular interactions between ATSCs and T cells were important, but not essential for the immunosuppressive effect of ATSCs. ATSCs produce cytokines like TGF- $\beta$ , IL-10 and hepatocyte growth factor (HGF) which has been suggested to be responsible for the immunosuppressive property of ATSCs. The immunomodulatory effect of ATSCs *in vivo* was also studied using a mouse model. Graft versus host disease (GVHD) was induced in mice after haploidentical hematopoietic transplantations. Infusion of ATSCs significantly increased the survival of transplanted mice and notably diminished the severity of tissue damage



by GVHD (Yanez, et al 2006).

The remarkable immunosuppressive property of MSCs including ATSCs allows transplantation across classical histocompatibility barriers and makes them the best candidate for allogeneic transplantation by preventing the incidence of GVHD. Recently, reports have been published on the evaluation of use of MSCs in GVHD treatment and preliminary results appear to be promising (Bacigalupo 2007, Le Blanc, et al 2004, Ringden, et al 2006).

#### **1.3.4 Proliferation Capacity of ATSCs**

One of the typical characteristics of stem cells is the ability to self-renew. In a study by Lee (Lee, et al 2004), the proliferation capacity of ATSCs was evaluated by its doubling time versus the passage number in culture. From their findings, the doubling time of ATSCs remained constant up to 15 passages and growth was stopped at 20 passages. However, in the case of BMSCs, the doubling time increases with the passage number and growth stopped at 15 passages. These findings are consistent with the microarray data in other studies (Wagner, et al 2005) that ATSCs has a higher expression of cell proliferation-associated genes like Ki-67, cell division cycle associated 8 (CDCA8) and cyclin B2 (CCNB2) than BMSCs. These all indicate that ATSCs has a better proliferation potential than BMSCs.

### **1.3.5 Multilineage Differentiation of ATSCs**

The abilities of ATSCs to differentiate along classic mesenchymal lineages into adipocytes, osteocytes, chondrocytes and myocytes have been well established (Dicker, et al 2005, Lee, et al 2004, Lin, et al 2006, Mizuno, et al 2003, Zuk, et al 2002). After the introduction of adult stem cell plasticity, their abilities to cross-germ differentiate have also been investigated and published. ATSCs can be induced into non-mesodermal lineages such as neural, endothelial, epithelial, pancreatic and hepatic lineages (Brzoska, et al 2005, Cao, et al 2005, Kokai, et al 2005, Planat-Benard, et al 2004b, Safford, et al 2002a, Seo, et al 2005, Timper, et al 2006), demonstrating their differentiation plasticity. In this study, we will focus on the chondrogenic lineage which is the most well established and widely studied to act as a model tool for identification of molecular pathways important for ATSC differentiations.

#### **1.3.5.1 Differentiation Capability of ATSCs : Adipogenesis**

ATSCs, which are isolated from adipose tissue, can readily differentiate along the adipocytic lineage. ATSCs are commonly induced in adipogenic medium containing isobutyl-methylxanthine (IBMX), dexamethasone, insulin, indomethacin and Rosiglitazone (Lee, et al 2004, Lin, et al 2006, Mizuno, et al 2003, Ryden, et al

2003). ATSC-derived adipocytes develop lipid laden intracellular vacuoles and stain positive with the triglyceride specific dye Oil Red O. They express several adipocytic genes including *lipoprotein lipase*, *aP2*, *PPAR $\gamma$ 2*, *leptin*, *Glut4* and *glycerol-3-phosphate dehydrogenase (GPDH)* (Dicker, et al 2005, Sen, et al 2001, Zuk, et al 2001, Zuk, et al 2002). ATSC-derived adipocytes also display lipolysis, which is another hallmark of adipogenesis. The lipolytic capacity, assessed by glycerol release in the medium after lipolytic agent stimulation, increased in differentiated cells compared to control (Dicker, et al 2005). Secretion of fat cell-specific proteins like leptin and adiponectin was also detected in adipocytes derived from ATSCs.

The ability of ATSCs to differentiate into adipocytic lineage *in vivo* has also been demonstrated. In these studies, different carrier materials were used including cell-seeded natural scaffolds like collagen and hyaluronic acid (Halbleib, et al 2003, von Heimburg, et al 2001a, von Heimburg, et al 2001b) as well as synthetic bioresorbable grafts like polyglycolic acid and PLGA (Lee, et al 2003, Patrick, et al 1999, Patrick, et al 2002).

#### **1.3.5.2 Osteogenesis**

Same as BMSCs, ATSCs have the ability to differentiate into the osteogenic

lineage (Dicker, et al 2005, Halvorsen, et al 2001, Lee, et al 2004, Lin, et al 2006, Zuk, et al 2002). In the presence of ascorbic acid,  $\beta$ -glycerophosphate and dexamethasone, ATSCs change into an osteoblastic morphology with a cuboidal shaped and tightly packed arrangement and eventually form bone-like nodules. Deposition of a calcium-rich mineralized extracellular matrix can be identified and confirmed by a calcium-specific stain Alizarin Red. ATSC-derived osteocytes express osteogenic marker genes and proteins including alkaline phosphatase, collagen type I, osteopontin, osteocalcin, osteonectin, cbfa-1, bone sialo protein, RunX-1, BMP-2, BMP-4, BMP receptors I and II, and PTH-receptor.

With the use of a variety of supportive 3D scaffolds such as beta-tricalcium phosphate ( $\beta$ -TCP) and polyglycolic acid (PGA), osteocytes derived from human ATSCs can be tissue-engineered and implanted in immunodeficient rodent ectopic bone models (Dragoo, et al 2003, Hattori, et al 2006, Hicok, et al 2004, Lee, et al 2003). The positive immuno-staining of human osteocalcin, which is an indicator for metabolically active bone cells, in the implanted ATSC scaffolds indicated that the implanted human ATSCs were successfully differentiated into osteoblasts and promoted the bone formation in the nude mice. Overall, the rate and extent of bone formation *in vivo* of ATSCs was similar to that of BMSCs.

More importantly, ATSCs have already been applied to clinical uses for bone



engineering, and the results are encouraging. In a case study of a 7-year-old girl suffering from widespread calvarial defects, repair was achieved by applying processed autologous ATSCs to the calvarial defects (Lendeckel, et al 2004). New bone formation and near complete calvarial continuity were detected three months after the reconstruction. This case report suggests the powerful therapeutic use of ATSCs in bone engineering as well as the clinical uses of ATSCs in human.

#### **1.3.5.3 Skeletal and Smooth Muscle Myogenesis**

By culturing ATSCs in the presence of hydrocortisone and horse serum, and/or co-culturing with myoblasts, ATSCs can be induced into myogenic lineage (Di Rocco, et al 2006, Lee, et al 2006, Mizuno, et al 2002, Zuk, et al 2002). ATSC-derived myocytes acquired a myoblast-like morphology with generation of long, multinucleate cells early in culture and formation of myofibrillar bundles after two week induction. These cells also express muscle-related genes in a time-dependent pattern, which is consistent with normal myogenesis. They express early myogenic markers MyoD1 and Myf5, Myf6, Desmin, Myogenin and Myosin, followed by expression of late markers including Myosin Heavy Chain and Alpha-skeletal Actin. ATSCs can be induced into smooth muscle differentiation using various protocols, including induction by heparin in MCDB131 medium

(Rodriguez, et al 2006) or by chemicals like mercaptoethanol (BME), ascorbic acid (AA) and retinoic acid (RA) (Lee, et al 2006). Differentiated cells express smooth muscle markers alpha-smooth muscle actin (aSMA), smoothelin, Calponin, Caldesmon, MHC, and SM22, that confirm the leiomyogenic lineage.

So far, not many studies have been done on the *in vivo* myogenesis capacity of ATSCs. Bacou et al. (2004) were the first to report on the muscle regeneration ability of ATSCs in animal models. They demonstrated that after the transplantation of ATSCs into injured regions of rabbit skeletal muscle, participation of ATSCs was detected in regenerated fibres, followed by the increased muscle weight and fiber cross section area. The maximal contractile force was significantly raised when compared to the damaged control muscle. These results are similar to those previously obtained after satellite cell transplantation. Another study (Rodriguez, et al 2005b) demonstrated the muscle regeneration ability of ATSCs in a mouse model with Duchenne muscular dystrophy. After transplantation, substantial expression of human dystrophin was detected in mice while no dystrophin-positive fibres were found in non-injected muscle.

The leiomyogenic differentiation potential of ATSCs also allows their uses in tissue engineering of the lower urinary tract, help curing disorders like urinary incontinence and bladder dysfunction. In a report by Jack et al. (Jack, et al 2005),

human ATSCs were isolated and injected into the bladder and urethra in multiple animal models using both Rnu athymic rats and SCID mice. After injection, ATSCs were found to incorporate into the recipient smooth muscle, followed by the *in vivo* expression of alpha-smooth muscle actin (aSMA), a smooth muscle marker, in the injected area. ATSCs, with their easy accessibility and ability to undergo myogenesis, provide a feasible and cost-effective cell source for muscle engineering and muscle cell-mediated therapy.

#### **1.3.5.4 Cardiomyogenesis**

Cardiovascular disease, which has become the leading cause of morbidity and mortality in the world, can also be benefited by the use of ATSCs. ATSCs had been successfully induced into cardiomyocytes using different differentiation protocols, e.g. addition of 5-azacytidine or cardiomyocytes extracts. In a compelling study by Planat-Bernard et al. (Planat-Bernard, et al 2004a), ATSCs were cultured in a semisolid methylcellulose medium containing interleukin (IL) -3, IL-6 and stem cell factor (SCF). Colonies of spontaneously beating cells were observed and positively expressed cardiac specific markers such as GATA-4, Nkx2.5, Atrial/Ventricular Myosin Light Chain (MLC-2a/MLC-2v), Myosin-enhancing Factor 2C (MEF2C),  $\beta$ -Myosin Heavy Chain ( $\beta$ MHC) and Connexins. The absence of the skeletal



muscle protein MyoD or the smooth muscle actin strongly supported that the beating cells identified were cardiomyocytes and not skeletal or smooth muscle cells. Moreover, these cells exhibited a pacemaker activity and responded to adrenergic and cholinergic stimuli.

The ability of ATSCs to repair injured myocardium *in vivo* has been demonstrated (Miyahara, et al 2006, Strem, et al 2005b), and the results are promising. Transplantation of monolayered ATSCs onto the scarred myocardium of an infarcted rat heart resulted in cardiomyogenesis with the expression of cardiomyocyte-specific markers (Miyahara, et al 2006). Angiogenesis was also induced in the transplanted area, with the wall thinning in scar area reversed and cardiac function improved. Although these data were exclusively from animal models, ATSCs could be a new therapeutic strategy for cardiac tissue regeneration in the near future.

#### **1.3.5.5 Chondrogenesis**

To induce ATSCs into chondrogenic lineage, the cells are cultured in a very high density to mimic the prechondrogenic cellular condensation, which is a critical first event of chondrogenesis *in vivo* (Ede 1983). Two culture techniques, called micromass culture (Ahrens, et al 1977) and pellet culture (Mackay, et al 1998), are



commonly used to create a high cell density culture of ATSCs for chondrogenic induction. Together with the supplement of chondrogenic induction agents such as transforming growth factor- $\beta$ , ascorbic acid and dexamethasone, ATSCs form a three dimensional spheroid structure (Dicker, et al 2005, Dragoo, et al 2003, Lee, et al 2004, Ogawa, et al 2004, Zuk, et al 2001, Zuk, et al 2002). A proteoglycan-rich extracellular matrix form around the spheroid and the cells express chondrogenic markers including collagen type II, aggrecan, collagen type X, as well as sulfated proteoglycans such as keratan sulfate and chondroitin sulfate. Apart from the high density culture methods, chondrogenesis of ATSCs can also be induced by suspending cells in spherical alginate beads in chondrogenic medium (Awad, et al 2003, Estes, et al 2006). By maintaining the cells in a three dimensional environment, expression of the chondrocytic phenotype can also be significantly promoted.

Due to the poor regenerative capacity and inferior repair of the cartilage, treatment of cartilage pathology and trauma faces great challenges. Current treatments for articular cartilage reconstruction include arthrodesis and arthroplasty, which are joint fusion and joint replacement respectively (Hunziker 2002). However, these synthetic implants may lead to problems like infection, rejection, poor longevity and unsatisfactory scarring. The recent discovery of the potential of adult stem cells in cartilage tissue engineering have provided a novel therapeutic approach

to cartilage repair.

Implantation of stem cell-derived chondrocytes requires scaffolds which can provide biodegradable and porous, mechanical support. Both natural (e.g. agarose, alginate, hyaluronic acid, gelatin) and synthetic biomaterials (e.g. polyglycolic acid) have been used in the *in vivo* studies of cartilage tissue engineering using human MSCs. In a study by Erickson et al. (Erickson, et al 2002), ATSCs were seeded onto alginate discs for 2 weeks *in vitro* and were implanted into nude mice for another 4 to 12 weeks. The implanted cells exhibited significant production of cartilage matrix molecules including collagen type II, VI and aggrecan. A recent study also evaluated the potential of ATSCs as a source for full-thickness cartilage repair in a rabbit model (Dragoo, et al 2007). Autologous ATSCs seeded in a fibrin glue scaffold were implanted into rabbits with chondral defects. Defects in articular surface were healed in 100% (12 of 12) implanted rabbits while only 1 of 12 healed in the control group. In addition, aggrecan, superficial zone protein and collagen type II messenger ribonucleic acid were identified in all implanted rabbits, with the exhibition of a collagen type II:I protein ratio similar to that of normal rabbit cartilage.

The ability to produce characteristic cartilage matrix molecules in both *in vitro* and *in vivo* models, as well as to repair cartilage defects *in vivo*, suggests ATSCs as a promising cell source for cartilage tissue engineering. However, further

work should still be done on the optimization of the culture and engineering procedures before ATSCs can be successfully applied in human clinical trials.

#### **1.3.5.6 Neurogenesis**

Lacking the ability of mature neurons to regenerate and repair in response to injury, tissue damage in the central nervous system is incapable of self-repair. Loss of neurons due to aging, neurodegenerative diseases, stroke or injury cannot be corrected by ordinary therapies such as organ transplantation. Grafting neural precursor cells may be one possible strategy to solve this problem of regenerating damaged nervous tissues.

Having the plasticity to transdifferentiate, ATSCs have been shown to acquire the potential to undergo neural differentiation. Even before any induction, undifferentiated MSCs, including ATSCs, already express neural progenitor markers such as Nestin, neuron-specific enolase (NSE) and Tuj-1 (Tondreau, et al 2004, Yang, et al 2004). To induce ATSCs into neurons, various protocols have been used, most involving the use of chemicals as induction agents. Similar to BMSCs (Woodbury, et al 2000), treatment of ATSCs with beta-mercaptoethanol (BME) resulted in rapid transition (in 30 minutes) of cells to a neuronal morphology with spherical cell bodies with multiple extensions (Zuk, et al 2002). The induced cells expressed early



neuronal markers including Nestin, neuron-specific enolase (NSE) and neuron-specific protein (NeuN). Similar results were also obtained using other inductive conditions such as indomethacin and isobutylmethylxanthine (Ashjian, et al 2003) or butylated hydroxyanisole (BHA) and forskolin (Safford, et al 2002b, Safford, et al 2004). In addition to Nestin, NSE and NeuN, expression of other neural markers such as Vimentin and Trk-A (a receptor of neural growth factor, NGF), GFAP, S-100, MAP2, Tau, h-III Tubulin were also detected or upregulated in the neural-induced ATSCs. Immunohistochemical analysis also revealed the presence of g-Aminobutyric acid (GABA), the NR-1 and NR-2 subunits of the glutamate receptor, GAP-43, synapsin I, and voltage-gated calcium channels in the induced ATSCs, raising the possibility of producing functional, mature neuronal cells (Safford, et al 2004).

Neural induction conditions using chemicals such as BME and BHA have been challenged by some reports (Bertani, et al 2005, Lu, et al 2004) suggesting that these rapid inductions (within minutes to hours) into neurons were likely due to cellular toxicity, cell shrinkage and changes in the cytoskeleton instead of a complicated cellular differentiation process. This was supported by the fact that time-lapse microscopy of the induced MSCs showed no new neurite growth but rather cellular shrinkage and retraction of the majority of existing cell extensions.



Besides, the neuronal induction using these protocols could also be reproduced in normal primary fibroblasts as well as mimicked by addition of drugs that elicit cytoskeletal collapse and disruption of focal adhesion contacts (Bertani, et al 2005).

In fact, neuronal differentiation cannot be concluded merely with neural-like morphology and the expression of some neural or glial markers. To confirm the genuine neuronal differentiation of adult stem cells, a demonstration of full neuronal functions through electrophysiology and complete neuronal gene expression is required. So far, all reports on *in vitro* neuronal differentiation of MSCs can only confirm the potential of these cells into neuronal progenitor cells. No group has succeeded in inducing MSCs, including ATSCs and BMSCs, into mature, functional neuronal cells *in vitro*. However, recent studies with ATSCs on their potential in *in vivo* neural repair are promising.

Several *in vivo* studies done by Kang et al. (Kang, et al 2003a, Kang, et al 2003b, Kang, et al 2006) suggested the clinical relevance and application for ATSCs. They first showed that human ATSCs may provide a supportive role for endogenous neural stem cells by co-culturing human ATSCs with mouse neural stem cells (NSCs) *in vitro*, supported by the result that the percentage of neurons in culture was significantly increased when compared to culture of NSCs alone. In another study they demonstrated that intracerebroventricular administration of neurally induced

human ATSC into rat brains resulted in cell migration to areas of ischemic injury. Significant recovery of motor and somatosensory behavior was found in transplanted animals, especially those with BDNF-transduced ATSCs. In their recent study (Kang, et al 2006), they confirmed the therapeutic effect of ATSC infusion in rat models of spinal cord injury. Intravenous infusion of the oligodendrocyte precursor cells derived from autologous rat ATSC improved the motor function in rats with spinal cord injury.

An *in vivo* study by another group (Jun, et al 2004) also showed that intraventricular injection of human ATSCs transfected with a retrovirus overexpressing the human telomerase gene, in ischemic rat brain, resulted in enhancement of functional recovery in these animals. In all these *in vivo* studies, significant functional recovery was exhibited after ATSC infusion in animal models. However, these functional improvements may be due to the release of trophic factors or cytokines by ATSCs instead of neuron formation. Nevertheless, these promising results strongly suggest the use of ATSCs as an alternative source of neuronal cells for treating disorders with neuronal function defects or neuron loss. Genetically engineered hATSCs expressing biologically active gene products can also act as effective vehicles for therapeutic gene transfer to the brain.

## 1.4 Signaling Pathways in Stem Cells

Inside the stem cell niche, multipotent stem cells are kept alive and undifferentiated by the physical contact between stem cells and their non-stem cell neighbors. The neighboring differentiated cell types form an extracellular matrix that secretes factors and support stem cells by keeping the balance between quiescence, self-renewal and cell commitment. Stem cell fates are regulated in a signal-dependent manner. To control the stemness and differentiation of stem cells, these growth factors act through multiple signaling pathways, including Wnt, Notch, transforming growth factor  $\beta$  (TGF $\beta$ ) and bone morphogenetic proteins (BMPs) signaling (Paratore, et al 2006).

### 1.4.1 Wnt Signaling

Wnt proteins play an important role in regulation of stem cell and differentiation (Cadigan, et al 1997). There are totally nineteen *Wnt* genes in mammalian genomes, and they give rise to proteins that participate in both gene transcription and cell adhesion. When Wnt signals bind the Frizzled receptors, the downstream signals lead to the accumulation of  $\beta$ -catenin.  $\beta$ -catenin is the central player of the canonical Wnt signaling pathway, and it is normally degraded in the absence of Wnt. The stabilization and accumulation of  $\beta$ -catenin results in the



formation of complex with TCF (T cell factor) and LEF (lymphoid enhancer factor). This complex activates many different target genes involved in cell development, maintenance of stemness in stem cells, as well as carcinogenesis. Cross-talk also occurs in the Wnt/ $\beta$ -catenin signaling with various other signaling pathways such as Notch, TGF $\beta$ , FGFs and Shh (De Strooper, et al 2001, Hecht, et al 2000, Nelson, et al 2004).

In undifferentiated ESCs, large-scale gene expression profiling revealed the expression of the main components of the canonical Wnt signaling pathway, which suggest a role of Wnt signaling in regulating stem cell stemness (Aubert, et al 2002, Sato, et al 2003). This was supported by an *in vitro* experiment that treatment of ESCs with GSK3 $\beta$  inhibitor that activated the canonical Wnt pathway and kept both mouse and human ESCs remain undifferentiated (Sato, et al 2004). Moreover, overexpression of Wnt1 or stabilized  $\beta$ -catenin in ESCs resulted in the inhibition of neural differentiation (Aubert, et al 2002, Haegel, et al 2003). Apart from ESCs, Wnt signaling is also important in other stem cells such as hematopoietic stem cells (HSCs) (Austin, et al 1997, Reya, et al 2003). Activation of the Wnt signal promotes HSC proliferation and limits their differentiation potential. This sustains the self-renewal of HSCs in long-term culture inside the bone marrow for later functional reconstitution of hematopoietic lineages *in vivo*.



### 1.4.2 Notch Signaling

The Notch signaling pathway is a highly conserved cell signaling system which is present in most multicellular organisms (Artavanis-Tsakonas, et al 1999, Harper, et al 2003, Lai 2004). In mammals, Notch possesses four receptors and is involved in various processes ranging from cell-fate specification, cell lineage decision to pattern formation. Once the notch receptors are activated by Delta-like ligands and Serrate-like ligands from neighboring cells, the pathway is initiated through the proteolytic cleavage of the Notch intracellular domain (NICD), recruitment of co-activators and expression of members of the Hairy enhancer of Split (HES) and HES-related (HERP) genes. These HES proteins participate in several lineage-specification processes by inhibiting the expression of lineage-specifying bHLH genes such as Neurogenins, MyoD and E2A (Iso, et al 2003). Cross-talk between Notch and TGF- $\beta$  signaling is common, by direct protein-protein interactions between the signal-transducing intracellular elements from both pathways such as *Hes-1* and Smad3 (Blokzijl, et al 2003). The converge of the two pathways occurs in differentiation of many cell types including myogenic, endothelial, pancreas and neural development (Blokzijl, et al 2003, Goumans, et al 2002, Kim, et al 2001, Shah, et al 1996a).

Like Wnt signaling, Notch signaling also has a role in maintaining stemness

of stem cells. In the central nervous system, reports have shown that activation of Notch signaling is associated with the inhibition of neuronal differentiation, whereas repression of Notch activity promotes neurogenesis (Artavanis-Tsakonas, et al 1999, Beatus, et al 1998). Similarly, interference with Notch signaling leads to premature neurogenesis and a depletion of the neural stem cell pool (Ishibashi, et al 1995, Lutolf, et al 2002, Nakamura, et al 2000).

### **1.4.3 Signaling Pathway of the TGF- $\beta$ Superfamily**

The TGF $\beta$  superfamily including TGF- $\beta$  isoforms, bone morphogenetic proteins (BMPs), activins and growth and differentiation factors (GDFs) are involved in many aspects of embryonic and adult development by regulating cell proliferation, differentiation and migration. They are also well-known for their capability to induce cartilage and bone formation in mammals (Wozney, et al 1988b). Activation of the TGF- $\beta$  receptors triggers the heterodimerization of type I and type II receptors and subsequent phosphorylation of specific SMAD proteins. These proteins then translocate into the nucleus and regulate the transcription of target genes (Shi, et al 2003, Zwijsen, et al 2003). Although there are only few receptors and SMADs in the TGF $\beta$  pathway, different combinatorial interactions between them can give rise to a great versatility of signaling.

In MSCs, members of TGF $\beta$  superfamily play an important role in regulating their differentiation. Extensive studies have been done on BMPs and shown that BMPs, including BMP2, BMP6 and BMP7, initiate, promote, and maintain chondrogenesis and osteogenesis in mesenchymal stem cells (Estes, et al 2006, Knippenberg, et al 2006). They induce specific transcription factors such as *Sox9*, *Dlx5* and *c-fos* that regulate the cell commitment into chondrogenic or osteogenic lineages (Shea, et al 2003).

In addition to cartilage and bone formation, BMPs are also involved in multiple processes during neural development in the CNS, including lineage commitment, proliferation, survival, apoptosis, differentiation and morphogenesis (Hogan 1996, Mehler, et al 1997). For example, BMP2, 4 and 7 are found to promote autonomic neurogenesis, both *in vitro* and *in vivo*, during the later stages of peripheral nervous system (PNS) development (Reissmann, et al 1996, Schneider, et al 1999, Shah, et al 1996b).

Like Wnt signaling, a recent study suggested that BMP4 might also support ESC self-renewal, probably through the MAPK pathways (Qi, et al 2004). It was supported by an experiment that introduced an inhibitor of the SMAD family members Smad6 and Smad7 and antagonized BMP signaling. This resulted in a decrease of self-renewal capacity of ESCs and induced differentiation (Ying, et al



2003).

### **1.5 Pathways Controlling Chondrogenesis**

Extensive studies have been done on the cellular and molecular mechanisms of chondrogenesis regulation. Many growth factors and cytokines are involved in cartilage development. Among them, the transforming growth factor-beta (TGF- $\beta$ ) superfamily is most widely studied (Centrella, et al 1991). BMPs, which are members of the TGF- $\beta$  superfamily, have proved to be important in chondrogenesis (Celeste, et al 1990, Wozney, et al 1988a). BMP-6 strongly upregulates the primary chondrogenic markers Aggrecan and Collagen Type II and, acting in a synergistic manner with TGF- $\beta$ 3, promotes chondrogenesis in MSCs (Estes, et al 2006, Indrawattana, et al 2004). BMP-7, which was found to have strong anabolic activity in young and adult cartilage (Chubinskaya, et al 2003), is also known to induce chondrogenesis in human and goat perichondrium tissue *in vitro* (Klein-Nulend, et al 1998, Nishihara, et al 2003). Treating ATSCs with recombinant BMP-7 upregulated important cartilage extracellular matrix proteoglycans aggrecan and biglycan and promoted chondrogenesis in the cells (Knippenberg, et al 2006). BMP-2 is identified in reports as an important regulator in osteogenesis (Knippenberg, et al 2006). However, many other reports have also demonstrated its role in the regulation and



promotion of chondrogenesis (Kim, et al 2003, Wei, et al 2006). In the TGF- $\beta$  signaling pathway, chondrogenic differentiation and maturation are mainly regulated through two pathways: TGF- $\beta$  signaling and BMP signaling (Chen, et al 1991, Fromigue, et al 1998, Suzuki 1992). Interplay of these two pathways determines the chondrocyte fate. TGF- $\beta$  promotes chondrogenesis by stimulating cell proliferation and matrix synthesis, but reversibly inhibits terminal differentiation of chondrocytes (Bohme, et al 1995, Kato, et al 1988, Serra, et al 1997). On the other hand, BMP stimulates DNA synthesis of chondrocytes and induces rapid maturation (Li, et al 2003, Nishihara, et al 2003). For both pathways, their effects on chondrogenesis involve SMAD activation. SMADs are a family of intracellular proteins that consist of three classes of signaling molecules: receptor-associated SMADs, the cofactor SMAD4 and the inhibitory SMADs (Heldin, et al 1997, Massague, et al 2000a, Massague, et al 2000b). Previous work has demonstrated that TGF- $\beta$ -related SMADs (SMAD2/3) inhibit chondrocyte maturation, whereas BMP-related SMADs (SMAD1/5/8) stimulate maturation (Ferguson, et al 2004, Li, et al 2003).

Besides BMPs, there are also other regulators that promote chondrogenesis, including fibroblast growth factors (FGF) (Awad, et al 2003, Stevens, et al 2004) and insulin-like growth factors (IGF) (Fukumoto, et al 2003b, Longobardi, et al 2006). In ATSCs, treatment of FGF-2 significantly upregulated Sox9, the critical transcription

factor for chondrogenesis, as well as two early mesenchymal condensation markers FGF-receptor 2 and N-Cadherin (Chiou, et al 2006). Expanding MSCs in the presence of FGF-2 enhanced the later chondrogenesis, possibly by selecting specific chondro-progenitors within the heterogeneous population of isolated MSCs (Chiou, et al 2006; Solchaga, et al 2005). IGF-1 has also been shown to significantly increase chondrogenesis in MSCs from bone marrow and periosteum (Fukumoto, et al 2003b, Longobardi, et al 2006). Both FGF-2 and IGF-1 most likely play supportive roles in chondrogenesis by acting in conjunction with TGF- $\beta$  (Centrella, et al 1994).

Although many pathways involved in chondrogenesis have been identified, there are more and more novel pathways and mediators being continually discovered. In fact, the control of chondrogenesis involves the interplay of complex gene networks. To control the rate and progression of the differentiation process, surely more than a single pathway is needed. A great interest has been aroused to completely dissect how all these networks interact but it will be a huge challenge. The recent discovery of a new gene regulator, microRNA, has suggested a novel mechanism to control chondrogenesis which allows previous questions to be answered.

## 1.6 MicroRNA

### 1.6.1 MicroRNA – A Novel Gene Regulator

MicroRNA (miRNA) is a novel class of small, non-coding RNAs of ~22 nucleotides. Although it was discovered just over a decade ago, miRNA has been recognized as one of the major regulatory gene families in eukaryotic cells. Nearly 1% of the predicted mammalian genes encode miRNAs (Lim, et al 2003). The first publication on miRNA appeared fourteen years ago by Victor Ambros and colleagues (Lee, et al 1993) in a screen for developmental timing mutants in *C. elegans*. They discovered that *lin-4*, a gene known to control the timing of *C. elegans* development, did not code for a protein but instead produced a pair of small non-coding RNAs, which were found later to be the first miRNA. Hundreds of miRNAs have been found in animals, plants and viruses. In humans, over 500 miRNAs have been identified, and certainly there are more to come. MicroRNAs regulate gene expression by mRNA degradation, or translational repression, or both. A miRNA can target numerous mRNAs. Several miRNAs can also act in combination on a specific target. Because of this, miRNAs offer a regulatory network with extremely high complexity.



### 1.6.2 Biogenesis of MicroRNAs

The maturation of miRNAs in animals is carried out in two steps, (i) the production of the miRNA precursors (pre-miRNAs) from the miRNA transcripts (pri-miRNAs), (ii) processing of pre-miRNAs to mature miRNAs (Fig. 1).

In the first step, miRNA genes are transcribed by RNA polymerase II (Pol II) to give long primary miRNA transcripts (pri-miRNAs) (Lee, et al 2004). The pri-miRNAs contain 7-methylguanosine caps and poly(A) tails, which are the unique properties of class II gene transcripts. They also contain a stem-loop structure which is then cleaved by the nuclear RNase III Droscha to give the precursor of miRNA (pre-miRNAs) (Lee, et al 2003). In the second step, the pre-miRNAs are exported out of the nucleus to the cytoplasm by exportin-5 (Exp5), which is a RanGTP-dependent dsRNA-binding protein which binds pre-miRNAs specifically in the presence of the Ran-GTP cofactor (Bohnsack, et al 2004, Kim 2004, Lund, et al 2004, Yi, et al 2003).

In cytoplasm, pre-miRNAs are then processed into ~22-nt miRNA duplexes by the cytoplasmic RNase III Dicer (Bernstein, et al 2001, Hutvagner, et al 2001, Ketting, et al 2001). The miRNA duplex will then quickly unwind and separate into two fragments. Usually only one strand of the duplex remains as the mature miRNAs, whereas the strand from the opposing arm, miRNA\*, disappears. The stabilities of



the two strands differ greatly that the recovery rate of miRNA\*s from endogenous tissues is ~100-fold lower than that of miRNAs (Schwarz, et al 2003).

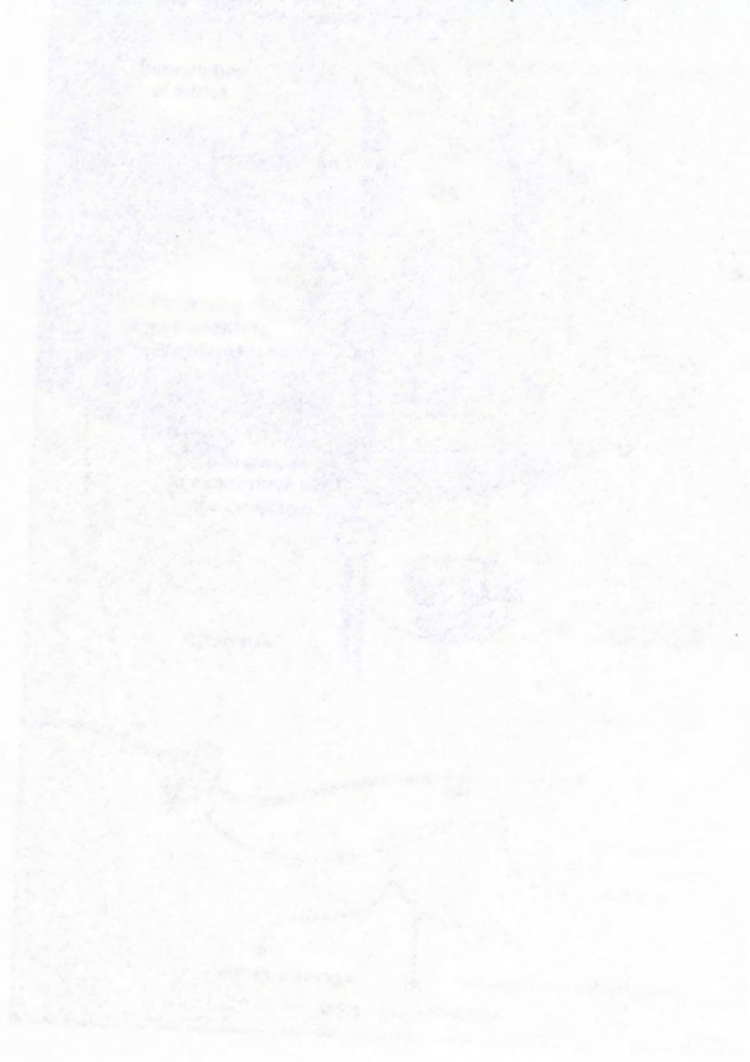
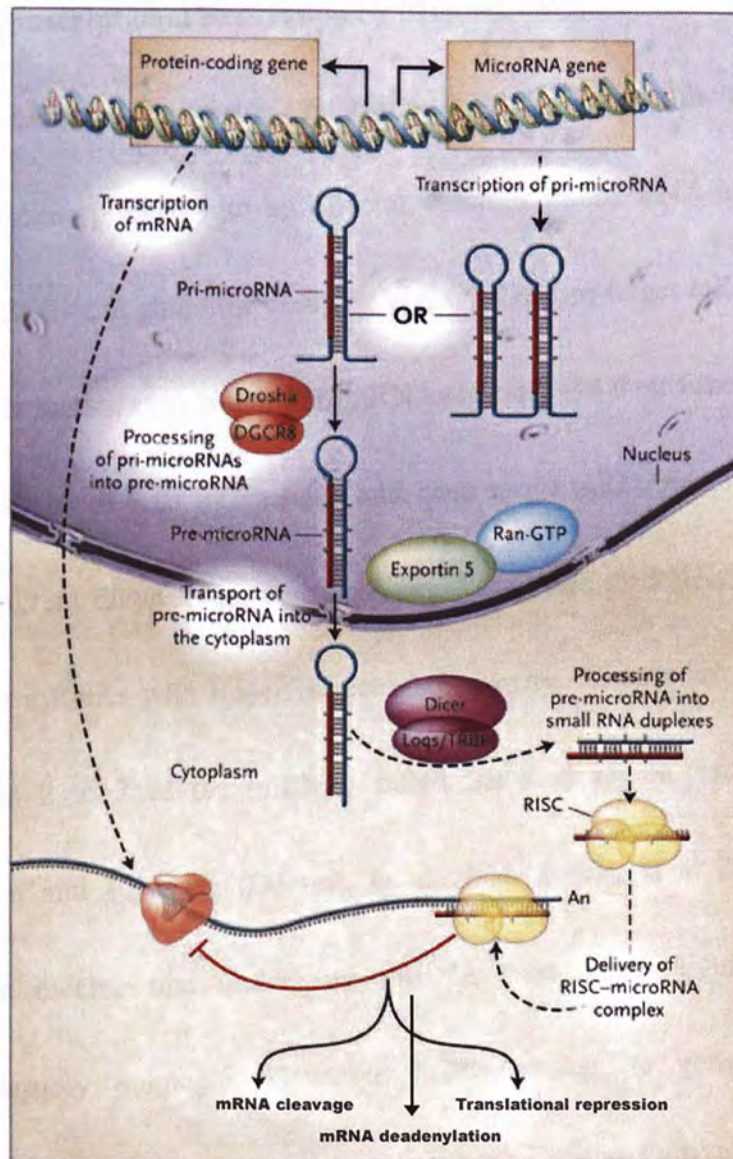


Fig. 1 Biogenesis of miRNA. miRNAs are transcribed from DNA by RNA polymerase II into primary miRNAs (pri-miRNAs) precursors. These pri-miRNAs are then processed in the nucleus into intermediate precursor miRNAs (pre-miRNAs) by the nuclear RNase III Drosha. The pre-miRNAs are then exported to the cytoplasm where they are processed by the RNase III Dicer into mature miRNAs. The mature miRNAs are then loaded into the RNA-induced silencing complex (RISC) and the miRNA guides the RISC to the target mRNA, leading to translational repression or mRNA degradation.



**Fig. 1 Biogenesis of MicroRNA** (modified from Chen 2005). The long primary miRNAs (pri-miRNAs) transcribed from the miRNA genes are processed in the nucleus into stem-loop precursors (pre-miRNA). The pre-miRNAs are then actively transported into the cytoplasm by exportin 5 and Ran-GTP and further processed into small RNA duplexes of approximately 22 nucleotides. The functional strand of the miRNA duplex is then loaded into the RNA-induced silencing complex (RISC) and the miRNA guides the RISC to the cognate mRNA target and regulates through translational repression, mRNA cleavage and mRNA deadenylation.

### 1.6.3 Post-transcriptional Repression by MicroRNAs

In similar fashion to small interfering RNAs (siRNAs), the mature miRNAs released are incorporated into an effector complex called RNA-induced silencing complex (RISC) and guide the complex to the 3'UTR of target mRNAs (Khvorova, et al 2003, Schwarz, et al 2003). For miRNAs to carry out their functions, a key issue is the specificity of their interactions with their target mRNAs and how interactions lead to different downstream consequences. In animals, miRNAs usually base pair with target mRNAs with imperfect complementarity. Reports have showed that the nucleotides 2 to 7 of the miRNA, called the seed region, is critical for target recognition and silencing (Doench, et al 2004, Lewis, et al 2005). The precise molecular mechanisms underlying miRNA post-transcriptional repression still remain largely unknown. However, miRNAs regulate genes by three main mechanisms: translational repression, mRNA cleavage and mRNA decay initiated by rapid deadenylation of mRNA.

Translational repression is the predominate mechanism in animals by which miRNAs negatively regulate their targets. It was first suggested by the observation that the lin-4 miRNA reduced the amount of lin-14 protein, without reducing the amount of the lin-14 mRNA (Lee, et al 1993, Wightman, et al 1993). Several reports have suggested that miRNAs may repress the mRNA translation by inhibition of



translation initiation, mainly supported by the accumulation of Argonaute proteins, miRNAs, and mRNA targets of miRNAs in P-bodies in a miRNA-dependent manner (Jakymiw, et al 2005, Liu, et al 2005, Pillai, et al 2005).

MicroRNAs can also control gene expression post-transcriptionally by directing endonuclease cleavage of the target mRNAs. The RISC identifies target mRNAs based on perfect or nearly perfect complementarity between the miRNAs, and the endonuclease of the RISC cleaves the mRNAs at a site near the middle of the miRNA complementarity (Elbashir, et al 2001a, Elbashir, et al 2001b). However, some reports have shown that extensive base-pairing between miRNAs and mRNAs may not always be sufficient to induce cleavage, suggesting other additional requirements for the endonucleolytic cleavage of the RISC complex, such as the presence of a specific Argonaute protein within RISC (Chen 2004, Liu, et al 2004).

Apart from the two well known mechanisms, translational repression and mRNA cleavage, recently a third mechanism of miRNA-directed gene regulation was proposed, namely mRNA deadenylation (Giraldez, et al 2006, Wu, et al 2006). A poly(A) tail is added to the 3' of the mRNA after mRNA transcription to enhance the stability mRNA and prevent mRNA decay (Coller, et al 2004). A report by Wu and colleagues, using miR-125b and let-7 as representative miRNAs, showed that miRNAs can reduce the concentration of mRNAs by accelerating mRNA



deadenylation, which leads to rapid mRNA decay (Wu, et al 2006). Through this mechanism, miRNA can regulate gene expression by reducing the concentration of target mRNA which is not perfectly or nearly-perfectly complementary to it (Wu, et al 2006).

#### **1.6.4 Role of MicroRNAs in Development**

Since the first discovery of miRNAs and their roles in gene regulation, researchers are eager to know the biological functions of miRNAs. MicroRNAs have been shown to play an important role in a wide variety of biological processes including cell cycle regulation, cell differentiation, apoptosis, maintenance of stemness and imprinting (Ambros 2004). Distinctive expression profiles of miRNAs were identified in different kinds of cells and tissue (Chen, et al 2007, Krichevsky, et al 2006a, Lee, et al 2007, Ryan, et al 2006, Sempere, et al 2004a, Suh, et al 2004, Tang, et al 2006, Tuddenham, et al 2006). These findings suggest that the expression of miRNAs is, not only spatiotemporal, but also tissue or cell-type specific, which imply their essential roles in developmental biology.

## **1.6.5 MicroRNAs in Stem Cell Differentiation**

### **1.6.5.1 MicroRNA Expression Profile in ESCs**

The miRNA expression profile of human and mouse ES cells have been well studied and unique sets of expressed miRNAs have been identified (Strauss, et al 2006, Suh, et al 2004, Tang, et al 2006). A study by Suh et al. describe 36 miRNAs identified by cDNA cloning in human ES cells (Suh, et al 2004). Most of them are specifically expressed in human ES cells and downregulated during embryoid body development. Some ES-specific miRNA genes are even organized as clusters and transcribed as polycistronic primary transcripts. These miRNA gene families have homologues in the mouse with similar genomic organizations and expression patterns, which suggests a conserved key regulatory network in mammalian pluripotent stem cells.

Dicer mutants have been commonly used in the study of miRNA functions in stem cells. Several studies have demonstrated the importance of dicer in ES cell differentiation. As demonstrated by three independent studies (Bernstein, et al 2003, Kanellopoulou, et al 2005, Murchison, et al 2005), dicer-null mice failed to process endogenous miRNAs and resulted in lethality in early mouse development as well as depletion of stem cells in mouse embryos. In dicer-deficient ES cells, severe defects were displayed in both proliferation and differentiation. These cells failed to

differentiate but only formed cell aggregates. These results strongly suggest a key role of endogenous miRNA processed by dicer in maintenance of embryonic development.

### **1.6.5.2 Lineage Differentiation**

Involvement of miRNAs has been identified in different lineage differentiation, such as neurogenesis, myogenesis, chondrogenesis, adipogenesis, angiogenesis, hematopoiesis and development of limb and epithelial cells (Chen, et al 2004, Chen, et al 2006, Esau, et al 2004, Harris, et al 2006, Hornstein, et al 2005, Krichevsky, et al 2006b, Naguibneva, et al 2006, Rao, et al 2006, Smirnova, et al 2005, Tuddenham, et al 2006, Yi, et al 2006). Here we focus on the differentiation of the neural, chondrogenic, myogenic and adiposal cell lineages.

#### ***Neurogenesis***

The expression profile of miRNAs in mammalian brain has been fully studied. A number of miRNAs are exclusively detected (miR-9, -124a, -124b, -135, -153, -219) or highly expressed (miR-9\*, -125a, -125b, -128, -132, -137, -139) in both human and mouse brain (Sempere, et al 2004b). These brain-specific and brain-enriched miRNAs are highly conserved in human and mouse, which suggest



their important role in mammalian neurogenesis.

Gain-of-function and loss-of-function approaches are commonly used to study the biological functions of these brain-specific miRNAs. A study showed that early overexpression of five brain-enrich miRNAs (miR-9, -9\*, -22, -124a, and -125b) in neural precursors reduced the number of Glial Fibrillary Acidic Protein (GFAP) positive cells (i.e. astrocytes) and slightly increased the number of Tuj1<sup>+</sup> cells (i.e. neurons) differentiated in culture. On the other hand, inhibition of miR-9 alone or in combination with miR-124a reduced the number of Tuj1<sup>+</sup> cells (neurons) in neural precursors (Krichevsky, et al 2006b). These results suggest a possible role of these miRNAs in neurogenesis and prevention of gliogenesis.

MicroRNA can also regulate dendritic spine development. A brain-specific miRNA, miR-134, negatively regulates the size of dentritic spines-postsynaptic sites of excitatory synaptic transmission, probably by translation suppression of Limk1, which is a protein kinase that controls spine development (Schratt, et al 2006).

### ***Chondrogenesis***

Not many studies have been done on the role of miRNAs in chondrogenesis. MicroRNA-140 was found to be specifically expressed in cartilagenous tissue using microarray and in situ hybridization in zebrafish embryos (Ason, et al 2006,



Wienholds, et al 2005). Based on these findings, the expression pattern of *miR-140* was further studied in mouse embryo. Similarly, miR-140 is also specifically expressed in cartilage tissues in mouse embryos during both long and flat bone development (Tuddenham, et al 2006). A regulator of chondrocyte hypertrophy, histone deacetylase 4 (HDAC4), was identified as a potential target of miR-140. After transfecting mouse 3T3 cells with siRNA-140 which targeting miR-140, the level of HDAC4 protein was found to be significantly down-regulated, while the level of HDAC4 protein remained unchanged for cells transfected with non-specific siRNA. Luciferase reporter assay also showed that a marked decrease in reporter activity occurred in mouse cells after siRNA-140 transfection (Tuddenham, et al 2006).

### ***Myogenesis***

Using northern blot and microarray, three microRNAs, miR-1, miR-133 and miR-206 were found to be enriched and specific in skeletal muscle and cardiac muscle of both human and mouse (Baskerville, et al 2005, Lagos-Quintana, et al 2002, Sempere, et al 2004c). Based on these findings, further studies were done to investigate the biological roles of these miRNAs. Using a gain-of-function approach, miR-1 (miR-1-1 and miR-1-2) was found to play a regulatory role in cardiomyocyte

proliferation in mouse (Zhao, et al 2005). Over-expression of miR-1 led to a significant decrease in the number of proliferating ventricular cardiomyocytes. In addition, over-expression of miR-1 also down-regulated Hand2 protein, which is a transcription factor that promotes ventricular cardiomyocyte expansion. This indicated that Hand2 was probably a target of miR-1. In the same study, a deletion assay showed that miR-1 genes are direct transcriptional targets of muscle differentiation regulators serum response factor, MyoD and Mef2, which further confirm the involvement of miR-1 in cardiogenesis.

MiR-1 and miR-133 are found to have distinct roles in proliferation and differentiation of skeletal muscle even though they are clustered on the same chromosomal loci and transcribed together (Chen, et al 2006). MiR-1 promotes myogenesis by targeting a transcriptional repressor of muscle gene expression histone deacetylase 4 (HDAC4), while miR-133 promotes myoblast proliferation by targeting serum response factor (SRF).

Another study by Rao et al. showed that the muscle-specific miRNAs: miR-1, miR-133 and miR-206 are significantly and specifically induced during myoblast-myotube transition, in both primary human myoblast and mouse mesenchymal stem cell line (Rao, et al 2006). Moreover, CHIP assay also demonstrated the activation of these miRNAs by the binding of the myogenic factors

Myogenin and MyoD to the upstream regions of the miRNA genes.

MiR-181 was also discovered to be involved in mammalian myoblast differentiation (Naguibneva, et al 2006). miR-181 is weakly expressed in adult muscle but is strongly upregulated in terminal muscle differentiation. In addition, knock down of miR-181 led to complete abolishment of myoblast differentiation. Hox-A11, which is a repressor of the myogenic differentiation process, was found to be the possible target of miR-181, based on the results that the protein level of Hox-A11 is inversely correlated to miR-181 expression.

### *Adipogenesis*

By combination of data from loss-of-function assay and miRNA microarray using cultured human pre-adipocytes, miR-143 was identified to participate in adipogenesis (Esau, et al 2004). Its expression was found to be increased in differentiating adipocytes. Inhibition of miR-143 significantly inhibited adipocyte differentiation. ERK5 protein was induced in adipocytes treated with antisense oligonucleotides (ASOs) complementary to miR-143, suggesting ERK5 as a possible target of miR-143.



## 1.7 Project Aims

Extensive studies have been done on the molecular characterization, proliferation capacity, multilineage differentiation potential and the immunogenicity of ATSCs. Promising results from the *in vivo* and pre-clinical studies have suggested that ATSCs represent one of the key stem cell types for tissue genesis, regeneration, and turnover. This notion has spawned the concept of regenerative medicine, or stem cell based therapies to supplement degenerating or damaged tissues. To ensure consistency of the stem cell's performance across different donors during future therapeutic uses, it is important to investigate factors influencing the yield or differentiation potential of the isolated ATSCs. Factors like age, region of adipose tissue used and tissue-harvesting procedure have been examined. However, the effect of the donor's reproductive and physiological status on the ATSC's performance has not been studied. Therefore, in this project, we first investigated the reproductive status and hormonal effect on the stem cell performance by comparing the cell yield and growth characteristics of ATSCs from donors at different reproductive status (pregnancy, pre-menopause and menopause).

The unique ability of ATSCs to self-renew and differentiate into multiple phenotypes implies that all stem cells might share a common transcriptional and miRNA signature. A better knowledge of the ATSC miRNA appears to be fundamental to fully achieve the potential of regenerative medicine. MiRNAs, though small, are recently found to be involved in the regulation of numerous biological processes including cell differentiation, cell proliferation and apoptosis. Elucidation of the microRNA expression profile and its molecular mechanisms which direct stem cell self-renewal and differentiation should provide key insights



into deciphering exactly how "stemness" is maintained, as well as the molecular basis of cell plasticity. Therefore, another aim of our project is, using ATSC-derived chondrocytes as a model, to investigate the involvement of miRNAs in stem cell differentiation. Candidate miRNAs identified were further investigated by functional studies using *in vitro* knock down and over-expression approaches.

### **1.8 Significance of Study**

This remarkable proliferation and differentiation capacity as well as their immunosuppressive property make ATSCs an excellent candidate for future regenerative medicine. Maintaining the consistency of the stem cell's performance across different donors will be an important concern for clinicians. By demonstrating the effect of donor's reproductive status on the differentiation power of ATSCs, the therapeutic uses of ATSCs can be further facilitated. Identifying miRNAs that are differentially expressed during stem cell differentiation provides new understanding of the molecular aspects and mechanisms regulating stem cell. The findings of miRNAs important in regulating chondrocyte differentiation and the identification of key pathways miRNAs act on give novel insights for stem cell research and cell therapy.

## **CHAPTER 2 MATERIALS AND METHODS**

### **2.1 Sample Collection**

Adipose tissue samples were obtained from abdomen of 15 women undergoing Caesarean section, vaginal hysterectomy (VH) and total abdominal hysterectomy (TAH). These 15 donors were divided into three groups according to their reproductive states: pregnancy, pre-menopause and menopause. Subjects with malignant tumors were excluded from this study.

### **2.2 Isolation and Culture of ATSCs**

To isolate human adipose tissue-derived stem cells (ATSCs), adipose tissues were washed extensively with sterile phosphate-buffered saline (PBS) to remove contaminants. Then the tissues were digested at 37°C for 1 hour with 0.075% type IV collagenase in plain Dulbecco's Modified Eagle Medium:Nutrient Mix F-12 (DMEM/F12). After digestion, cells released from the adipose tissues were collected by centrifugation at 1200g for 10 minutes. Then the pellet was resuspended with plain DMEM/F12 and centrifuged for another 10 minutes. Finally, the cells in pellet were seeded on 100mm plastic tissue culture dishes in control medium containing DMEM/F12, 10% fetal bovine serum (FBS), 100 units/ml penicillin, and 100µg/ml streptomycin. The cells were incubated in a humidified atmosphere of 5% CO<sub>2</sub> at 37°C. New control medium was replaced after 24 hours to remove residual non-adherent red blood cells. ATSCs were passaged five times prior to differentiation. All culture mediums and reagents were purchased from Gibco BRL Life Technologies, Inc. (Carlsbad, CA, USA).



### **2.3 Measurement of Cell Growth**

ATSCs were seeded in 6-well-plates at cell density of  $2.5 \times 10^4$  cells/well. Cells were counted every 3 or 4 days using a histocytometer for 2 weeks. A growth curve (cell numbers versus time) was plotted and the growth rate was the slope of the growth curve.

### **2.4 Effect of Estrogen Treatment on ATSC Proliferation**

ATSCs at passage 5 were seeded in 24-well-plate at a density of  $1 \times 10^4$  cells/well in DMEM/F12 medium plus 10% charcoal-treated FBS (Gibco). Before treatment, they were serum-starved for 24 hours. Then the cells were treated with 0 or  $10^{-8}$  mol/l of  $17\beta$ -estradiol (or E2) (Sigma, St. Louis, MO, USA) in DMEM/F12 medium with 2% charcoal-treated FBS for 9 days.

The proliferation rates of ATSCs with and without E2 treatment were compared. The cell proliferation was monitored by MTT assay at day 1 (1 day after plating), day 3, day 6 and day 9. At each timepoint,  $300 \mu\text{l}$ /well MTT reagent (Sigma) were added to cells from each well, 2 hours prior to harvest. The supernatant in all wells was removed, and the cells were treated with  $400 \mu\text{l}$ /well dimethylsulphoxide for 10 minutes. Reabsorbance at 570 nm, which is proportional to the number of living cells in each well, was recorded using an enzyme-linked immunosorbent assay plate reader and a growth curve of reabsorbance against day was plotted.

### **2.5 Multilineage Differentiation of ATSCs**

At passage 4 (one passage before induction), ATSCs were pretreated with 5ng/ml fibroblast growth factor-basic (bFGF) (Invitrogen, Carlsbad, CA, USA).

### **2.5.1 Chondrogenic Differentiation**

Chondrogenic differentiation was induced using the micromass culture technique (Ahrens, et al 1977). Ten microlitres of a concentrated ATSC suspension at concentration of  $1 \times 10^7$  cells/ml was plated into the center of each well and allowed to attach at 37°C for 3 hours. Chondrogenic medium containing DMEM/F12, 10% FBS, 10 ng/ml transforming growth factor- $\beta$ 1 (TGF- $\beta$ 1) (Sigma), 100 nM dexamethasone (Sigma), 6.25  $\mu$ g/ml insulin (Sigma), 50 nM ascorbate-2-phosphate (Sigma), 110 mg/l sodium pyruvate (Gibco) and 1% P/S was added gently on the cell nodules and the cells were collected after 3, 7, 14, 21 and 28 days of culturing.

### **2.5.2 Neural Differentiation**

To induce neural differentiation, plates and coverslips were first pre-coated with poly-L-lysine (0.01% w/v) (Sigma) for 2 hours then laminin (10ng/ml) overnight before cell seeding. Then ATSCs at passage 5 were seeded in 24-well-plates with coverslips at cell density of  $1 \times 10^4$  cells/well (for immunocytochemistry) and 6-well-plates with coverslips at cell density of  $3.5 \times 10^4$  cells/well (for RNA extraction) in control medium. On the next day, the control medium was replaced with neural medium containing  $\alpha$ -MEM, 2% FBS, 20ng/ml NGF (Nerve Growth Factor) 2.5S (Invitrogen), 50ng/ml NGF 7S (Invitrogen), 10ng/ml BDNF (Brain-derived Neurotrophic Factor) (Invitrogen), 1% P/S and collected on day 3, 7, 10 and 14. On day 7, the neurally differentiating ATSCs were split in a ratio of 1:3 and seeded again in pre-coated plates in neural medium for another 7 days.



## 2.6 Immunocytochemical Analysis of Surface Markers and Lineage Specific Markers

After differentiation, non-induced or induced cell, which are seeded in monolayer on coverslips, were collected and fixed in 4% buffered paraformaldehyde for 3 hours. Then they can be used directly for the immunostaining.

For ATSCs induced into the chondrogenic lineage, spheroids were formed during the micromass culture. Therefore, after they were fixed in 4% buffered paraformaldehyde overnight, the spheroids first needed to be dehydrated, embedded in parafilm blocks and cut into sections of 5nm before they were ready for immunostaining.

To perform the immunostaining, the monolayered cells on coverslips were permeabilized in 2.5% Triton X in PBS.T for 10mins; while sections of the spheroids had their antigens retrieved by microwaving at high power for 4 minutes in citrate buffer (pH 6.0). Then the cells were blocked in 3% bovine serum albumin at room temperature for 30 minutes. Then they were incubated at room temperature for 2 hours with the following antibodies.

- ◆ CD44 [BD Biosciences, mouse IgG, dilution 1:100]
- ◆ CD90 [BD Biosciences, mouse IgG, dilution 1:100]
- ◆ Anti-gial Fibrillary Acidic Protein (GFAP) [DAKO Corp., mouse IgG, dilution 1:100]
- ◆ Neuron-Specific Enolase (NSE) [Dako Corp., mouse IgG, dilution 1:100]
- ◆ Nestin [Chemicon International, Inc., rabbit IgG, dilution 1:500]
- ◆ Tau [Chemicon International, Inc., goat IgG, dilution 1:300]
- ◆ SOX9 [Chemicon International, Inc., rabbit IgG, dilution 1:130]
- ◆ Aggrecan [Santa Cruz Biotechnology, Inc., goat IgG, dilution 1:80]

- ◆ Collagen Type II [MP Biomedicals, Inc. mouse IgG, dilution 1:80]

Sequentially, the cells were then incubated for 1 hour with either anti-mouse Alexa 555 (Ex 555/Em 565, Invitrogen), anti-rabbit Alexa 488 (Ex 495/Em 519, Invitrogen) or anti-goat Alexa 555 (Ex 555/Em 565, Invitrogen) for immunofluorescent labeling. Sections were then mounted with ProLong Gold antifade mount with DAPI (Ex 358/Em 461, Invitrogen) and kept in 4°C for microscopy.

## **2.7 Alcian Blue Staining**

Cells after chondrogenic differentiation was first fixed with 4% buffered paraformaldehyde. Then they were stained in 1% aqueous Alcian Blue solution (Sigma) for 30 mins and washed in distilled water. After washing, the cells were dehydrated, cleared and mounted for microscopy. Non-induced ATSCs were used as control.

## **2.8 RNA Extraction**

Total RNA was extracted from differentiated ATSCs by Trizol Reagent (Molecular Research Center Inc, Cincinnati, Ohio). Cells were homogenized by adding 250µl Trizol Reagent per well and were frozen at -20°C overnight to ensure complete lysis. Next, the homogenate was thawed at room temperature for 5 minutes and 200µl of chloroform was added, followed by vigorous shaking for 15 seconds. The mixture was centrifuged at 12,000g for 15 minutes at 4°C. After the centrifugation, the aqueous phase (about 150µl) was transferred to a fresh tube and mixed with 125µl of isopropanol. It was left at room temperature for 10 minutes and



centrifuged at 12,000g for 10 minutes at 4°C. The RNA pellet was then washed with 250µl of 75% ethanol and subsequently centrifuged at 7,500g for 5 minutes at 4°C. The RNA pellet was air-dried for 15 minutes and the RNA was dissolved in 20 µl of DEPC-treated water.

The yield and purity of RNA were determined by spectrophotometry. An absorbance of 1 unit at 260 nm corresponds to 40 µg of RNA per ml of distilled water. The ratio between the absorbance values at 260 and 280 nm gives an estimate of RNA purity. For pure RNA, the A<sub>260</sub>/A<sub>280</sub> ratio should be close to 2.0.

## **2.9 Reverse Transcription**

Extracted RNA was reverse-transcribed to cDNA by SuperScript™ First-Strand Synthesis Kit (Invitrogen Life Technology, Carlsbad, California). For each sample, 100 ng total RNA, 100 ng random primers, and 1µl 10mM dNTP in 12 µl reaction mixture were first heated at 65°C for 5 minutes and quickly chilled in ice for 1 minute. 4 µl 5XFirst-Strand Buffer, 1µl 0.1M DTT, and 40 IU RNaseOUT and 200 IU SuperScript III reverse transcriptase were added to the reaction mixture. The reaction mixture was heated to 25°C for 5 minutes, 50°C for 50 minutes, and 70°C for 15 minutes.

## **2.10 Quantitative Real-time Polymerase Chain Reaction**

Primers for 6 lineage marker genes and a house-keeping gene were self-designed and purchased from Invitrogen Life Technology (Carlsbad, California) The primer sequences are summarized in the following table.



**Table 3 Primer sequences for lineage marker genes**

Marker Genes	Primer set	Tm (°C)	Product Size (bp)
Sox9 (SRY (sex determining region Y)-box 9)	Forward: 5'- TGC TCA AAG GCT ACG ACT GG -3' Reverse: 5'- GCG GCT GGT ACT TGT AAT CC -3'	60	291
COL2A1 (Collagen type II, alpha 1)	Forward: 5'- TGG TGG AGC AGC AAG AGC -3' Reverse: 5'- CAG GCG TAG GAA GGT CAT -3'	58	136
COL10A1 (Collagen type X, alpha 1)	Forward: 5'- CAC AGT TCT TCA TTC CCT AC -3' Reverse: 5'- CTG GTC CAA CAT CTC CTT T -3'	56	254
NEF3 (Neurofilament triplet M protein)	Forward: 5'-TGG GAA ATG GCT CGT CAT TT-3' Reverse: 5'-CTT CAT GGA AGC GGC CAA TT-3'	60	333
TUBB3 (Beta Tubulin III)	Forward: 5'- CAT GGA CAG TGT CCG CTC AG -3' Reverse: 5'- CAG GCA GTC GCA GTT TTC AC -3'	62	175
MAP2 (Microtubule-associated protein 2)	Forward: 5'- AGT CAG GGT CCC ACA GCG -3' Reverse: 5'- ATG CTC CTA TCA TCA TCT TGA G -3'	60	289
GAPDH - House Keeping Gene	Forward: 5'- GAA GGT GAA GGT CGG AGT C -3' Reverse: 5'- GAA GAT GGT GAT GGG ATT TC -3'	55	226

To check the transcript expression of the candidate genes and *GAPDH*, real-time PCR was performed thereafter in a 5  $\mu$ l volume of the final reaction solution containing 2  $\mu$ l of the RT reaction product (diluted at 1:20X), 2.5  $\mu$ l of 2X Power SYBR® Green PCR Master Mix (Applied Biosystems, Foster City, California), 0.25  $\mu$ l each of forward and reverse primers. The amplification conditions were: 95°C for 10 minutes, 45 cycles of 94°C for 30 seconds, 55-62°C for 1 minute, and 72°C for 30 seconds. The fluorescence signal emitted was collected by ABI PRISM® 7900HT Sequence Detection System and the signal was converted into numerical values by SDS 2.1 software (Applied Biosystems).

### **2.11 Statistical Analysis of Real-time PCR Data**

The expression level of a gene was first calculated from the Relative Standard Curve Method by the SDS 2.1 software. The threshold cycle ( $C_T$ ) value, which represents the relative expression of each target gene, was determined from the corresponding curve. Then the relative expression of each target gene was determined by dividing the target amount by *GAPDH* amount to obtain a normalized target value. Then the normalized values of the target genes were compared between induced and non-induced cells and across time points.

### **2.12 MicroRNA Profiling**

TaqMan® MicroRNA Assays, Human Panel Early Access Kit from Applied Biosystems was used in the microRNA profiling. The kit contains reverse transcription primers and TaqMan probes specific for 157 miRNAs.

### **2.12.1 Reverse Transcription**

Total RNA of the samples extracted by TRIZOL Reagent reverse-transcribed to cDNA using High Capacity cDNA archive kit (Applied Biosystems) following the manufacturer's protocol with little modification. One to five nanogram of the total RNA was used as the starting material according to manufacturer's protocol, but a total 5- $\mu$ l reaction volume protocol was applied, instead of a 15- $\mu$ l reaction volume protocol suggested by the manufacturer. The reverse transcription reaction mixture contain 0.05 $\mu$ l dNTP (100mM with dTTP), 0.35 $\mu$ l Reverse Transcriptase, 0.5 $\mu$ l Reverse Transcription Buffer, 0.063 $\mu$ l RNase Inhibitor (20U/ $\mu$ l), 1-5ng of extracted total RNA in 3.037 $\mu$ l DEPC-treated H<sub>2</sub>O and 1 $\mu$ l specific miRNA primer from the microRNA assay kit. The reaction condition for the reverse transcription was as follows: 16°C for 30 minutes, 42°C for 30 minutes, and 85°C for 5 minutes. cDNA products were then be diluted 3 fold by nuclease-free water.

### **2.12.2 Quantitative Real-time Polymerase Chain Reaction**

Transcript expressions of the miRNAs were quantified by performing real time PCR. The 5 $\mu$ l reaction mixture contained 1.4 $\mu$ l cDNA, 2.5 $\mu$ l TaqMan 2X Universal PCR Master Mix (Applied Biosystems), 0.5 $\mu$ l TaqMan probes from the microRNA assay kit and 0.6 $\mu$ l nuclease-free water. The amplification conditions were: 50°C for 2 minutes, 95°C for 10 minutes, 45 cycles of 95°C for 15 seconds, 60°C for 1 minute.



### 2.13 mRNA Target Prediction of MicroRNAs

A web-based database called miRGen *Targets* was used (<http://www.diana.pcbi.upenn.edu/cgi-bin/miRGen/v3/Targets.cgi>) to predict the potential mRNA targets of any miRNA.

### 2.14 MicroRNA Knockdown Assay

The anti-miR<sup>TM</sup> miRNA inhibitor against hsa-miR-199a was purchased from Ambion (Austin, TX, USA). Transfection of the microRNA inhibitor into ATSCs was performed using Lipofectamine<sup>TM</sup> 2000.  $5 \times 10^4$  cells/well were seeded in a 6-well plate and allowed overnight attachment. For each well of transfection, 1  $\mu$ l of 20  $\mu$ M miRNA inhibitor and 7.5  $\mu$ l of Lipofectamine<sup>TM</sup> 2000 reagent were diluted in 0.5ml of plain DMEM/F12 separately and mixed gently. Stealth<sup>TM</sup> RNAi negative control (Invitrogen) or lipofectamine alone were used as controls. After 5 minutes of incubation at room temperature, the diluted plasmid and Lipofectamine<sup>TM</sup> 2000 reagent were mixed and allowed to stand for 20 minutes at room temperature. Then growth media in the 6-well plate were aspirated and each well was replaced with 1 ml of DMEM/F12 containing the Lipofectamine<sup>TM</sup> 2000-DNA complex. After 8-hour incubation at 37°C, the Lipofectamine<sup>TM</sup> 2000-DNA complex was removed and replaced with fresh growth DMEM/F12 with the selection antibiotics Zeocin. The cells were then maintained overnight at 37°C.

To perform the microRNA knockdown assay during chondrogenic differentiation of ATSCs, similar protocols were used. However, before transfection, cells were first seeded in micromass culture and incubated at 37°C for 2 hours. Then the cells were transfected with the same protocols as previously mentioned. The cells were harvested at day 2, 3, 7 and 14 and the protein and mRNA expression level of

chondrogenic markers were assessed by immunostaining and real-time PCR respectively.

## 2.15 MicroRNA Over-expression Assay

### 2.15.1 Vector Amplification

#### 2.15.1.1 Transformation

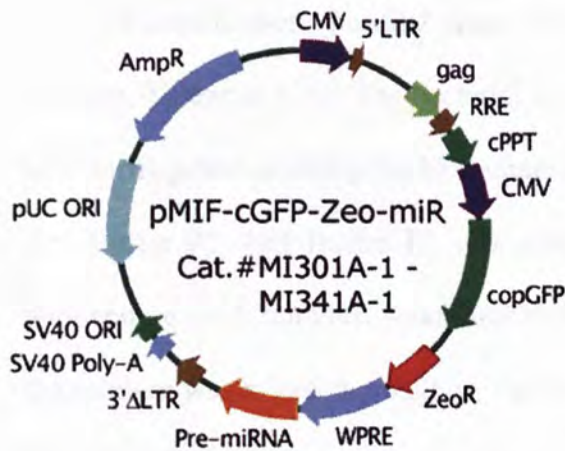


**Fig 2** The lentiviral vector containing the miR-199a-1 precursor

The construct pMIF-cGFP-Zeo-miR expressing precursor of has-miR-199a-1 (Fig.2) was purchased from System Biosciences (Mountain View, CA). To amplify the plasmid, they were first transformed into competent *E. coli* DH5 $\alpha$  strain by transient period of heat shock. 2 $\mu$ l of the purchased constructs were first mixed with 30 $\mu$ l of competent cells and incubated on ice for 30 minutes allowing the plasmids to attach on the competent cells. The mixture was then introduced to a heat shock period of 45 seconds at 42°C in which the extracellular plasmids rapidly influx into the bacterium. After the heat shock period, the mixture was stood on ice for another 2 minutes before recovery. 30 $\mu$ l of SOC medium (Invitrogen) was added to the



bacterium and the suspension mixture was allowed to recover at 37°C for 60 minutes with shaking. Then the transformed bacteria were plated onto LB agar plate (with 100 µg/ml ampicillin) and incubated at 37°C overnight. Single bacterial colony was then picked and inoculated in LB broth, with 100 µg/ml ampicillin at 37°C overnight for plasmid production.

#### **2.15.1.2 Purification of Plasmid DNA**

Plasmids were purified from bacteria using QIAfilter Plasmid Midi Kits (Qiagen, Valencia, CA). The bacterial cells in the overnight culture were harvested by centrifugation at 6000g for 15 minutes at 4°C. The pellet was then resuspended in 4ml Buffer P1. 4ml Buffer P2 was added to the mixture and incubated at room temperature for 5 minutes. Next, 4ml chilled Buffer P3 was added to the lysate and the mixture was mixed thoroughly. The lysate was then poured into the barrel of the QIAfilter Cartridge and was incubated at room temperature for 10 minutes. A plunger was gently inserted into the QIAfilter Cartridge and the cell lysate was filtered into a QBT-equilibrated QIAGEN-tip 100. The cleared lysate was allowed to enter the resin by gravity flow and the QIAGEN-tip was washed with 10ml Buffer QC twice. The purified DNA was then eluted with 5ml Buffer QF and precipitated with 3.5ml isopropanol. The mixture was mixed and centrifuged immediately at 15,000g for 30 minutes at 4°C. The supernatant was carefully decanted and the DNA pellet was washed with 2ml 70% ethanol followed by centrifugation at 15,000g for 10 minutes. After the supernatant was carefully decanted, the DNA was allowed to air-dry for 10 minutes and redissolved in 100µl sterilized water.



### **2.15.1.3 Confirmation of Construct Insertion**

Restriction enzyme digestion was performed to confirm the presence of construct in the plasmid. The reaction mixture contained 1µl restriction enzyme NheI (5U/µl) (New England Biolabs, Beverly, MA, USA), 1µl 10x Buffer2, 1.357µg purified plasmid, 1µl BSA(10x), 6µl sterilized water in a total volume of 10µl. The mixture was incubated at 37°C overnight. And the length of the linear construct was determined by gel electrophoresis. A band around 7300bp confirmed the presence of has-miR-199a-1 precursor constructs.

### **2.15.2 Transfection of Plasmid and Establishment of MicroRNA Precursor Expressing Cell Lines**

To establish an ATSC cell line expressing the miR-199a-1 precursor, the plasmid were transfected into ATSCs using Lipofectamine™ 2000.  $5 \times 10^4$  cells/well were seeded in a 6-well plate and allowed overnight attachment. For each well of transfection, 5 µg of plasmid and 7.5 µl of Lipofectamine™ 2000 reagent were diluted in 0.5ml of plain DMEM/F12 separately and mixed gently. After 5 minutes of incubation at room temperature, the diluted plasmid and Lipofectamine™ 2000 reagent were mixed and allowed to stand for 20 minutes at room temperature. Then growth media in the 6-well plate were aspirated and each well was replaced with 1 ml of DMEM/F12 containing the Lipofectamine™ 2000-DNA complex. After 8-hour incubation at 37°C, the Lipofectamine™ 2000-DNA complex was removed and replaced with fresh growth DMEM/F12 containing the selection antibiotics Zeocin (Invivogen, San Diego, CA) in a concentration of 150µg/ml. The cells were then maintained overnight at a 37°C incubator. After 24hours of recovery, the transfection efficiency was checked by the presence of green fluorescent signal from the

transfected cells under microscopy. The cells were cultured with necessary passage so as to select out the transfected cells.

## **2.16 Gene Expression Microarray**

To study the effect of miR-199a in gene expression of ATSCs, the cells were first transfected with anti-miR-199a inhibitor or miR-199a precursor construct for miR-199a knockdown or overexpression respectively. They were harvested 48 hours after transfection and their total RNAs were extracted using Trizol Reagent. And a microarray was performed to study the gene expression profiles of these samples, using the protocol of One-Color Microarray-Based Gene Expression Analysis by Agilent Technologies (Santa Clara , CA 95051, USA)

### **2.16.1 Preparation of Amplification and Labeling Reaction**

For each sample, 500ng of total RNA extracted by Trizol Reagent was used. 1.2µl of T7 Promoter Primer was added to the RNA and the mixture was topped up to 11.5µl using nuclease-free water. Then the RNA template and primer in the mixture were denatured at 65°C for 10 minutes followed by quick chill on ice for 5 minutes. A cDNA Master Mix with total volume of 8.5µl containing 4µl of 5X First Strand Buffer, 2µl of 0.1M DTT, 1µl of 10mM dNTP mix, 1µl of MMLV-RT and 0.5µl of RNaseOut was added to the each sample and mixed gently. Then the samples were incubated at 40°C for 2 hours, 65°C for 15 minutes and cooled in ice for another 5 minutes. Next, a Transcription Master Mix with total volume of 60µl containing 20µl of 4X Transcription Buffer, 6µl of 0.1M DTT, 8µl of NTP mix, 6.4µl of PEG, 0.5µl of RNaseOut, 0.6µl of inorganic pyrophosphatase, 0.8µl of T7 RNA



Polymerase, 2.4 $\mu$ l of Cyanine 3-CTP and 15.3 $\mu$ l of nuclease-free water was added to each sample and the mixture was incubated at 40°C for 2 hours.

### **2.16.2 Purification of the Labeled/Amplified RNA**

For each cRNA sample prepared from the previous step, 20 $\mu$ l of nuclease-free water was added to a total volume of 100 $\mu$ l. Then 350 $\mu$ l of Buffer RLT and 250 $\mu$ l of ethanol (96-100%) was added to the sample and they were mixed gently. The sample was then applied to an RNeasy® Mini column and centrifuged at 4°C for 30 seconds at 13,000rpm. 500 $\mu$ l of buffer RPE was added to the column and centrifuged at 4°C for 30 seconds at 13,000rpm for RNA washing. Another 500  $\mu$ l of buffer RPE was added to the column and centrifuged at 4°C for 60 seconds at 13,000rpm. To elute the cleaned cRNA sample, 30 $\mu$ l of RNase-free water was applied directly onto the RNeasy filter membrane and centrifuged at 4°C for 30 seconds at 13,000rpm. The cRNA yield was determined by measuring the absorbance at 260nm using NanoDrop® ND-1000 UV-Vis Spectrophotometer. The quality of purified and labeled cRNA was checked by 2100 Bioanalyzer RNA 6000 Series II Pico kits.

### **2.16.3 RNA Fragmentation**

For a 4x44K microarray, the fragmentation mix was prepared from 1.65 $\mu$ g cyanine 3-labeled, linearly amplified cRNA, 11 $\mu$ l 10X blocking agent, 2.2 $\mu$ l 25X Fragmentation Buffer and nuclease-free water to a final volume of 55 $\mu$ l. The reaction mixture was incubated at 60°C for 30 minutes. After the fragmentation, 55 $\mu$ l of 2X GX Hybridization Buffer HI-RPM was added to stop the reaction.



#### **2.16.4 Hybridization**

For the hybridization, the Agilent SureHyb chamber was used. 100µl of the hybridization sample was slowly dispensed onto the gasket well and the 4x44K microarray was gently placed on the gasket slide and was tightened on the chamber. The array was slowly rotated at 10rpm and allowed to hybridize at 65°C for 17 hours in the Hybridization Oven.

#### **2.16.5 Array Washing and Scanning**

After hybridization, the slide was first washed with Gene Expression Wash Buffer 1 at room temperature for 1 minute and then with Gene Expression Wash Buffer 2 at 37°C for another minute. Then the slide was washed in acetonitrile at room temperature for 1 minute followed by stabilization and drying solution for 30 seconds. The slide was removed from the final wash slowly to prevent water droplet retention on the array. Finally the slide was spun at 400 x g for 3 minutes to further removed water droplets from the slide.

After the washing, the array was scanned by Agilent DNA Microarray Scanner, Model G2565BA, at 5µm. The intensities of the scanned images were digitized into numerical values by using Agilent Feature Extraction Software Version 9.5.3.

#### **2.16.6 Statistical Analysis of Microarray Data**

The microarray data was analyzed by the software Genespring GX version 7.3.1 (<http://www.chem.agilent.com/scripts/pds.asp?lpage=27881>). The data was normalized by intensity dependent (Lowess) normalization and statistically significant genes were determined using parametric test in Colvano plot, with 2-fold

cut off (for over-expression) or 0.5-fold cut off (for knockdown) and p-value equal to 0.05. KEGG pathway imported into the Genespring software was used to study the pathways involved by those differentially expressed genes.

### 3.1 Isolation and Characterization of ATSCs

In total 15 adipose samples were collected from 15 unrelated women undergoing Gynaecology section, VH and TAH. Among the 15 donors, two were parous and five were pregnant and six were pre-menopausal (Table 4). ATSCs from the human adipose tissues were successfully isolated and cultured. On the day after isolation, approximately  $1 \times 10^6$  adipogenic cells were yielded from each fat sample, and the yield varied with the size of tissue collected. The cells were maintained in DMEM/F12 growth medium with 10% FBS and could be expanded easily in vitro.

Isolated ATSCs exhibited a fibroblast-like morphology (Fig. 3A) and were similar to mesenchymal stem cells [14] that other nature people have reported. However, their morphology may change along passage. Some of the cells may exhibit a distinct, larger, squamous morphology with obvious contractile filaments (Fig. 3B). Immunocytochemistry was performed against CD44, CD90, CD105, CD133, CD147, CD166, CD184, CD188, CD200, CD244, CD268, CD271, CD274, CD281, CD300, CD309, CD319, CD320, CD325, CD326, CD327, CD328, CD329, CD330, CD331, CD332, CD333, CD334, CD335, CD336, CD337, CD338, CD339, CD340, CD341, CD342, CD343, CD344, CD345, CD346, CD347, CD348, CD349, CD350, CD351, CD352, CD353, CD354, CD355, CD356, CD357, CD358, CD359, CD360, CD361, CD362, CD363, CD364, CD365, CD366, CD367, CD368, CD369, CD370, CD371, CD372, CD373, CD374, CD375, CD376, CD377, CD378, CD379, CD380, CD381, CD382, CD383, CD384, CD385, CD386, CD387, CD388, CD389, CD390, CD391, CD392, CD393, CD394, CD395, CD396, CD397, CD398, CD399, CD400, CD401, CD402, CD403, CD404, CD405, CD406, CD407, CD408, CD409, CD410, CD411, CD412, CD413, CD414, CD415, CD416, CD417, CD418, CD419, CD420, CD421, CD422, CD423, CD424, CD425, CD426, CD427, CD428, CD429, CD430, CD431, CD432, CD433, CD434, CD435, CD436, CD437, CD438, CD439, CD440, CD441, CD442, CD443, CD444, CD445, CD446, CD447, CD448, CD449, CD450, CD451, CD452, CD453, CD454, CD455, CD456, CD457, CD458, CD459, CD460, CD461, CD462, CD463, CD464, CD465, CD466, CD467, CD468, CD469, CD470, CD471, CD472, CD473, CD474, CD475, CD476, CD477, CD478, CD479, CD480, CD481, CD482, CD483, CD484, CD485, CD486, CD487, CD488, CD489, CD490, CD491, CD492, CD493, CD494, CD495, CD496, CD497, CD498, CD499, CD500, CD501, CD502, CD503, CD504, CD505, CD506, CD507, CD508, CD509, CD510, CD511, CD512, CD513, CD514, CD515, CD516, CD517, CD518, CD519, CD520, CD521, CD522, CD523, CD524, CD525, CD526, CD527, CD528, CD529, CD530, CD531, CD532, CD533, CD534, CD535, CD536, CD537, CD538, CD539, CD540, CD541, CD542, CD543, CD544, CD545, CD546, CD547, CD548, CD549, CD550, CD551, CD552, CD553, CD554, CD555, CD556, CD557, CD558, CD559, CD560, CD561, CD562, CD563, CD564, CD565, CD566, CD567, CD568, CD569, CD570, CD571, CD572, CD573, CD574, CD575, CD576, CD577, CD578, CD579, CD580, CD581, CD582, CD583, CD584, CD585, CD586, CD587, CD588, CD589, CD590, CD591, CD592, CD593, CD594, CD595, CD596, CD597, CD598, CD599, CD600, CD601, CD602, CD603, CD604, CD605, CD606, CD607, CD608, CD609, CD610, CD611, CD612, CD613, CD614, CD615, CD616, CD617, CD618, CD619, CD620, CD621, CD622, CD623, CD624, CD625, CD626, CD627, CD628, CD629, CD630, CD631, CD632, CD633, CD634, CD635, CD636, CD637, CD638, CD639, CD640, CD641, CD642, CD643, CD644, CD645, CD646, CD647, CD648, CD649, CD650, CD651, CD652, CD653, CD654, CD655, CD656, CD657, CD658, CD659, CD660, CD661, CD662, CD663, CD664, CD665, CD666, CD667, CD668, CD669, CD670, CD671, CD672, CD673, CD674, CD675, CD676, CD677, CD678, CD679, CD680, CD681, CD682, CD683, CD684, CD685, CD686, CD687, CD688, CD689, CD690, CD691, CD692, CD693, CD694, CD695, CD696, CD697, CD698, CD699, CD700, CD701, CD702, CD703, CD704, CD705, CD706, CD707, CD708, CD709, CD710, CD711, CD712, CD713, CD714, CD715, CD716, CD717, CD718, CD719, CD720, CD721, CD722, CD723, CD724, CD725, CD726, CD727, CD728, CD729, CD730, CD731, CD732, CD733, CD734, CD735, CD736, CD737, CD738, CD739, CD740, CD741, CD742, CD743, CD744, CD745, CD746, CD747, CD748, CD749, CD750, CD751, CD752, CD753, CD754, CD755, CD756, CD757, CD758, CD759, CD760, CD761, CD762, CD763, CD764, CD765, CD766, CD767, CD768, CD769, CD770, CD771, CD772, CD773, CD774, CD775, CD776, CD777, CD778, CD779, CD780, CD781, CD782, CD783, CD784, CD785, CD786, CD787, CD788, CD789, CD790, CD791, CD792, CD793, CD794, CD795, CD796, CD797, CD798, CD799, CD800, CD801, CD802, CD803, CD804, CD805, CD806, CD807, CD808, CD809, CD810, CD811, CD812, CD813, CD814, CD815, CD816, CD817, CD818, CD819, CD820, CD821, CD822, CD823, CD824, CD825, CD826, CD827, CD828, CD829, CD830, CD831, CD832, CD833, CD834, CD835, CD836, CD837, CD838, CD839, CD840, CD841, CD842, CD843, CD844, CD845, CD846, CD847, CD848, CD849, CD850, CD851, CD852, CD853, CD854, CD855, CD856, CD857, CD858, CD859, CD860, CD861, CD862, CD863, CD864, CD865, CD866, CD867, CD868, CD869, CD870, CD871, CD872, CD873, CD874, CD875, CD876, CD877, CD878, CD879, CD880, CD881, CD882, CD883, CD884, CD885, CD886, CD887, CD888, CD889, CD890, CD891, CD892, CD893, CD894, CD895, CD896, CD897, CD898, CD899, CD900, CD901, CD902, CD903, CD904, CD905, CD906, CD907, CD908, CD909, CD910, CD911, CD912, CD913, CD914, CD915, CD916, CD917, CD918, CD919, CD920, CD921, CD922, CD923, CD924, CD925, CD926, CD927, CD928, CD929, CD930, CD931, CD932, CD933, CD934, CD935, CD936, CD937, CD938, CD939, CD940, CD941, CD942, CD943, CD944, CD945, CD946, CD947, CD948, CD949, CD950, CD951, CD952, CD953, CD954, CD955, CD956, CD957, CD958, CD959, CD960, CD961, CD962, CD963, CD964, CD965, CD966, CD967, CD968, CD969, CD970, CD971, CD972, CD973, CD974, CD975, CD976, CD977, CD978, CD979, CD980, CD981, CD982, CD983, CD984, CD985, CD986, CD987, CD988, CD989, CD990, CD991, CD992, CD993, CD994, CD995, CD996, CD997, CD998, CD999, CD1000.

## CHAPTER 3 RESULTS

### **3.1 Isolation and Characterization of ATSCs**

In total 15 adipose samples were collected from 15 un-related women undergoing Caesarean section, VH and TAH. Among the 15 donors, four were menopausal, five were pregnant and six were pre-menopausal (Table 4). ATSCs from the human adipose tissues were successfully isolated and cultured. On the day after isolation, approximately  $1 \times 10^5$  nucleated cells were yielded from each fat sample, but the yield varied with the size of tissue collected. The cells were maintained in DMEM/F12 growth medium with 10% FBS and could be expanded easily *in vitro*.

Isolated ATSCs exhibited a fibroblast-like morphology (Fig.3A), which is similar to mesenchymal stem cells from other tissues previously reported. However, their morphology may change along passage. Some of the cells may exhibit a flatter, bigger, squamous morphology with obvious cytoskeleton (Fig. 3B). Immunocytochemistry was performed against two mesenchymal stem cell markers, CD44 and CD90, to confirm the MSC nature of the isolated cells. All of the cells expressed CD44 (Fig. 4A). Most of the cells also expressed CD90, but their expression intensity was lower and varied in different samples (Fig. 4B).



Groups	Pregnancy	Pre-menopause	Menopause
# of sample collected	5	6	4
Average Age (yr)	38.7 ( $\pm$ 0.6)	35.3 ( $\pm$ 15.5)	59.25 ( $\pm$ 12.01)

Table 4 Summary of adipose tissue samples collected from three groups of individuals.

Fig. 3 (A) Morphology of ATSCs derived from various adipose tissue under light microscopy (x100) is illustrated. (B) Some ATSCs may exhibit a flatter, bigger, squamous morphology with cytoplasmic vacuoles (arrow). (C) Hematoxylin and eosin staining of ATSCs (scale = 100  $\mu$ m).

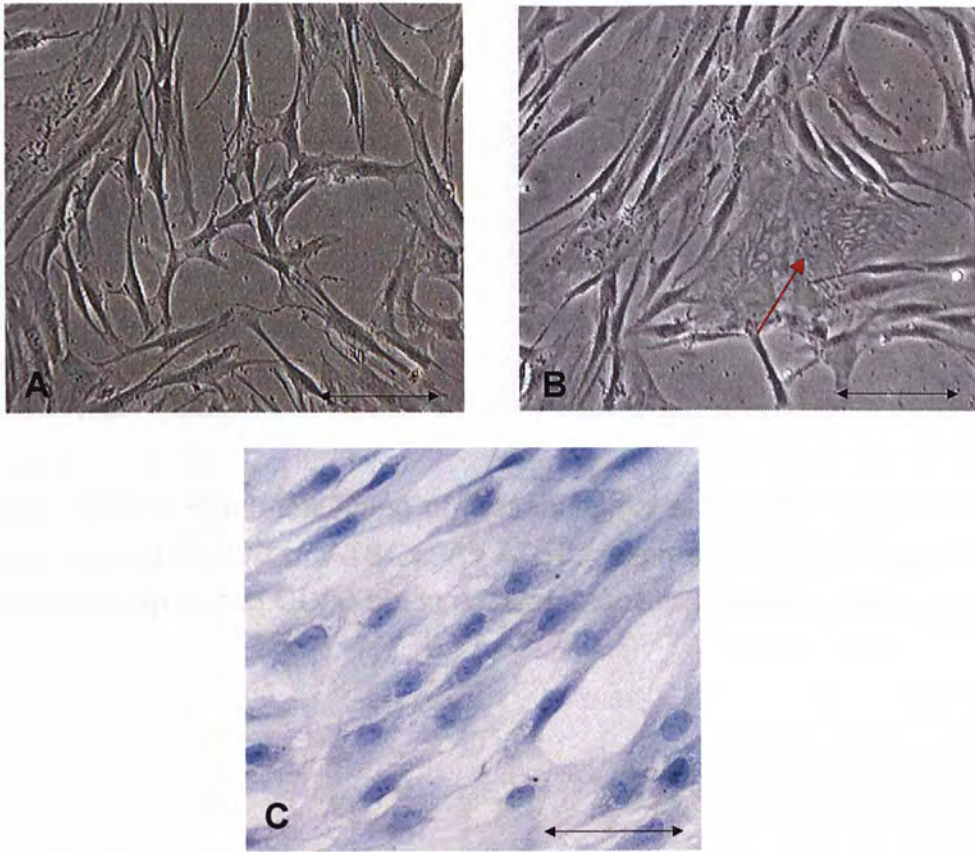


Fig. 3 (A) Morphology of ATSCs derived from human adipose tissue under light microscopy (x100) is fibroblast-like. (B) Some ATSCs may exhibit a flatter, bigger, squamous morphology with cytoskeleton obviously seen (arrow). (C) Hematoxylin and eosin staining of ATSCs (Scale = 100  $\mu$ m)

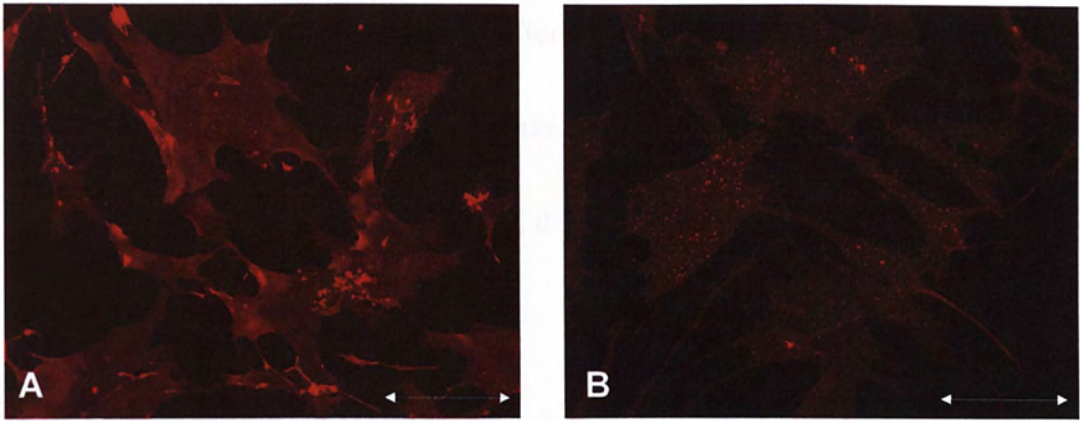


Fig. 4 Positive immunostaining of mesenchymal stem cell markers (A) CD44 and (B) CD90 of ATSCs. All ATSCs expressed CD44. Most of them also expressed CD90 but in a lower intensity. (Scale = 100  $\mu$ m)



### **3.2 ATSCs Exhibited Multilineage Differentiation**

To examine the multilineage differentiation capacity of ATSCs, the cells were induced towards chondrogenic or neural differentiation.

#### **3.2.1 Chondrogenic Differentiation**

For chondrogenic differentiation, ATSCs were induced in Micromass Culture with chondrogenic medium containing TGF- $\beta$  and dexamethasone for 28 days. As soon as one day after cell seeding, the cells started to aggregate into a three-dimensional spherical structure (Fig. 5B). The spheroids formed, which were about 1mm in diameter, were clearly visible to the naked eye in the tissue culture dish. Each sample was performed in duplicate; they all appeared identical in shape and size within the same sample. In each well, only one spheroid was formed, regardless of the length of treatment time.

In the control set, cells were also seeded in micromass culture, but they were grown in ATSC growth medium instead of chondrogenic medium. A multilayer, three-dimensional structure was also formed in the control cells. However, they could only form a semi-spheroid structure (Fig. 5A). Cells were loosely packed and the semi-spheroid formed was flatter and spread out. Outside the spheroid, monolayer cells attached on the wells continued to grow and confluence was reached

after one week. In contrast, ATSC induced into chondrogenic lineage proliferated at a much slower rate than control and histological examination showed that inside the spheroid, chondrogenic differentiating cells were more densely packed (Fig.5). Light microscope examination revealed that as ATSCs continued to differentiate, the spheroid contracted and was more firmly packed. In addition, cells on the outer edge of the induced spheroid acquired a more elongated, bipolar shape (Fig.5 C & D).

### **3.2.2 Expression of Chondrogenic Markers**

To confirm the success of chondrogenic differentiation, quantitative real-time PCR and immunohistochemical analysis were performed to assess the expression of lineage specific markers. Immunostaining against chondrogenic markers revealed the translocation of SOX9 in the nuclei and the accumulation of Collagen Type II and Aggrecan on the outer edge of the spheroids (Fig. 6). Chondrogenic differentiated ATSCs have a significantly higher (7 to 15 folds increment) mRNA expression of chondrogenic markers *SOX9*, *COL2A1* and *COL10A1* compared to controls (Fig. 7). The results of real-time PCR also showed a time-dependent manner in the expression profile of these markers. The *SOX9* and *COL2A1* transcripts were expressed in the early stage and peaked at Day 14 of the differentiation while *COL10A1* was expressed highly in the later stage (Day 28). Alcian Blue staining was also performed



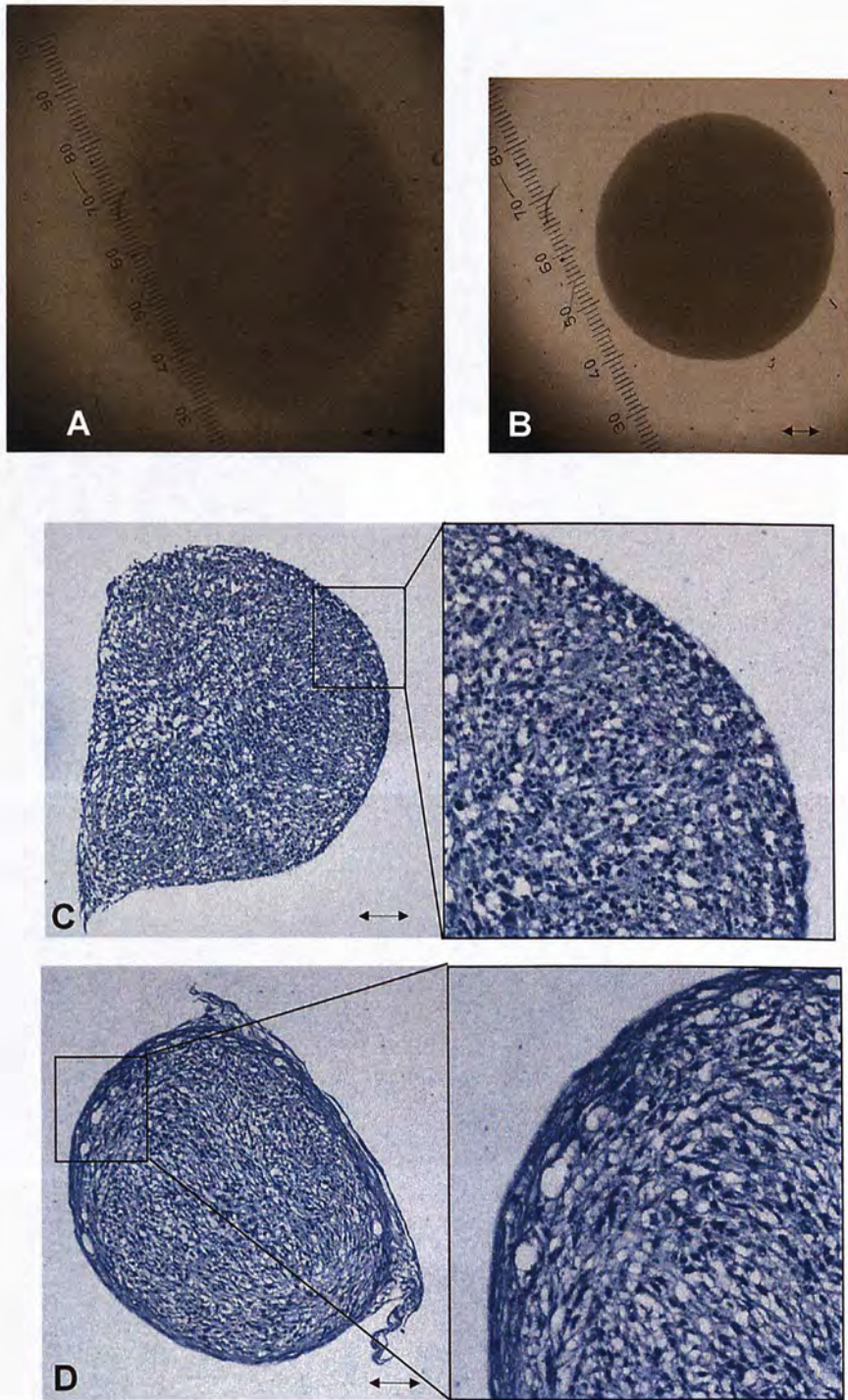


Fig. 5 Morphology of spheroids formed in micromass culture in (A) normal growth medium and (B) chondrogenic medium. Spheroids formed in chondrogenic medium were firmly packed and exhibited a perfect spherical shape. Hematoxylin staining of (C) non-induced spheroid and (D) chondrogenic induced-spheroid. (Scale = 100  $\mu$  m)



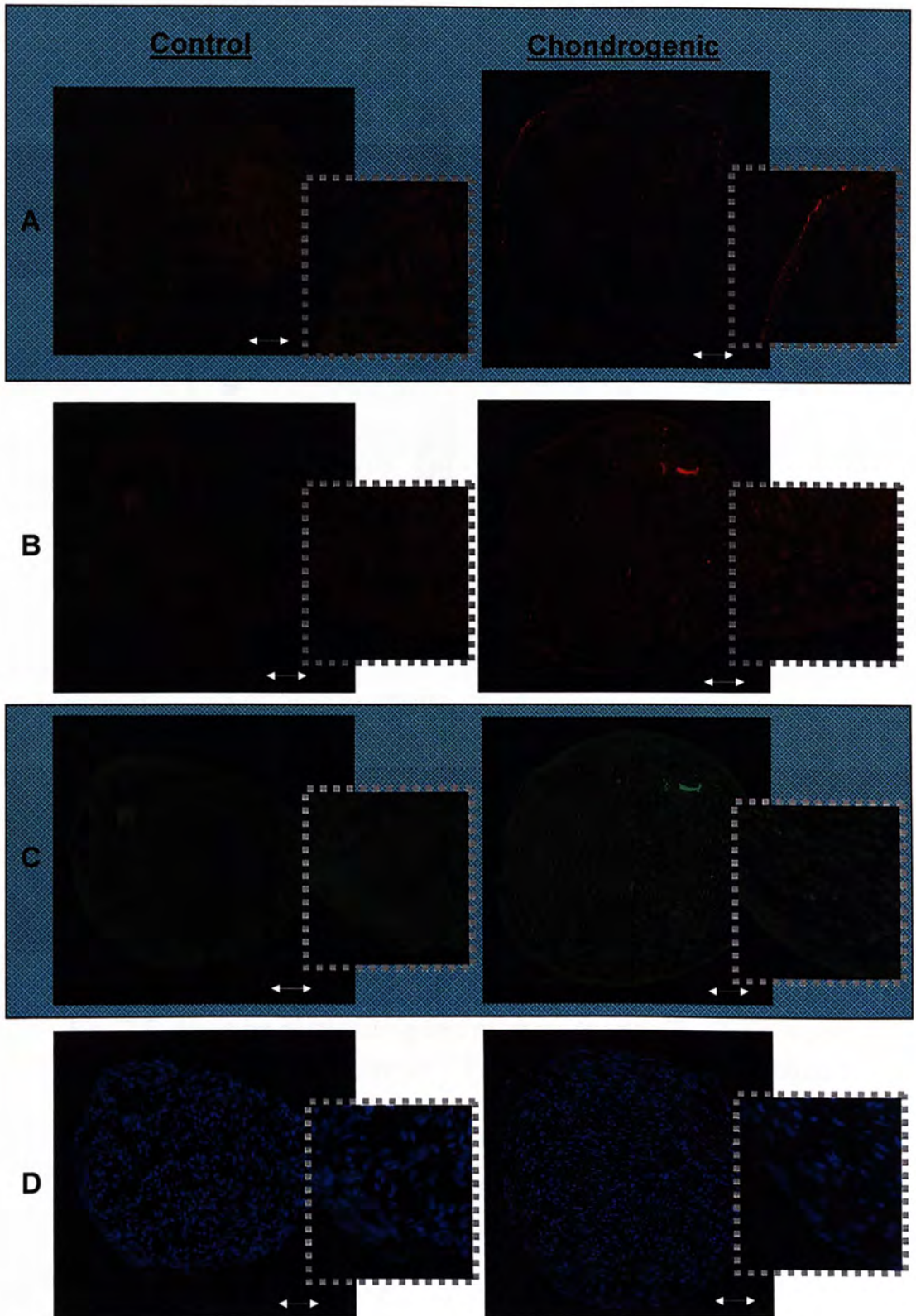
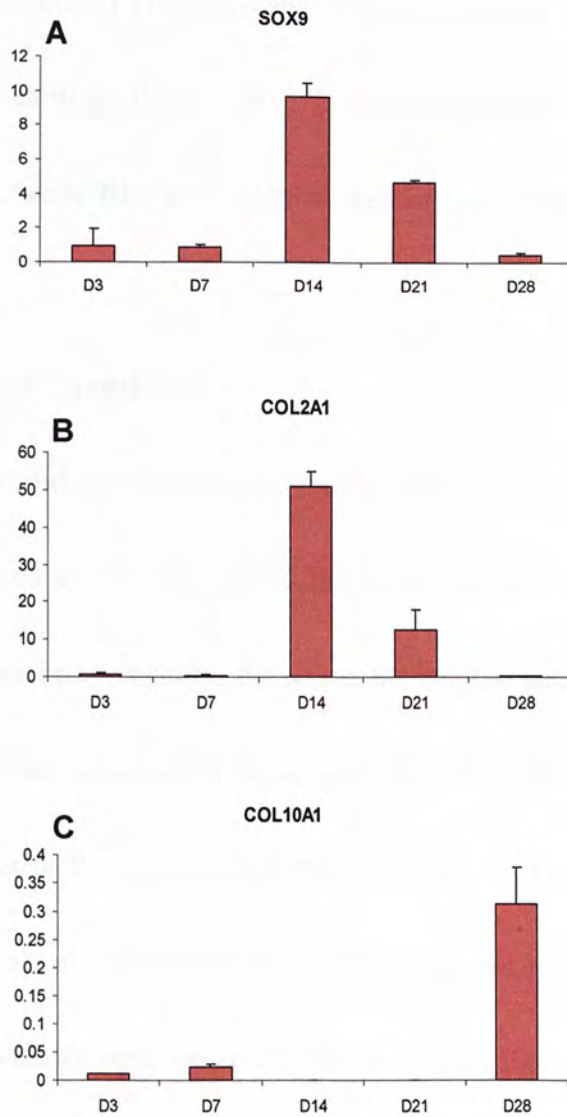


Fig. 6 Immunostaining of spheroids in control and chondrogenic medium against chondrogenic markers (A) Aggrecan, (B) Collagen Type II and (C) Sox9 as well as (D) nucleus staining DAPI. Chondrogenic markers expressed in chondrogenic induced-spheroid but weakly or not expressed in control. (Scale = 100 $\mu$ m)



**Fig. 7** Expression of chondrogenic markers (A) SOX9, (B) Collagen Type II and (C) Collagen Type X during chondrogenic differentiation of ATSCs normalized with GAPDH. Their expressions were time-dependent. *SOX9* and *COL2A1*, which are early chondrogenic markers, expressed in the middle of the differentiation. *COL10A1*, which is a late marker, expressed in the late stage of the differentiation.

to test the presence of proteoglycans, which is normally secreted in the extracellular matrix of the cartilage (Fig. 8). ATSCs differentiated into chondrocytes were stained positive with Alcian Blue with a higher intensity than control.

### **3.2.3 Neural Differentiation**

ATSCs could differentiate into neural cell by inducing in neural medium for 14 days. Compared to control, cell proliferation rate was slowed down in the neural medium. About one week after induction, the induced cells started to exhibit a neural appearance. They acquired a more fibroblast-like morphology with cytoplasmic retraction towards the nucleus (Fig. 9B). With increased time, the cell bodies became increasingly spherical and refractile, and multiple neurite-like cytoplasmic extensions extending outwards were observed. We monitored the induced cells until 24 days after induction, and they remained vital. In the control group, cells grew in ATSC growth medium instead of neural medium. They proliferated at a much faster speed and acquired a bigger, flatter morphology without any neural characteristics (Fig. 9A).



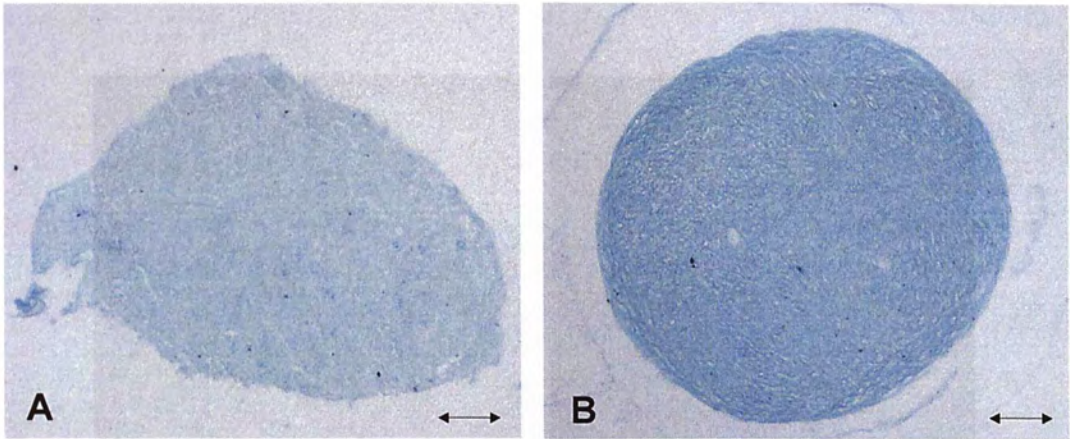


Fig. 8 Alcian Blue staining of spheroids in (A) non-induced and (B) chondrogenic medium. Chondrogenic induced-spheroids were stained positive with Alcian Blue with a higher intensity than control. (Scale = 100  $\mu$  m)

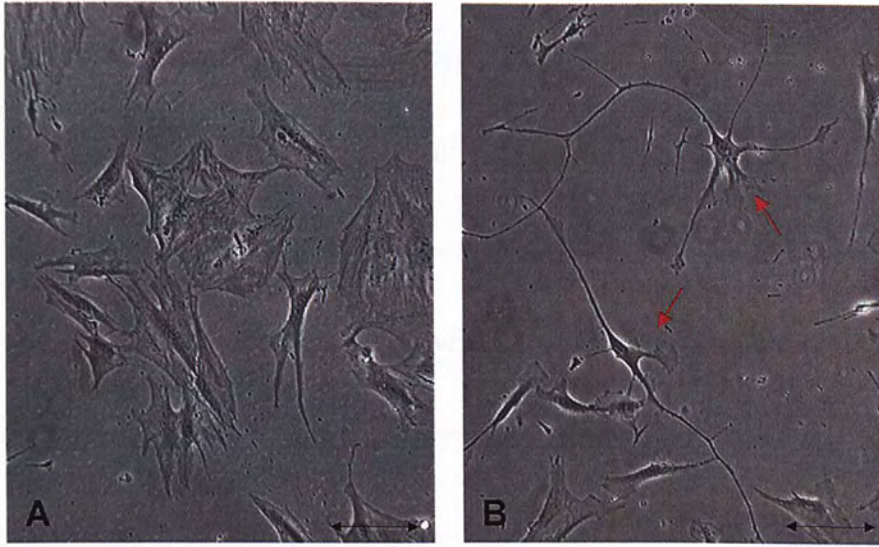


Fig. 9 Morphology of (A) non-induced and (B) neurally induced ATSCs in culture. Neurally induced ATSCs (arrow) acquired a typical neural morphology with small, round cell bodies and multiple cytoplasmic extensions. (Scale = 100  $\mu$ m)

### **3.2.4 Expression of Neural Markers**

Immunohistochemistry and real-time PCR against neural markers were performed to confirm the establishment of neurons differentiated from ATSCs (Fig. 10 & 11). After neural differentiation, the cells express neuronal progenitor markers *Nestin* and *GFAP*, early markers *NSE*, *NEF3* and *TUBB3*, and late markers *MAP2* and *TAU*. Real-time PCR revealed an increasing trend of *NEF3* and *TUBB3* mRNA expression along the induction and highest expression levels were reached on Day 14. Undifferentiated ATSCs also expressed progenitor markers and some early markers at a lower level, but they lacked the expression of late neuronal markers.

### **3.3 Effect of Donor's Reproductive Status on the Proliferation and Differentiation Capacity of ATSCs**

The ATSCs from the 15 samples were classified into three different groups according to their respective reproductive states (pregnancy, pre-menopause and menopause). We further compared their proliferation and differentiation capacities using chondrogenic lineage differentiation as a model.



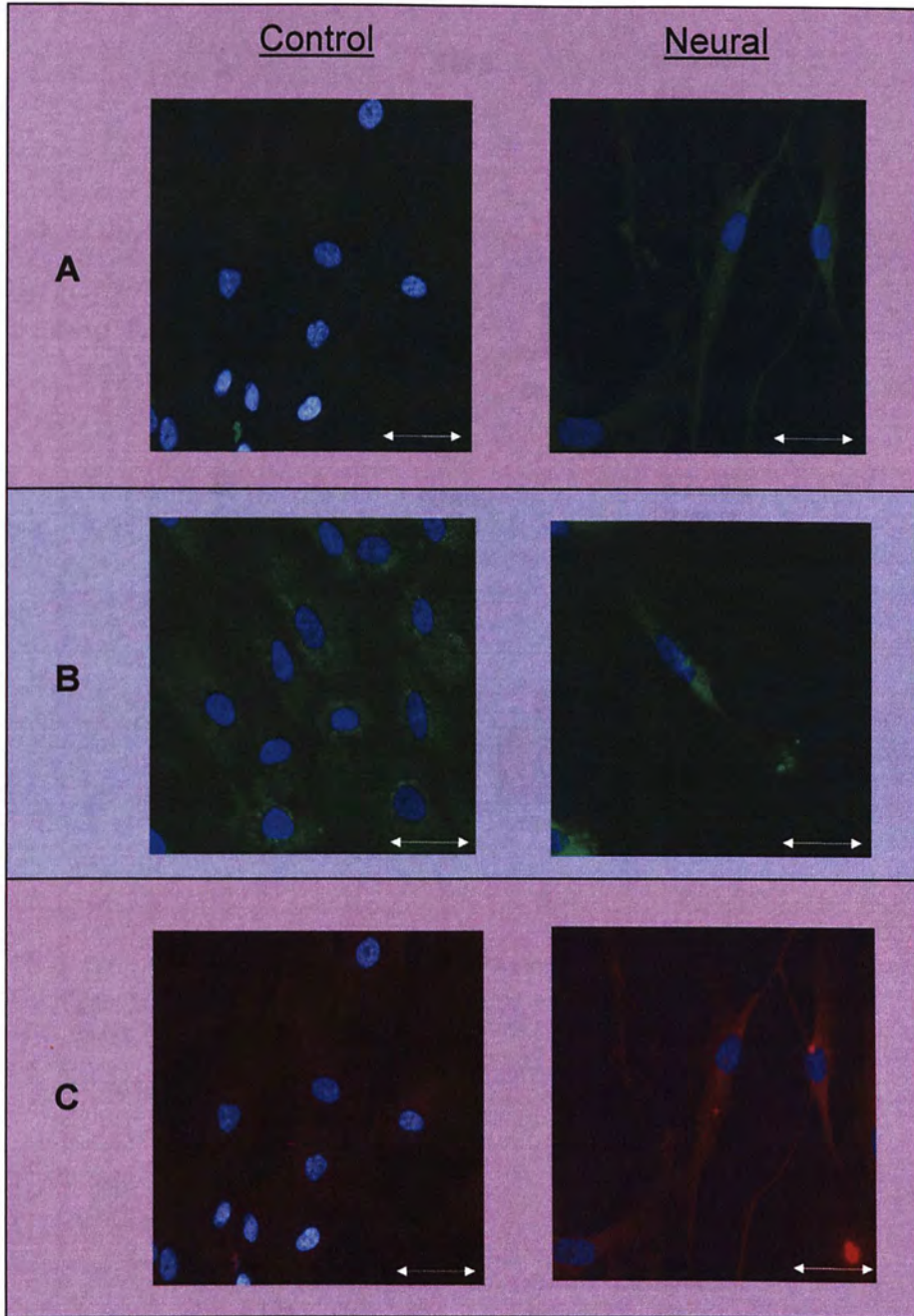


Fig. 10 Immunostaining of ATSCs in control and neural medium against neural markers (A) Nestin, (B) NSE and (C) TAU counterstained with DAPI. Neural markers expressed in neurally induced ATSCs. Except NSE, they weakly or not expressed in control except NSE. (Scale = 50  $\mu$ m)

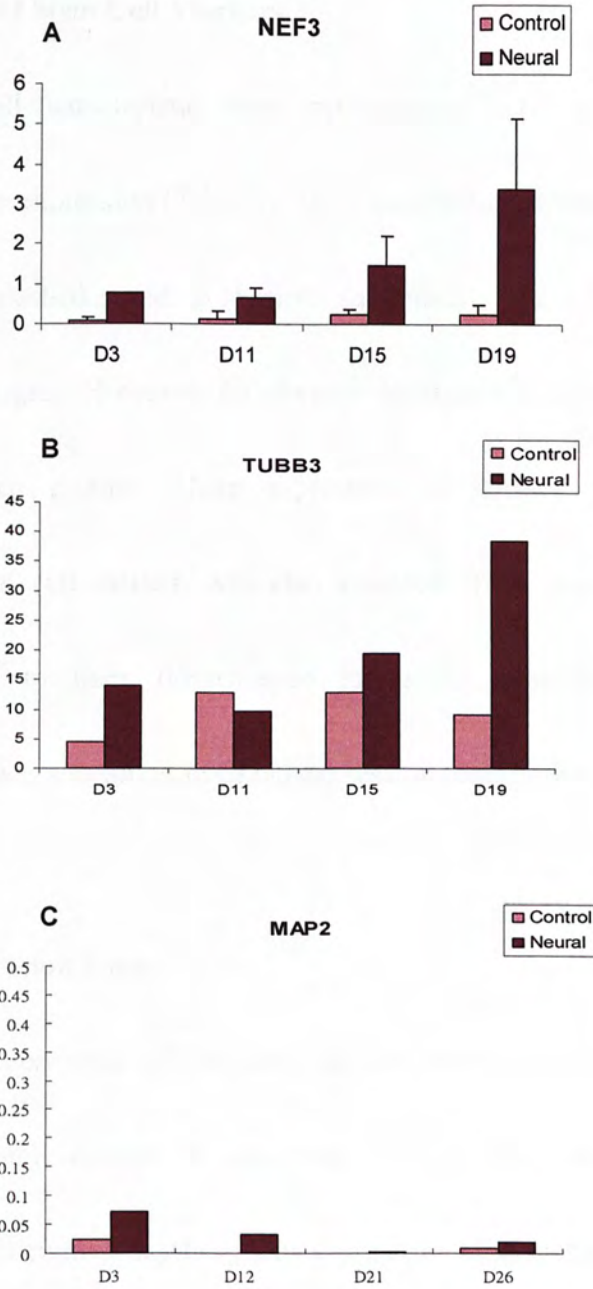


Fig. 11 Real-time PCR revealed a higher expression of early neural markers (A) NEF3, (B) TUBB3 and (C) late neural markers MAP2 in neurally induced ATSCs compared to control. Data was normalized with GAPDH.

### **3.3.1 Expression of Stem Cell Markers**

Their stem cell characteristics were first compared in terms of their morphology and surface marker expression (Table 5). Their morphologies were scored from 1 to 5 (1 is most fibroblast-like and 5 is most squamous). The 15 samples exhibited different morphologies. However, no obvious difference in morphology was found between the three groups. Their expression of surface protein CD90, the mesenchymal stem cell marker, was also assessed. Their expression levels were scored according to their fluorescence intensities after immunostaining. No significant difference was found in CD90 expression level between the three groups.

### **3.3.2 Cell Proliferation Assay**

The proliferation rates of the three groups were compared by cell count to investigate the total number of surviving ATSCs. The cell proliferation was monitored every alternative day from Day 1 (one day after plating) to Day 21. Using non-parametric Kruskal-Wallis test, the proliferation rate of the pregnancy group was significantly higher than the other two groups ( $p < 0.05$ ) (Fig. 12).



<u>Physiological State</u>	<u>Sample</u>	<u>Growth Rate</u> (cell no. / time)	<u>CD90 Intensity</u> + Weakest ++++ Strongest	<u>Morphology</u> Squamous ↔ Fibroblastic 1 ↔ 5
<b>Pregnancy</b>	P-1	2.5	+	4
	P-2	1.0317	++++	5
	P-3	0.8215	++	2
	P-4	0.3461	++	3
	P-5	1.2679	+	1
<b>Menopause</b>	M-1	1.2331	++	5
	M-2	0.6214	+++	2
	M-3	0.8308	++	2
	M-4	0.5347	+	2
<b>Pre-menopause</b>	PM-1	0.4971	++++	1
	PM-2	0.5329	++	4
	PM-3	0.3275	++++	3
	PM-4	0.4477	++	1
	PM-5	0.2379	++	2
	PM-6	0.4737	+++	1



Table 5 Table summarized the growth rate, CD90 expression intensity and morphology of ATSCs derived from three reproductive groups.

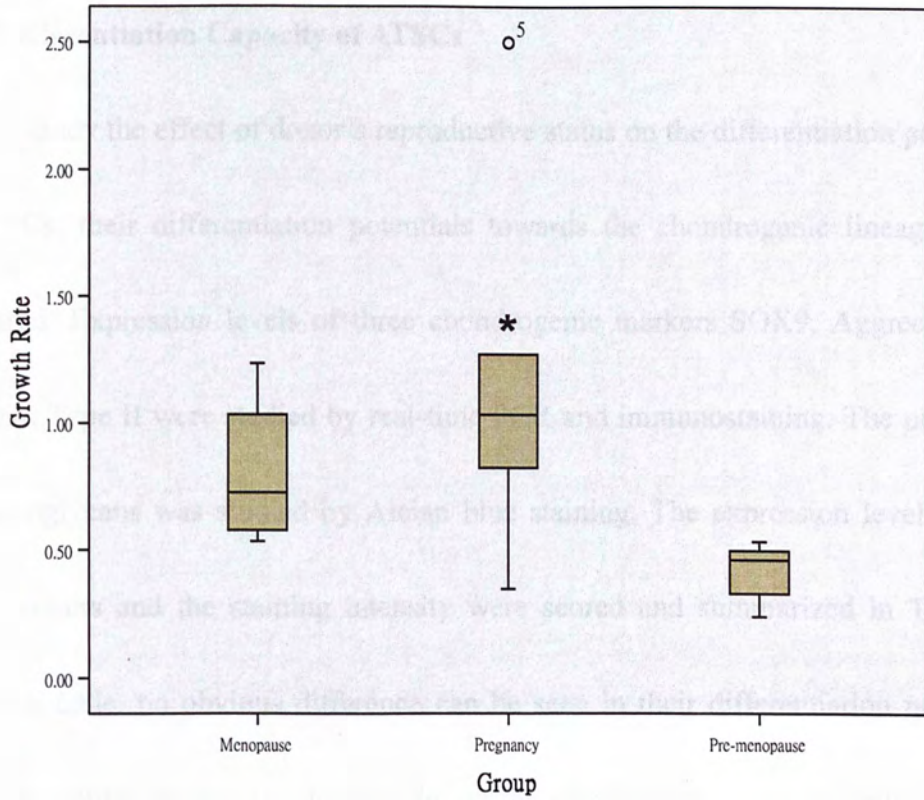


Fig. 12 Boxplot comparing the growth rates of ATSCs derived from the three reproductive groups. Growth rate of the pregnancy group is significantly higher than the other two groups (Kruskal-Wallis Test,  $p < 0.05$ ).

### **3.3.3 Differentiation Capacity of ATSCs**

To study the effect of donor's reproductive status on the differentiation potential of ATSCs, their differentiation potentials towards the chondrogenic lineage were compared. Expression levels of three chondrogenic markers SOX9, Aggrecan and Collagen Type II were studied by real-time PCR and immunostaining. The presence of proteoglycans was studied by Alcian blue staining. The expression level of the three markers and the staining intensity were scored and summarized in Table 6. From the table, no obvious difference can be seen in their differentiation potential among the three groups. In addition, due to the small sample size, no statistical test was significant for their comparison.

### **3.4 Effect of E2 Treatment on the Proliferation Rate of ATSCs**

To determine whether the higher proliferation rate in the pregnancy group was due to the higher level of estrogen in pregnant women, the effect of E2 treatment on the ATSC proliferation was studied by MTT assay. The growth rates of ATSCs with and without E2 treatment were compared. By comparing the slope of the growth curve, our result showed that there was no significant difference between the two groups of samples (data not shown). In addition, no significant up-regulations of *ERalpha* and *ERbeta* were found in either E2-treated or control ATSCs (data not shown).



Physiological State	Sample	% of Spheroid Formation		IHC			Alcian Blue Staining
		Control	Chondrogenic	SOX9	COL2A1	AGGRECAN	
Pregnancy	P-1	100	100	+	+	+++	++
	P-2	100	100	+	+/-	+++	++
	P-3	39	43	+	+/-	++	++
	P-4	0	0				
	P-5	100	100	+	+	+++	+
Menopause	M-1	54	77	+/-	-	+	+
	M-2	21	80	++	++	+++	++
	M-3	50	4	+/-	+/-	+	+
	M-4	100	100	+	+/-	++	+
Pre-menopause	PM-1	0	43	+	+/-	+++	+
	PM-2	4	59	+	++	+++	+
	PM-3	100	95	+	+	+++	++
	PM-4	0	12.5	+	+	++	++
	PM-5	100	96	+/-	+/-	+	++
	PM-6	95	100	+	+	++	+

Table 6 Comparison of the chondrogenic differentiation capacity of ATSCs from three reproductive groups in terms of the percentage of spheroid formation, expression intensity of immunostaining of chondrogenic markers and staining intensity of Alcian Blue.

### **3.5 MicroRNA**

#### **3.5.1 MicroRNA Expression Profile of Undifferentiated and Chondrogenic Differentiated ATSCs**

A quantitative real-time PCR based assay was used to establish the expression profiles of 157 miRNAs in 3 ATSC samples subjected to chondrogenic differentiated or left undifferentiated. Their miRNA expression levels were normalized by three endogenous control miRNAs *hsa-let-7a*, *hsa-miR-16* and small nuclear RNA *U6* (Fig. 13). Among the 157 miRNAs, 104 and 95 miRNAs were consistently expressed in undifferentiated and differentiated ATSCs respectively. Overall, the miRNA expression profiles between the differentiated and undifferentiated ATSCs of the same individuals were similar.

#### **3.5.2 Clustering Analysis Identified MicroRNAs Segregate with ATSCs**

To assess whether the expression patterns of the 157 miRNAs characterize ATSCs from other cell types, a bootstrap resampling analysis was conducted comparing undifferentiated and chondrogenic differentiated ATSCs with microRNA data generated in our lab by other team member (Tang Tao) including two normal cervix epithelium samples (L226 and L229) and 5 cervical cancer cell lines (C33A, HeLa, CC3, ME180 and Siha) (Fig. 14). Using data after global median-normalization,

hierarchical clustering successfully discriminated the ATSC samples from the cervix tissues and cervical cancer cell lines. The ATSCs were clustered into an independent terminal branch. These results confirm that ATSCs displayed unique miRNA expression profiles that can be successfully distinguished from other tissues and cancer cell lines.



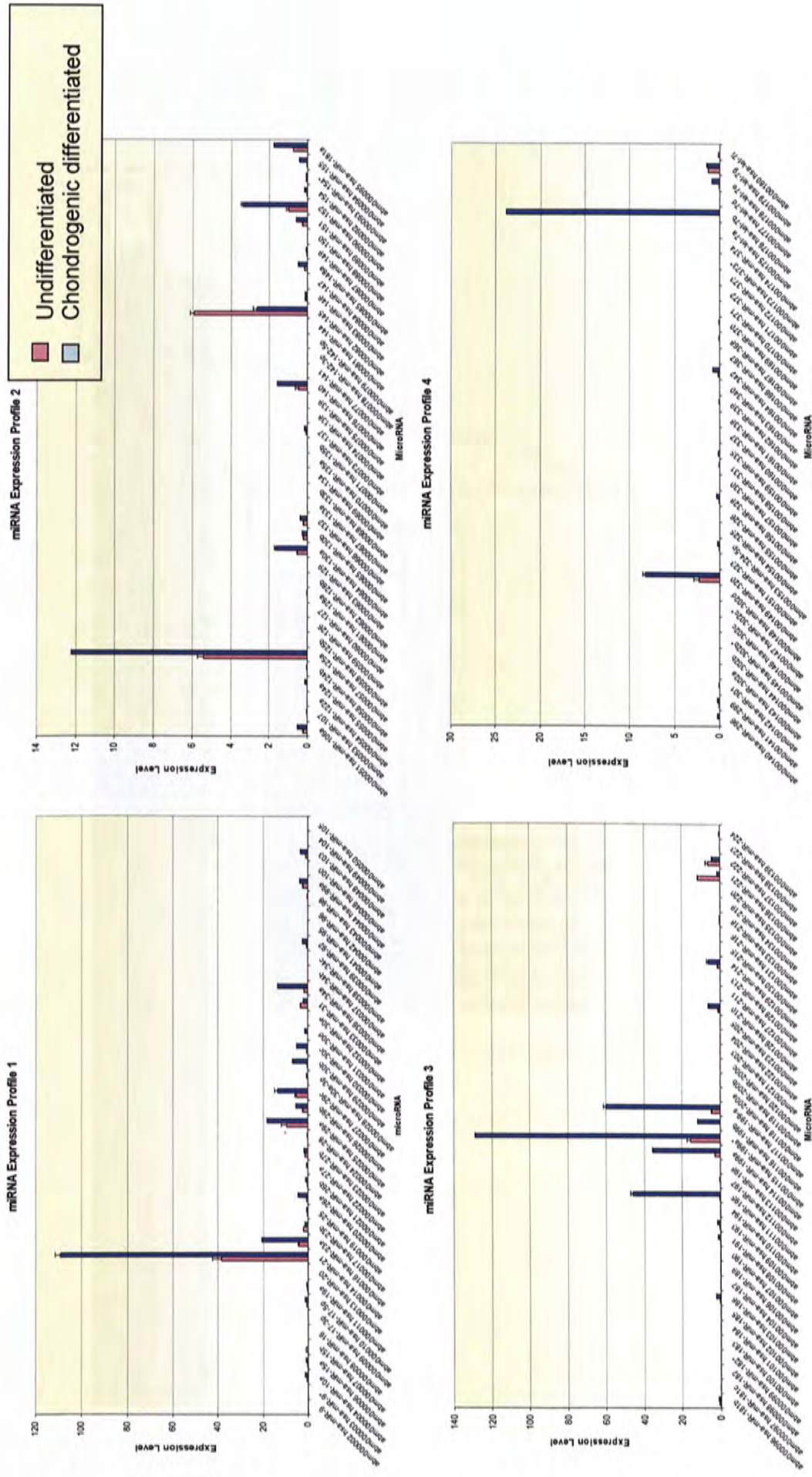


Fig 13 Expression profile of 157 miRNAs in undifferentiated and chondrogenic differentiated ATSCs. The data was normalized with U6.

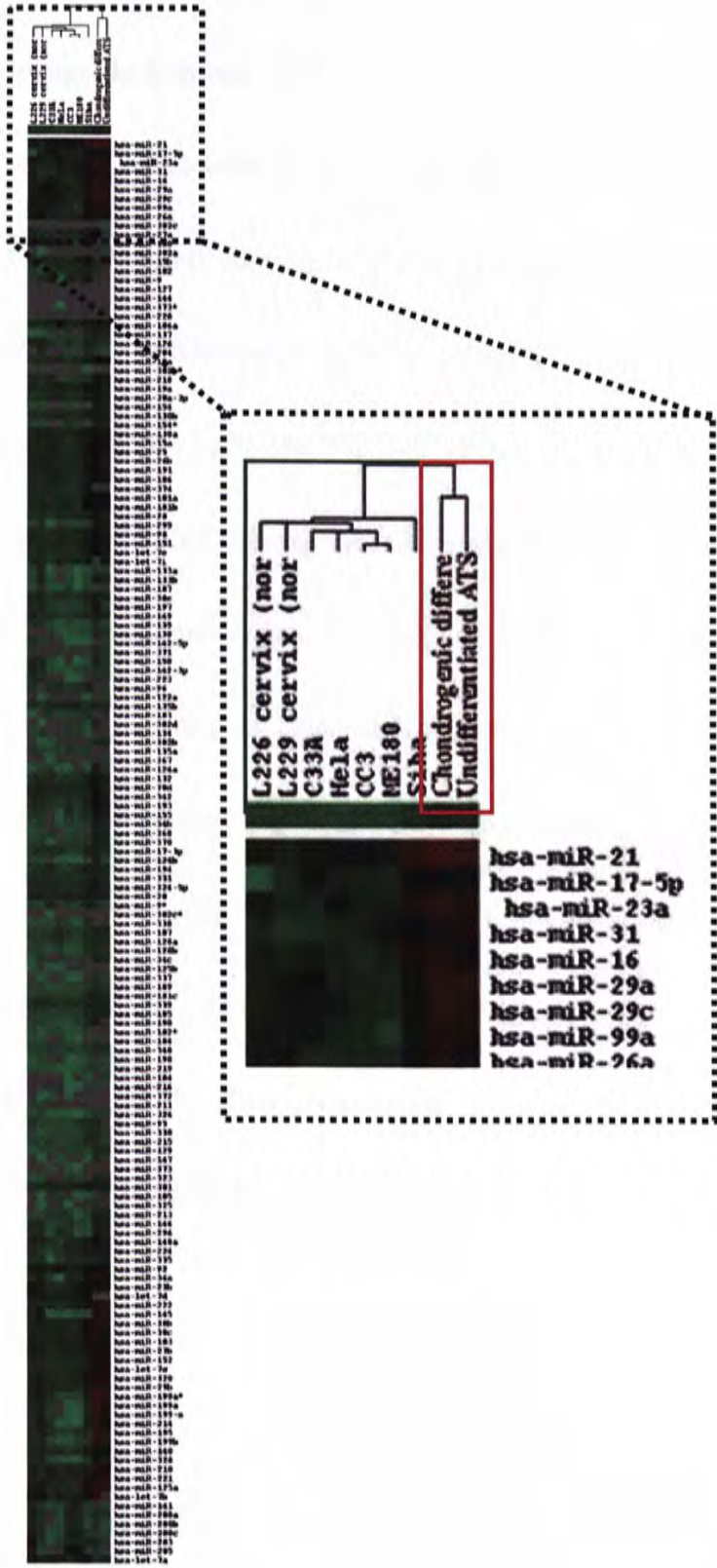


Fig. 14 Hierarchical clustering comparing 157 miRNA expression profile of undifferentiated ATSCs and chondrogenic differentiated ATSCs with two normal cervix tissues (L226 and L229) and 5 cervical cancer cell lines (C33A, Hela, CC3, ME180 and Siha) using data after global medium-normalization.

### **3.5.3 Identification of Differentially Expressed MiRNAs in Chondrogenic-induced ATSCs**

We used a threshold of > 2-fold changes in all three samples after normalization with the endogenous controls, to identify miRNAs that were uniquely expressed in chondrogenic differentiated ATSCs. Based on these criteria, 11 aberrantly expressed miRNAs (miR-30c, 30e, 34a, 124b, 191, 197, 199a, 199a\*, 199b, 199s and 328) were identified among the 157 miRNAs. Their average fold changes and expression levels are summarized in Fig. 15. We have identified the miRNA-199 family which consists of four miRNAs: miR-199a, 199a\*, 199b and 199-s. They were highly expressed and consistently up-regulated in all differentiated ATSCs. Therefore, we suspect that they may play a role in the chondrogenesis of ATSCs. Although miRNAs like miR-197 and miR-124b showed large fold changes (>25) in differentiated ATSCs than controls, the difference is not trustworthy, since their endogenous expression levels are very low (Fig. 15).



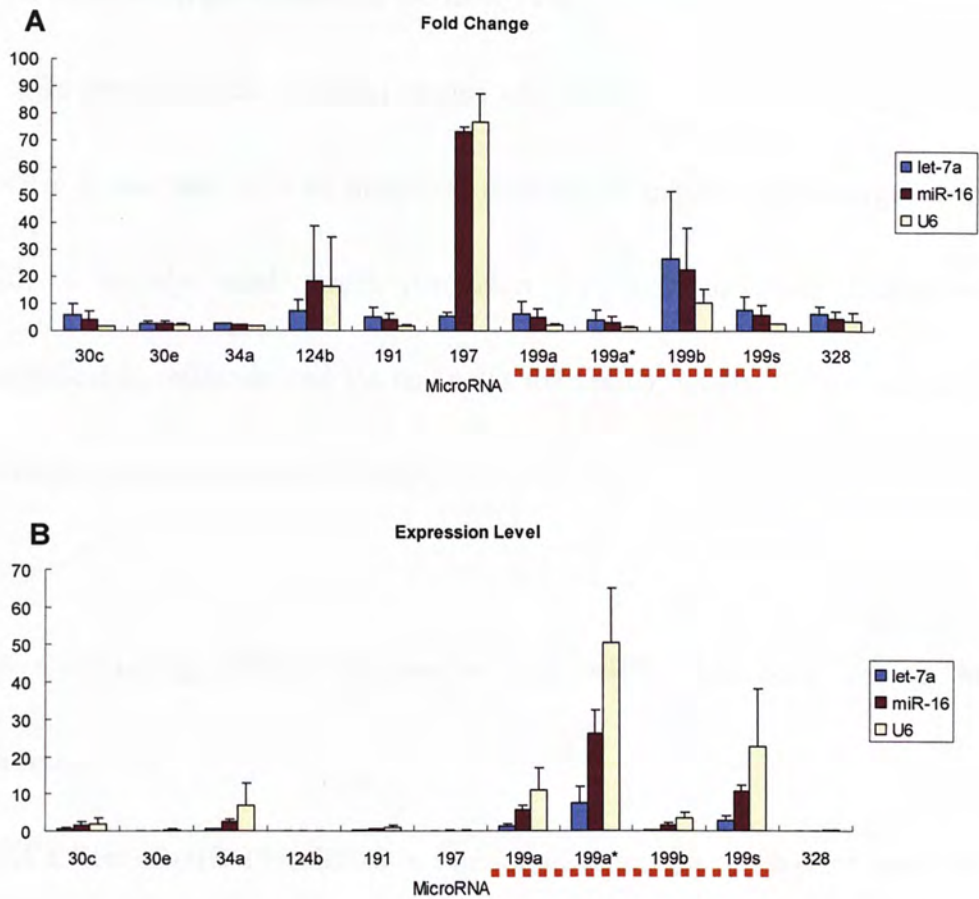


Fig. 15 (A) Average fold change and (B) expression level of 11 aberrantly expressed miRNAs in ATSCs after chondrogenic induction. Data was normalized with endogenous controls let-7a, miR-16 and U6. MicroRNA-199 families, which expressed in a relatively high level, were selected for further investigation.

### **3.5.4 mRNA Target Prediction for miR-199a**

To prediction the potential targets of miRNAs, miRGen *Targets*, a web-based database, was used. It is an integrated database of animal miRNA targets combined with 4 widely used target prediction programs including DIANA-microT, TargetScanS, miRanda and PicTar. After the search, totally 1275 predicted targets were found for miR-199a in human.

## **3.6 Correlating MiRNA Expression and mRNA Levels: Clues to MiRNA Function**

### **3.6.1 Effect of miR-199a RNAi in Phenotypic Changes of Chondrogenic-induced ATSCs.**

Due to the limited availability of reagents, among the four members of the miR-199 family, we chose miR-199a for further study. We knockdowned the endogenous miR-199a in ATSCs during chondrogenic differentiation using RNAi, an anti-miR199a specific miRNA inhibitor, to investigate the biological role of miR-199a in chondrogenic differentiation of ATSCs. Knockdown of the *miR-199a* was confirmed by real-time PCR. In monolayered ATSCs, the miRNA inhibitor knockdowned *miR-199a* effectively (knockdown by >85%) (Fig. 16A). However, in micromass culture during chondrogenic differentiation, knockdown of *miR-199a* was

reduced to 18-30% on D2, D3 and D7. And the knockdown effect was diminished on D14 (Fig. 16B).

Both protein and mRNA expression levels of chondrogenic markers were accessed by immunostaining and real-time PCR respectively. Compared to control (without knockdown), *miR-199a* knockdown greatly reduced the expression of chondrogenic markers (*SOX9*, *COL2A1* and *COL10A1*) in D2, D3, and D7 spheroids (Fig. 17). Immunostaining against the chondrogenic markers also showed a lower expression in spheroids with *miR-199a* knockdown including Aggrecan (Fig.18). However, their expressions re-gained greatly on D14. The cell culture model revealed a direct correlation between expressions of *miR-199a* and increased expression of chondrogenic markers. Consistently, in samples with lower (knockdowned) *miR-199a* expression, chondrogenic markers were also expressed in a lower level. These results suggested a positive role of *miR-199a* in regulation of chondrogenic marker expression.



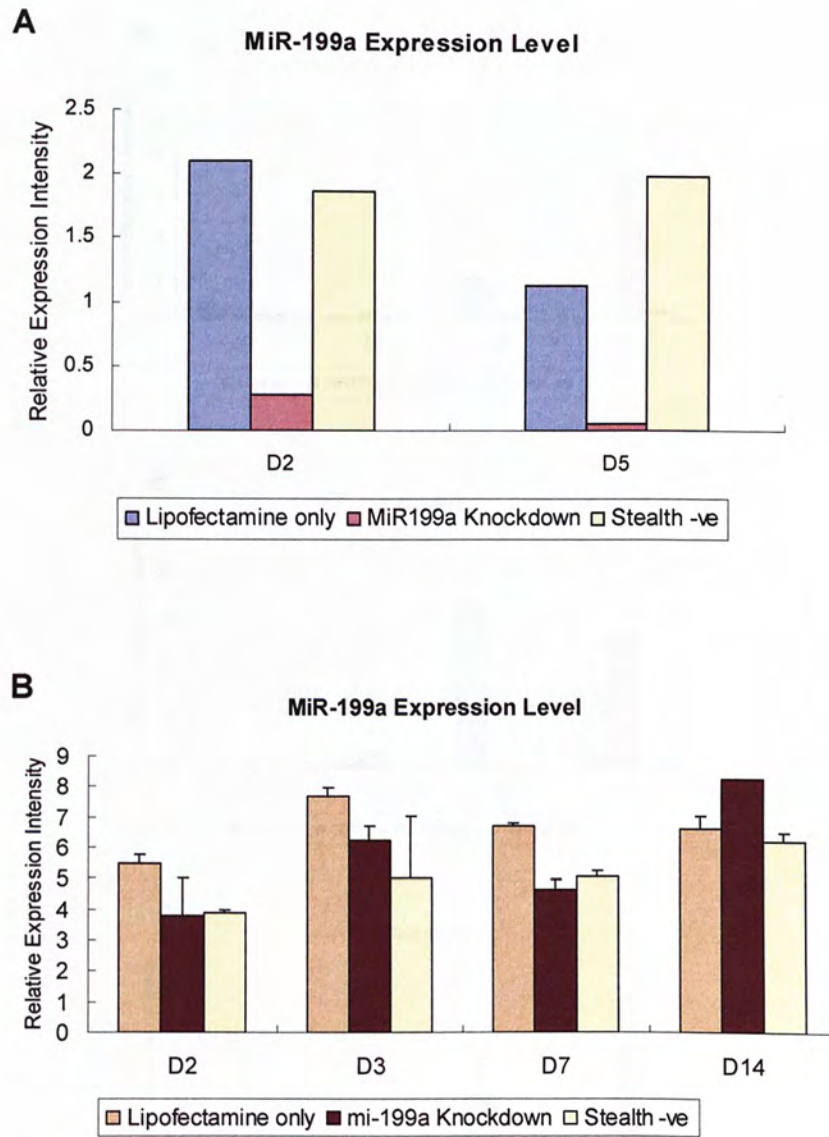


Fig. 16 Change in miR-199a expression (normalized with U6) (A) in monolayer undifferentiated ATSCs (B) during chondrogenic differentiation of ATSCs with and without miR-199a knockdown.

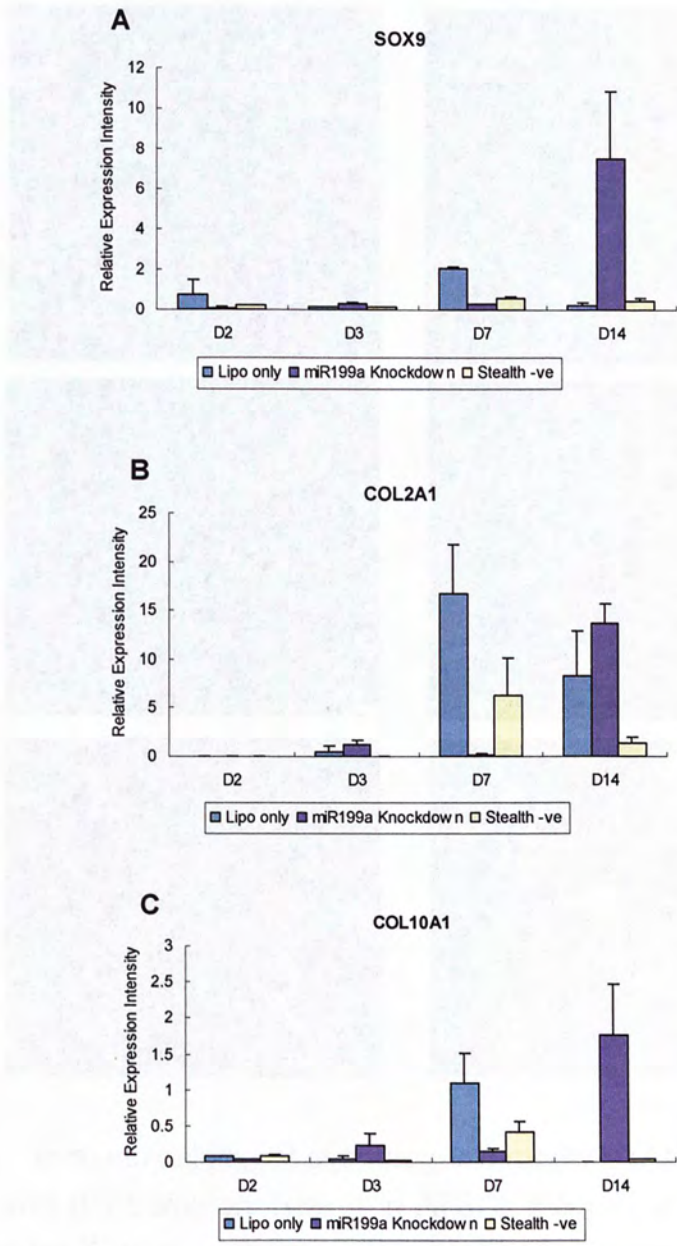


Fig. 17 Real-time PCR results showing the change in expressions of three chondrogenic markers (A)SOX9, (B) Collagen Type II and (C) Collagen Type X during ATSC chondrogenic differentiation. Marker expressions were suppressed in the first week (D2-D7) but re-expressed on D14, which is consistent with the high expression of miR-199a in the sample.

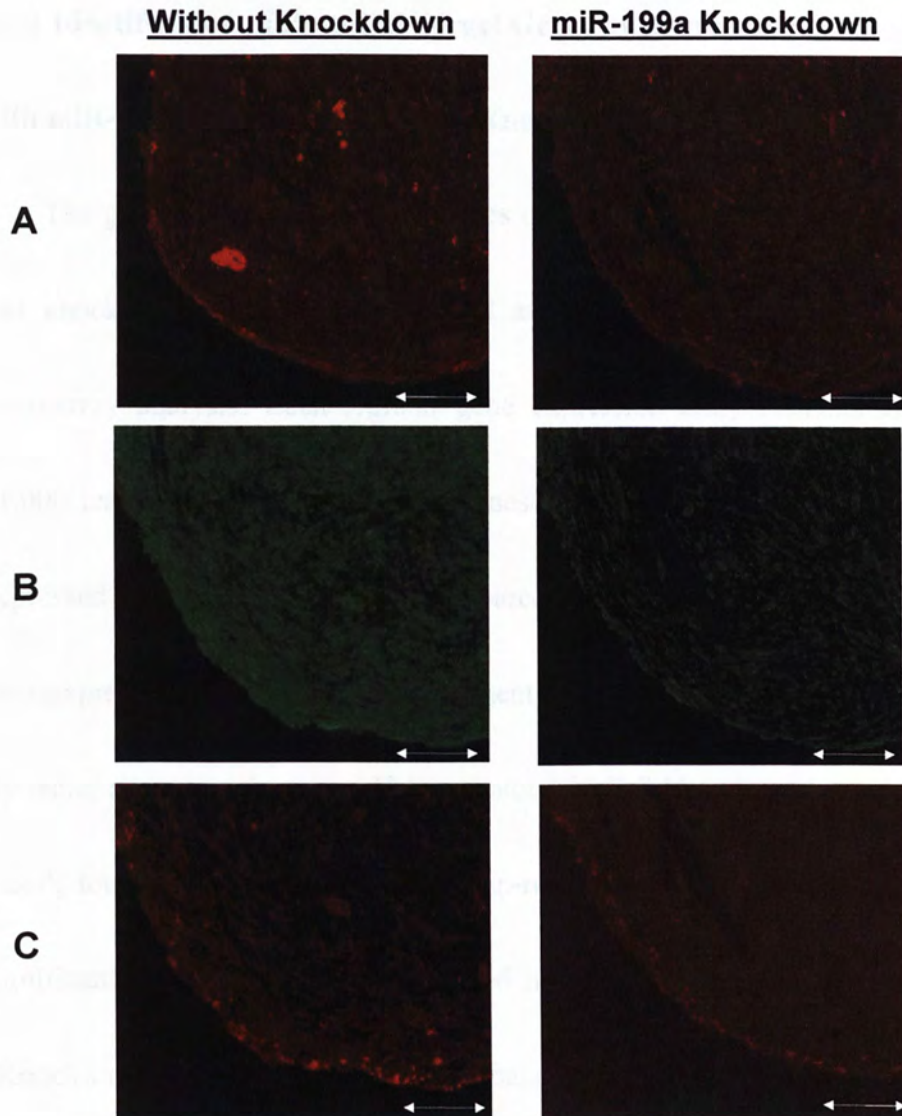


Fig. 18 Immunostaining of chondrogenic markers (A) Aggrecan, (B) SOX9 and (C) Collagen Type II in ATSCs induced in chondrogenic medium for 7 days, with and without miR-199a knockdown. ATSCs with miR-199a knockdown showed a decrease in expression of all three chondrogenic markers. (Scale = 100  $\mu$ m)



### **3.6.2 Identification of Potential Target Genes by Microarray Analysis of ATSCs with miR-199a Over-expression and Knockdown**

The global gene expression profiles of ATSCs with miR-199a over-expression and knockdown for 48 hours as well as untreated ATSCs were studied by the microarray analysis. Each Agilent gene expression array contains approximately 41,000 features with unique human genes and transcripts. To identify differentially expressed genes, data was compared between samples with *miR-199a* over-expression and knockdown treatment, using stealth RNAi as negative control. By using a parametric test in Volcano plot with 2-fold and p-value equal to 0.05 as cutoff, totally 9611 transcripts (2614 up-regulated and 6997 down-regulated) were significantly altered and were identified in the “Over-expression” sample. For the “Knockdown” sample, a lower fold change cutoff value, 0.5-fold, was used as a lower change in miR-199a expression was obtained in the knockdown (decreased by 85%) than the over-expression treatment (increased by 6489%). A total of 1215 differentially expressed transcripts (710 up-regulated and 505 down-regulated) were identified in the “Knockdown” sample.

By importing the Kyoto Encyclopedia of Genes and Genomes (KEGG) pathway database into GeneSpring GX 7.3.1, differentially expressed genes overlapping with members of any signaling pathway were identified. Among all the differentially

expressed genes, genes were mostly involved in cell biological processes such as cell cycle (3.0% of genes in Overexpression/2.7% of genes in Knockdown), cytokine-cytokine receptor interaction (2.3%/3.3%), cell communication (1.1%/1.9%) as well as various signaling pathways including MAPK signaling pathway (3.4%/4.7%), Wnt signaling pathway (2.1%/2.1%), Jak-STAT signaling pathway (1.5%/1.9%) and TGF-beta signaling pathway (1.2%/2.2%).

As the TGF- $\beta$  signaling pathway is known to be important for chondrogenic condensation and differentiation, we further investigated the possible involvement of genes participating in the TGF- $\beta$  pathways. Among all differential expressed genes, 36 genes in “Over-expression” and 15 genes in “Knockdown” were identified that involved in the TGF- $\beta$  pathways (Appendix 1). These genes in the TGF- $\beta$  signaling pathway showed varied expression changes after altered *miR-199a* level in ATSCs. Over-expression of *miR-199a* resulted in a down-regulation of important mediators in TGF- $\beta$  signaling pathway including *SMAD2*, *SMAD3*, *THBS1* and *MAPK3* by at least two folds. On the other hand, other key genes in chondrocyte differentiation including *TGFB3*, *BMP2* and *BMP6* were up-regulated (from three to eleven folds). Consistently, the expression changes of most of these genes were found opposite in ATSCs with *miR-199a* knockdown. Expression of *TGFB1* was also up-regulated (1.6 folds).

## **CHAPTER 4 DISCUSSION**

Recently, the multipotent MSCs isolated from adipose tissue have shown great ability to differentiate into a variety of cell types across all three germ layers. In our project, we have demonstrated that MSCs can be successfully isolated from human adipose tissues. Similar to BMSCs, ATSCs show a fibroblastic morphology with self-renewing ability. Almost all of the cultured ATSCs expressed mesenchymal stem cell markers CD44 and CD90, indicating that the cell population we isolated were mostly mesenchymal stem cells. Most importantly, this study showed the ability of ATSCs to differentiate into chondrocytes as well as transdifferentiate into neurons. This confirms the multipotent nature of ATSCs. We used this model to study the effect of the donor's physiological status on ATSCs, establishing the first miRNA profile in ATSCs and identifying microRNAs important for ATSC differentiation.

### **Effect of Donor's Reproductive Status on the Proliferation and Differentiation**

#### **Capacity of ATSCs**

To determine the effect of donor's reproductive status on the performance of ATSCs, we divided the samples into three groups according to their physiological status: pregnancy, pre-menopause and menopause and their isolated ATSC



phenotypes, proliferation and differentiation capacities were compared. Although the morphology and the MSC marker expression varied in different samples, no obvious difference was found between the three sample groups. We have also compared their differentiation capacities towards the chondrogenic lineage in terms of their abilities to form spheroids as well as the expression level of chondrogenic markers after the induction. Similarly, no obvious difference was found between the three groups. These results provide important information for future therapeutic uses as they suggest that ATSCs can be isolated from different individuals of different reproductive status without affecting their stem cell nature. As ATSCs acquired similar differentiation power regardless of the donor's reproductive status, cell therapies or transplantations involving the use of ATSCs can be applied in any individual without the concern of individual variation, although we haven't confirmed our findings between male and female yet.

Interestingly, we found that the proliferation rate of ATSCs in the pregnancy group was significantly higher than the other two groups. There are reports showing that estrogen can stimulate proliferation in mouse ESCs as well as affecting the differentiation capacities of human MSCs (Han, et al 2006, Hong, et al 2006). Therefore, we hypothesized that it might be the difference in the estrogen level in the pregnancy group that accounts for the variation. To verify our hypothesis, ATSCs

were treated with estrogen ( $17\beta$ -Estradiol) and their proliferation rates were compared with untreated ATSCs. However, no significant difference was found between the two groups. This suggested that the variation of the estrogen level among the three sample groups may not be the cause of their difference in the proliferation rate. Other possibilities might be the involvement of hormones other than estrogen, or other factors that are still unknown which require further investigation.

### **Unique MicroRNA Expression Profile in ATSCs**

The miRNA expression assay revealed a unique miRNA expression profile in ATSCs that can be easily distinguished from that of other tissues and cancer cell lines, using cluster analysis. To identify specific miRNAs that are involved in the chondrogenic differentiation of ATSCs, the miRNA expression profiles of undifferentiated ATSCs and chondrogenic-induced ATSCs were further studied and compared. Overall, they displayed similar expression profiles. For example, they both highly expressed miR-21, which has been reported to be an anti-apoptotic factor in human glioblastoma cells as well as tumor cells (Chan, et al 2005). Among the 157 miRNAs studied in the assay, we have identified 11 aberrantly expressed miRNAs that were up-regulated ( $\geq$  folds) after chondrogenic differentiation. Among them,

*miRNA-140*, which is the only miRNA so far reported as being involved in chondrogenesis (Tuddenham, et al 2006), was also found to be up-regulated in chondrogenic differentiated ATSCs. However, it is not included in the list of aberrantly expressed miRNAs as it had a fold change less than two.

### **MicroRNA-199a Does Play a Role in Chondrogenesis of ATSCs**

The 11 aberrantly expressed miRNAs include *miR-30c*, *30e*, *34a*, *124b*, *191*, *197*, *199a*, *199a\**, *199b*, *199s* and *328* and they are possibly involved in the chondrogenic differentiation of ATSCs. To further our investigation, we selected the miR-199 family (*199a*, *199a\**, *199b*, *199s*), particularly *miR-199a* as the candidate miRNA as they were highly expressed and consistently up-regulated in chondrogenic differentiated ATSCs. Other aberrantly expressed miRNAs such as *miR-197* and *miR-124b* also showed large fold changes; however, their endogenous expression level was relatively low which made them a difficult candidate target for the RNAi knockdown approach.

Using RNAi knockdown assay, a correlation was observed between the expression of *miR-199a* and the expression of chondrogenic markers in ATSCs. The result suggests that *miR-199a* may participate in the chondrogenesis of ATSCs. Using real-time PCR, we confirmed that the knockdown of *miR-199a* was successful and



lasted until Day 7 of the *in vitro* induction of ATSCs into chondrocytes. Immunohistochemical analysis and real-time PCR demonstrated a decrease in the expression level of various chondrogenic markers among *miR-199a*-knockdown ATSCs. However, on Day 14 when the knockdown effect was diminished, the expression level of the chondrogenic markers started to rise. This correlation suggests that *miR-199a* does play a positive role in the chondrogenic differentiation of ATSCs.

### **MiR-199a Promotes Chondrogenesis Through TGF- $\beta$ Signaling Pathway**

The fate of a chondrocyte greatly depends on the interplay of the TGF- $\beta$  signaling and BMP signaling (Chen, et al 1991, Fromigue, et al 1998, Suzuki 1992). TGF- $\beta$  promotes chondrocyte proliferation while BMP induces its maturation. For both pathways, SMAD proteins participate as the key mediators. From the miRNA expression profiling, *miR-199a* was consistently up-regulated in chondrogenic-induced ATSCs. Moreover, the knockdown of *miR-199a* partially inhibited the chondrogenic differentiation of ATSCs, evidenced by the reduced expression of chondrogenic markers. In our microarray results, over-expression of *miR-199a* in ATSCs significantly down-regulated the expression of TGF- $\beta$  signaling genes including *SMAD2*, *SMAD3*, *TGFB3* and *TGFBR2* and significantly

up-regulated BMP signaling genes such as *BMP2* and *BMP6*. In contrast, knockdown of *miR-199a* significantly up-regulated TGF- $\beta$  signaling genes and down-regulated BMP signaling genes. Both results suggest a stimulatory effect of *miR-199a* on the chondrogenesis of ATSCs, probably through targeting an inhibitor in the differentiation pathways. These strongly suggest that *miR-199a* promotes chondrogenic differentiation and maturation by inhibiting TGF- $\beta$  and stimulating BMP signaling.

In fact, the inhibitory effect of TGF- $\beta$  on chondrocyte maturation is mainly mediated by *SMAD2* and *SMAD3* as has been suggested by others (Ferguson, et al 2000, Li, et al 2006). In the report by Li et al., chondrocytes isolated from *Smad3*<sup>-/-</sup> mice exhibited accelerated differentiation and maturation compared to the wild type. A shift from TGF- $\beta$  towards BMP signaling was observed, supported by the increased expression of *SMAD1*, *SMAD5*, *BMP2*, *BMP6* and decreased expression of *TGFB1* and *TGFBR1*. Similarly, our microarray data of *miR-199a*-overexpressed ATSCs also showed an up-regulation in BMP signaling genes (*BMP2*, *BMP6*) and down-regulation in TGF- $\beta$  signaling genes (*SMAD2*, *SMAD3*), suggesting that *miR-199a* may promote chondrogenesis by targeting and suppressing *SMAD2* or *SMAD3*. Interestingly, *SMAD3* was one of the predicted targets of *miR-199a* (Appendix 2). This further supports the hypothesis that *miR-199a* promote



chondrocyte differentiation and maturation by suppressing SMAD3.

To verify the microarray data, quantitative real-time PCR will be done to confirm the aberrant expression of those genes in TGF- $\beta$  signaling pathway. Western blotting will also be done to confirm the changes in expression of potential target genes in protein level as well. To validate the hypothesis that SMAD3 is the direct target of miR-199a, functional assays such as luciferase reporter assay will be done to determine if there is any interaction between them.

### **Chondrogenic Differentiation of ATSCs**

In a highly dense environment with the supplement of appropriate growth factors, ATSCs are readily induced into chondrocytes. We showed that using supplements such as TGF- $\beta$ , dexamethasone, insulin and ascorbic acid in a micromass culture, ATSCs can be induced into chondrocytes exhibiting three-dimensional cellular structures with cartilaginous characteristics. The TGF- $\beta$  signaling pathway is well known for its important role in bone and cartilage formation. The addition of TGF- $\beta$  in ATSC micromass culture can certainly trigger the chondrogenic differentiation process (Lee, et al 2004, Zuk, et al 2002). Furthermore, the addition of insulin and ascorbic acid accelerated the growth of the ATSCs and further supported the condensation process.



The chondrogenic nature of differentiated ATSCs was supported by various features from mRNA expression to biochemical findings. Three-dimensional spheroids, which were condensed as early chondrogenesis proceeded, were formed soon after the induction (Fig. 3). Expressions of cartilaginous matrix, such as collagens and proteoglycans, were identified within the spheroids, using histological staining with Alcian blue and immunohistochemical analyses. Expressions of mRNA of various chondrogenic marker genes were detected in the spheroids using reverse transcription PCR assays.

The immunohistochemical analyses showed the expression of matrix proteins Collagen Type II and Aggrecan throughout the spheroids. Their expressions were found to be concentrated along the outer layer of the spheroids. This may be due to the higher differentiation rate of the cells in the outer layer as they had more contact with the differentiation medium. Therefore, they expressed these matrix proteins in a higher level than cells in the inner part of the spheroids (Fig 6 & 16). In addition, Alcian blue staining also confirmed the presence of sulfated proteoglycans within the spheroids. Similar to Collagen Type II and Aggrecan, a higher level of sulfated proteoglycans was also shown along the outer layer of the spheroids.

In the reverse transcription PCR assays, we observed a time-dependent increment of mRNA expression of chondrogenic markers (Fig. 5). The mRNAs of

*SOX9* and *COL2A1* appeared after 2 weeks of induction, while the mRNA of *COL10A1* appeared in the last week of the 4-week induction. These findings were in accordance with the *in vivo* expression patterns of these markers in real cartilage. *SOX9* is a key nuclear transcription factor which expresses early during chondrogenesis (Goldring, et al 2006). Its expression is required for the trigger of chondrogenesis as well as for the expression of some cartilage-specific matrix proteins including Collagen Type II and Aggrecan. In our samples, *SOX9* expressed in the highest level on Day 14 and its expression started to decline afterwards, as its expression was no longer needed in the later stage. In similar fashion to *SOX9*, the mRNA of Collagen Type II also appeared on Day 14, which supported that its expression being triggered by the expression of *SOX9*. Collagen Type X is a marker for chondrocyte hypertrophy which often expresses in the terminal stage of chondrogenesis. Consistently, in our samples, it expressed in the last week of the differentiation.

We have noticed that even in control medium without the addition of growth factors, ATSCs cultured in micromass were also able to form spheroids, although in a lower frequency. Moreover, they also showed some expression of chondrogenic markers. This result suggests that, although in a lower rate, ATCSs have the potential to undergo spontaneous differentiation towards chondrogenic lineages in a cell dense



environment.

### **Neural Differentiation of ATSCs**

The introduction of adult stem cell plasticity suggests that ATSCs are not restricted to differentiation along lineages of their tissue origin and can also be induced into non-mesenchymal lineages. Previous studies suggested the induction of ATSCs into neurons using chemical such as BME and BHA (Zuk, et al 2002). However, these rapid inductions of ATSCs into neurons were likely due to cellular toxicity causing shrinkage of cytoplasm instead of a real neurogenesis (Lu, et al 2004). In our project, we demonstrated that ATSCs were capable of differentiating into neural cells when stimulated by neural growth factors including bFGF, NGF and BNGF. The differentiated cells exhibited a neural appearance with cytoplasmic extensions and spherical cell bodies, and their neural lineage was confirmed by the expressions of several specific, both early and late, neural markers.

In undifferentiated ATSCs cultured in control medium, expression of some neural markers including Nestin, NEF3, NSE and TUBB3 was already detected. This finding is consistent with previous studies that undifferentiated ATSCs and BMSCs already express specific neural proteins before any differentiation (Tondreau, et al 2004, Yang, et al 2004), suggesting that these undifferentiated stem cells may already



acquire some characteristics of neural progenitor cells. They are ready to differentiate into neural lineage, once they are cultured with appropriate neural growth factors.

After neural induction for 2 weeks, the expression of NSE remained high in the cells while that of other markers such as Nestin and TUBB3 increased significantly after differentiation. The induced cells expressed late neural markers TAU and MAP2 as well. As ATSCs contain a highly heterogeneous population, their differentiation power may vary. It is difficult to obtain a 100% differentiation towards a specific lineage. The immunohistochemical analyses showed that, among the differentiated cells, most of them (>90%) expressed early neural markers Nestin and NSE. However, for the late neural marker TAU, expression was found only in ~50% of the induced cells, and was mainly expressed in cells with elongated cytoplasm with neuron-like morphology instead of those with squamous morphology.

## CHAPTER 5 CONCLUSION

In this study, we have successfully replicated previous *in vitro* studies to induce ATSCs into chondrogenic and neural lineages in four and two weeks respectively. By investigating the mRNA and protein expression of differentiated lineage markers, we compared the proliferation and differentiation capacity of ATSCs isolated from three reproductive groups (pregnancy, pre-menopause and menopause). We found that the differentiation capacity towards chondrogenic lineage was totally unaffected by the donor's reproductive status. However, the proliferation rate of ATSCs from pregnant women was significantly higher than the other two groups. By treating ATSCs with estrogen *in vitro*, we further concluded that the difference in proliferation were due to unknown factors other than the difference in estrogen level in pregnant women.

By quantifying the expression of 157 miRNAs between differentiated and undifferentiated ATSCs, this study clearly shows that a unique miRNA profile was identified in ATSCs comparing to other normal or cancerous tissues. Most significantly a group of miRNAs belonging to the miR-199 family (miR-199a, -199a\*, -199b, -199s) was identified to be important for ATSC differentiated into chondrogenic lineage. Further investigations *by in vitro* knockdown and over-expression of *miR-199a* during chondrogenic induction indicate that miR-199a

influenced the expression of chondrogenic markers, suggesting a positive role of miR-199a in chondrogenesis of ATSC. Although miRNAs might have many predicted targets, studies by gene expression array identified genes (SMAD2/3, and BMP2/6) that are involved in the TGF- $\beta$  signaling pathway were differentially regulated in response to miR-199a, particularly down-regulated in TGF- $\beta$  and up-regulated BMP signaling. These indicated that miRNAs, in particular *miR-199a*, may play important roles in the differentiation process of human ATSC cells. This study shows that *miR-199a* could be a novel regulator in ATSC chondrogenesis by shifting the balance towards BMP signaling which stimulates chondrocyte differentiation and maturation.

*(Table content is extremely faint and illegible)*



## APPENDICES

### Appendix 1 Predicted Targets of MiR-199a Involved in TGF- $\beta$ Signaling Pathway

Gene Name	Symbol	Accession
Bone morphogenetic protein 7 precursor	BMP7	NM_001719
DNA-binding protein inhibitor ID-1	ID1	NM_002165
Mitogen-activated protein kinase kinase kinase 7-interacting protein 1 (TAK1-binding protein 1)	MAP3K7IP1	NM_153497
Transforming growth factor beta-2 precursor	TGFB2	NM_003238
Growth/differentiation factor 2 precursor	GDF2	NM_016204
Mothers against decapentaplegic homolog 3	SMAD3	NM_005902

### Appendix 2 Differentially Expressed Genes Involved in TGF- $\beta$ Signaling Pathway in ATSCs after MiR-199a Over-expression and Knockdown

<u>Overexpression</u>			
Gene Name	Symbol	Accession	Expression Fold Change
Homo sapiens latent transforming growth factor beta binding protein 1 (LTBP1)	LTBP1	NM_206943	0.208
Homo sapiens cartilage oligomeric matrix protein	COMP	NM_000095	2.518
Homo sapiens thrombospondin 1	THBS1	NM_003246	0.341
Homo sapiens SMAD, mothers against DPP homolog 2	SMAD2	NM_005901	0.479
Homo sapiens SMAD, mothers against DPP homolog 3	SMAD3	NM_005902	0.398
Homo sapiens E1A binding protein p300	EP300	NM_001429	2.554

Homo sapiens cyclin-dependent kinase inhibitor 2B	CDKN2B	NM_004936	3.425
Homo sapiens v-myc myelocytomatosis viral oncogene homolog	MYC	NM_002467	2.362
Homo sapiens inhibitor of DNA binding 1	ID1	NM_002165	0.19
Homo sapiens inhibitor of DNA binding 2	ID2	NM_002166	0.175
Homo sapiens inhibitor of DNA binding 3	ID3	NM_002167	0.271
Homo sapiens Rho-associated, coiled-coil containing protein kinase 1	ROCK1	NM_005406	0.287
Homo sapiens Rho-associated, coiled-coil containing protein kinase 2	ROCK2	NM_004850	0.204
Homo sapiens zinc finger, FYVE domain containing 9	ZFYVE9	NM_004799	0.128
Homo sapiens mitogen-activated protein kinase 3	MAPK3	NM_002746	0.464
Homo sapiens SMAD specific E3 ubiquitin protein ligase 2	SMURF2	NM_022739	0.125
Homo sapiens transforming growth factor, beta receptor II	TGFBR2	NM_001024847	0.182
Homo sapiens transforming growth factor, beta 3	TGFB3	NM_003239	3.208
Homo sapiens bone morphogenetic protein receptor, type II	BMPR2	NM_001204	0.406
Homo sapiens bone morphogenetic protein receptor, type IA	BMPR1A	NM_004329	0.237
Homo sapiens bone morphogenetic protein 8a	BMP8A	NM_181809	2.079
Homo sapiens bone morphogenetic protein 2	BMP2	NM_001200	11.31
Homo sapiens bone morphogenetic protein 6	BMP6	NM_001718	8.707



<b><u>Knockdown</u></b>			
<b>Gene Name</b>	<b>Symbol</b>	<b>Accession</b>	<b>Expression Fold Change</b>
Homo sapiens thrombospondin 1	THBS1	NM_003246	1.365
Homo sapiens SMAD, mothers against DPP homolog 4	SMAD4	NM_005359	1.375
Homo sapiens SMAD, mothers against DPP homolog 2	SMAD2	NM_005901	0.873
Homo sapiens SMAD, mothers against DPP homolog 3	SMAD3	NM_005902	1.343
Homo sapiens Sp1 transcription factor	SP1	NM_138473	0.79
Homo sapiens CREB binding protein	CREBBP	NM_004380	1.32
Homo sapiens E1A binding protein p300	EP300	NM_001429	1.425
Homo sapiens cyclin-dependent kinase inhibitor 2B	CDKN2B	NM_078487	1.875
Homo sapiens v-myc myelocytomatosis viral oncogene homolog	MYC	NM_002467	1.518
Homo sapiens inhibitor of DNA binding 2, dominant negative helix-loop-helix protein	ID2	NM_002166	0.534
Homo sapiens protein phosphatase 2 catalytic subunit, beta isoform	PPP2CB	NM_00100955 2	2.071
Homo sapiens zinc finger, FYVE domain containing 9	ZFYVE9	NM_004799	1.927
Homo sapiens mitogen-activated protein kinase 3	MAPK3	NM_002746	1.354
Homo sapiens transforming growth factor, beta 1	TGFB1	NM_000660	1.645
Homo sapiens bone morphogenetic protein 6	BMP6	NM_001718	2.033



## REFERENCES

- Ahrens PB, Solursh M, Reiter RS. Stage-related capacity for limb chondrogenesis in cell culture. *Dev.Biol.* 1977;60:69-82.
- Ambros V. The functions of animal microRNAs. *Nature* 2004;431:350-355.
- Artavanis-Tsakonas S, Rand MD, Lake RJ. Notch signaling: cell fate control and signal integration in development. *Science* 1999;284:770-776.
- Ashjian PH, Elbarbary AS, Edmonds B, DeUgarte D, Zhu M, Zuk PA, et al. In vitro differentiation of human processed lipoaspirate cells into early neural progenitors. *Plast.Reconstr.Surg.* 2003;111:1922-1931.
- Ason B, Darnell DK, Wittbrodt B, Berezikov E, Kloosterman WP, Wittbrodt J, et al. Differences in vertebrate microRNA expression. *Proc.Natl.Acad.Sci.U.S.A.* 2006;103:14385-14389.
- Aubert J, Dunstan H, Chambers I, Smith A. Functional gene screening in embryonic stem cells implicates Wnt antagonism in neural differentiation. *Nat.Biotechnol.* 2002;20:1240-1245.
- Austin TW, Solar GP, Ziegler FC, Liem L, Matthews W. A role for the Wnt gene family in hematopoiesis: expansion of multilineage progenitor cells. *Blood* 1997;89:3624-3635.
- Awad HA, Halvorsen YD, Gimble JM, Guilak F. Effects of transforming growth factor beta1 and dexamethasone on the growth and chondrogenic differentiation of adipose-derived stromal cells. *Tissue Eng.* 2003;9:1301-1312.
- Bacigalupo A. Management of acute graft-versus-host disease. *Br.J.Haematol.* 2007;137:87-98.
- Bacou F, el Andaloussi RB, Daussin PA, Micallef JP, Levin JM, Chammas M, et al. Transplantation of adipose tissue-derived stromal cells increases mass and

- functional capacity of damaged skeletal muscle. *Cell Transplant.* 2004;13:103-111.
- Baskerville S, Bartel DP. Microarray profiling of microRNAs reveals frequent coexpression with neighboring miRNAs and host genes. *RNA* 2005;11:241-247.
- Beatus P, Lendahl U. Notch and neurogenesis. *J.Neurosci.Res.* 1998;54:125-136.
- Bernstein E, Caudy AA, Hammond SM, Hannon GJ. Role for a bidentate ribonuclease in the initiation step of RNA interference. *Nature* 2001;409:363-366.
- Bernstein E, Kim SY, Carmell MA, Murchison EP, Alcorn H, Li MZ, et al. Dicer is essential for mouse development. *Nat.Genet.* 2003;35:215-217.
- Bertani N, Malatesta P, Volpi G, Sonogo P, Perris R. Neurogenic potential of human mesenchymal stem cells revisited: analysis by immunostaining, time-lapse video and microarray. *J.Cell.Sci.* 2005;118:3925-3936.
- Blokzijl A, Dahlqvist C, Reissmann E, Falk A, Moliner A, Lendahl U, et al. Cross-talk between the Notch and TGF-beta signaling pathways mediated by interaction of the Notch intracellular domain with Smad3. *J.Cell Biol.* 2003;163:723-728.
- Bohme K, Winterhalter KH, Bruckner P. Terminal differentiation of chondrocytes in culture is a spontaneous process and is arrested by transforming growth factor-beta 2 and basic fibroblast growth factor in synergy. *Exp.Cell Res.* 1995;216:191-198.
- Bohnsack MT, Czaplinski K, Gorlich D. Exportin 5 is a RanGTP-dependent dsRNA-binding protein that mediates nuclear export of pre-miRNAs. *RNA* 2004;10:185-191.
- Bongso A, Lee EH. *Stem cells: From Bench to Bedside.* : World Scientific Publishing Co. Pte. Ltd., 2005.



- Bremer S, Hartung T. The use of embryonic stem cells for regulatory developmental toxicity testing in vitro--the current status of test development. *Curr.Pharm.Des.* 2004;10:2733-2747.
- Brennecke J, Hipfner DR, Stark A, Russell RB, Cohen SM. bantam encodes a developmentally regulated microRNA that controls cell proliferation and regulates the proapoptotic gene hid in *Drosophila*. *Cell* 2003;113:25-36.
- Brzoska M, Geiger H, Gauer S, Baer P. Epithelial differentiation of human adipose tissue-derived adult stem cells. *Biochem.Biophys.Res.Commun.* 2005;330:142-150.
- Cadigan KM, Nusse R. Wnt signaling: a common theme in animal development. *Genes Dev.* 1997;11:3286-3305.
- Cao B, Zheng B, Jankowski RJ, Kimura S, Ikezawa M, Deasy B, et al. Muscle stem cells differentiate into haematopoietic lineages but retain myogenic potential. *Nat.Cell Biol.* 2003;5:640-646.
- Cao Y, Sun Z, Liao L, Meng Y, Han Q, Zhao RC. Human adipose tissue-derived stem cells differentiate into endothelial cells in vitro and improve postnatal neovascularization in vivo. *Biochem.Biophys.Res.Commun.* 2005;332:370-379.
- Caspar-Bauguil S, Cousin B, Galinier A, Segafredo C, Nibbelink M, Andre M, et al. Adipose tissues as an ancestral immune organ: site-specific change in obesity. *FEBS Lett.* 2005;579:3487-3492.
- Celeste AJ, Iannazzi JA, Taylor RC, Hewick RM, Rosen V, Wang EA, et al. Identification of transforming growth factor beta family members present in bone-inductive protein purified from bovine bone. *Proc.Natl.Acad.Sci.U.S.A.* 1990;87:9843-9847.
- Centrella M, Horowitz MC, Wozney JM, McCarthy TL. Transforming growth factor-beta gene family members and bone. *Endocr.Rev.* 1994;15:27-39.
- Centrella M, McCarthy TL, Canalis E. Transforming growth factor-beta and remodeling of bone. *J.Bone Joint Surg.Am.* 1991;73:1418-1428.



- Chan JA, Krichevsky AM, Kosik KS. MicroRNA-21 is an antiapoptotic factor in human glioblastoma cells. *Cancer Res.* 2005;65:6029-6033.
- Chen CZ. MicroRNAs as oncogenes and tumor suppressors. *N.Engl.J.Med.* 2005;353:1768-1771.
- Chen CZ, Li L, Lodish HF, Bartel DP. MicroRNAs modulate hematopoietic lineage differentiation. *Science* 2004;303:83-86.
- Chen JF, Mandel EM, Thomson JM, Wu Q, Callis TE, Hammond SM, et al. The role of microRNA-1 and microRNA-133 in skeletal muscle proliferation and differentiation. *Nat.Genet.* 2006;38:228-233.
- Chen P, Carrington JL, Hammonds RG, Reddi AH. Stimulation of chondrogenesis in limb bud mesoderm cells by recombinant human bone morphogenetic protein 2B (BMP-2B) and modulation by transforming growth factor beta 1 and beta 2. *Exp.Cell Res.* 1991;195:509-515.
- Chen X. A microRNA as a translational repressor of APETALA2 in Arabidopsis flower development. *Science* 2004;303:2022-2025.
- Chen Y, Stallings RL. Differential patterns of microRNA expression in neuroblastoma are correlated with prognosis, differentiation, and apoptosis. *Cancer Res.* 2007;67:976-983.
- Chiou M, Xu Y, Longaker MT. Mitogenic and chondrogenic effects of fibroblast growth factor-2 in adipose-derived mesenchymal cells. *Biochem.Biophys.Res.Commun.* 2006;343:644-652.
- Chubinskaya S, Kuettner KE. Regulation of osteogenic proteins by chondrocytes. *Int.J.Biochem.Cell Biol.* 2003;35:1323-1340.
- Coller J, Parker R. Eukaryotic mRNA decapping. *Annu.Rev.Biochem.* 2004;73:861-890.
- De Bari C, Dell'Accio F, Tylzanowski P, Luyten FP. Multipotent mesenchymal stem cells from adult human synovial membrane. *Arthritis Rheum.* 2001;44:1928-1942.

- De Strooper B, Annaert W. Where Notch and Wnt signaling meet. The presenilin hub. *J.Cell Biol.* 2001;152:F17-20.
- Dennis JE, Carbillet JP, Caplan AI, Charbord P. The STRO-1+ marrow cell population is multipotential. *Cells Tissues Organs* 2002;170:73-82.
- Department of Health and Human Services. Regenerative Medicine 2006. 2006.
- Department of Health and Human Services. Stem Cells: Scientific Progress and Future Research Directions. 2001.
- Di Rocco G, Iachininoto MG, Tritarelli A, Straino S, Zacheo A, Germani A, et al. Myogenic potential of adipose-tissue-derived cells. *J.Cell.Sci.* 2006;119:2945-2952.
- Dicker A, Le Blanc K, Astrom G, van Harmelen V, Gothstrom C, Blomqvist L, et al. Functional studies of mesenchymal stem cells derived from adult human adipose tissue. *Exp.Cell Res.* 2005;308:283-290.
- Doench JG, Sharp PA. Specificity of microRNA target selection in translational repression. *Genes Dev.* 2004;18:504-511.
- Dominici M, Le Blanc K, Mueller I, Slaper-Cortenbach I, Marini F, Krause D, et al. Minimal criteria for defining multipotent mesenchymal stromal cells. The International Society for Cellular Therapy position statement. *Cytotherapy* 2006;8:315-317.
- Dragoo JL, Carlson G, McCormick F, Khan-Farooqi H, Zhu M, Zuk PA, et al. Healing Full-Thickness Cartilage Defects Using Adipose-Derived Stem Cells. *Tissue Eng.* 2007.
- Dragoo JL, Samimi B, Zhu M, Hame SL, Thomas BJ, Lieberman JR, et al. Tissue-engineered cartilage and bone using stem cells from human infrapatellar fat pads. *J.Bone Joint Surg.Br.* 2003;85:740-747.
- Ede DA. Cellular condensations and chondrogenesis. *Cartilage: Development, Differentiation, and Growth* New York: Academic Press; 1983: 143-185.



- Elbashir SM, Lendeckel W, Tuschl T. RNA interference is mediated by 21- and 22-nucleotide RNAs. *Genes Dev.* 2001a;15:188-200.
- Elbashir SM, Martinez J, Patkaniowska A, Lendeckel W, Tuschl T. Functional anatomy of siRNAs for mediating efficient RNAi in *Drosophila melanogaster* embryo lysate. *EMBO J.* 2001b;20:6877-6888.
- Erickson GR, Gimble JM, Franklin DM, Rice HE, Awad H, Guilak F. Chondrogenic potential of adipose tissue-derived stromal cells in vitro and in vivo. *Biochem.Biophys.Res.Commun.* 2002;290:763-769.
- Esau C, Kang X, Peralta E, Hanson E, Marcusson EG, Ravichandran LV, et al. MicroRNA-143 regulates adipocyte differentiation. *J.Biol.Chem.* 2004;279:52361-52365.
- Estes BT, Wu AW, Guilak F. Potent induction of chondrocytic differentiation of human adipose-derived adult stem cells by bone morphogenetic protein 6. *Arthritis Rheum.* 2006;54:1222-1232.
- Ferguson CM, Schwarz EM, Puzas JE, Zuscik MJ, Drissi H, O'Keefe RJ. Transforming growth factor-beta1 induced alteration of skeletal morphogenesis in vivo. *J.Orthop.Res.* 2004;22:687-696.
- Ferguson CM, Schwarz EM, Reynolds PR, Puzas JE, Rosier RN, O'Keefe RJ. Smad2 and 3 mediate transforming growth factor-beta1-induced inhibition of chondrocyte maturation. *Endocrinology* 2000;141:4728-4735.
- Friedenstein AJ, Piatetzky-Shapiro II, Petrakova KV. Osteogenesis in transplants of bone marrow cells. *J.Embryol.Exp.Morphol.* 1966;16:381-390.
- Fromigue O, Marie PJ, Lomri A. Bone morphogenetic protein-2 and transforming growth factor-beta2 interact to modulate human bone marrow stromal cell proliferation and differentiation. *J.Cell.Biochem.* 1998;68:411-426.
- Fukumoto T, Sperling JW, Sanyal A, Fitzsimmons JS, Reinholz GG, Conover CA, et al. Combined effects of insulin-like growth factor-1 and transforming growth



- factor-beta1 on periosteal mesenchymal cells during chondrogenesis in vitro. *Osteoarthritis Cartilage* 2003;11:55-64.
- Giraldez AJ, Mishima Y, Rihel J, Grocock RJ, Van Dongen S, Inoue K, et al. Zebrafish MiR-430 promotes deadenylation and clearance of maternal mRNAs. *Science* 2006;312:75-79.
- Goldring MB, Tsuchimochi K, Ijiri K. The control of chondrogenesis. *J.Cell.Biochem.* 2006;97:33-44.
- Goumans MJ, Valdimarsdottir G, Itoh S, Rosendahl A, Sideras P, ten Dijke P. Balancing the activation state of the endothelium via two distinct TGF-beta type I receptors. *EMBO J.* 2002;21:1743-1753.
- Gronthos S, Franklin DM, Leddy HA, Robey PG, Storms RW, Gimble JM. Surface protein characterization of human adipose tissue-derived stromal cells. *J.Cell.Physiol.* 2001;189:54-63.
- Gronthos S, Graves SE, Ohta S, Simmons PJ. The STRO-1+ fraction of adult human bone marrow contains the osteogenic precursors. *Blood* 1994;84:4164-4173.
- Guillot PV, Gotherstrom C, Chan J, Kurata H, Fisk NM. Human first-trimester fetal MSC express pluripotency markers and grow faster and have longer telomeres than adult MSC. *Stem Cells* 2007;25:646-654.
- Guillot PV, O'Donoghue K, Kurata H, Fisk NM. Fetal stem cells: betwixt and between. *Semin.Reprod.Med.* 2006;24:340-347.
- Haegeler L, Ingold B, Naumann H, Tabatabai G, Ledermann B, Brandner S. Wnt signalling inhibits neural differentiation of embryonic stem cells by controlling bone morphogenetic protein expression. *Mol.Cell.Neurosci.* 2003;24:696-708.
- Halbleib M, Skurk T, de Luca C, von Heimburg D, Hauner H. Tissue engineering of white adipose tissue using hyaluronic acid-based scaffolds. I: in vitro differentiation of human adipocyte precursor cells on scaffolds. *Biomaterials* 2003;24:3125-3132.

- Halvorsen YD, Franklin D, Bond AL, Hitt DC, Auchter C, Boskey AL, et al. Extracellular matrix mineralization and osteoblast gene expression by human adipose tissue-derived stromal cells. *Tissue Eng.* 2001;7:729-741.
- Han HJ, Heo JS, Lee YJ. Estradiol-17beta stimulates proliferation of mouse embryonic stem cells: involvement of MAPKs and CDKs as well as protooncogenes. *Am.J.Physiol.Cell.Physiol.* 2006;290:C1067-75.
- Harper JA, Yuan JS, Tan JB, Visan I, Guidos CJ. Notch signaling in development and disease. *Clin.Genet.* 2003;64:461-472.
- Harris KS, Zhang Z, McManus MT, Harfe BD, Sun X. Dicer function is essential for lung epithelium morphogenesis. *Proc.Natl.Acad.Sci.U.S.A.* 2006;103:2208-2213.
- Hattori H, Masuoka K, Sato M, Ishihara M, Asazuma T, Takase B, et al. Bone formation using human adipose tissue-derived stromal cells and a biodegradable scaffold. *J.Biomed.Mater.Res.B.Appl.Biomater.* 2006;76:230-239.
- Hausman DB, DiGirolamo M, Bartness TJ, Hausman GJ, Martin RJ. The biology of white adipocyte proliferation. *Obes.Rev.* 2001;2:239-254.
- Hecht A, Kemler R. Curbing the nuclear activities of beta-catenin. Control over Wnt target gene expression. *EMBO Rep.* 2000;1:24-28.
- Heldin CH, Miyazono K, ten Dijke P. TGF-beta signalling from cell membrane to nucleus through SMAD proteins. *Nature* 1997;390:465-471.
- Hicok KC, Du Laney TV, Zhou YS, Halvorsen YD, Hitt DC, Cooper LF, et al. Human adipose-derived adult stem cells produce osteoid in vivo. *Tissue Eng.* 2004;10:371-380.
- Hogan BL. Bone morphogenetic proteins: multifunctional regulators of vertebrate development. *Genes Dev.* 1996;10:1580-1594.
- Holtzer H. Cell lineages, stem cells and the 'quantal' cell cycle concept. In: *Stem cells and tissue homeostasis.* Cambridge, New York: Cambridge University Press, 1978.



- Hong L, Colpan A, Peptan IA. Modulations of 17-beta estradiol on osteogenic and adipogenic differentiations of human mesenchymal stem cells. *Tissue Eng.* 2006;12:2747-2753.
- Hornstein E, Mansfield JH, Yekta S, Hu JK, Harfe BD, McManus MT, et al. The microRNA miR-196 acts upstream of Hoxb8 and Shh in limb development. *Nature* 2005;438:671-674.
- Hunziker EB. Articular cartilage repair: basic science and clinical progress. A review of the current status and prospects. *Osteoarthritis Cartilage* 2002;10:432-463.
- Hutvagner G, McLachlan J, Pasquinelli AE, Balint E, Tuschl T, Zamore PD. A cellular function for the RNA-interference enzyme Dicer in the maturation of the let-7 small temporal RNA. *Science* 2001;293:834-838.
- Indrawattana N, Chen G, Tadokoro M, Shann LH, Ohgushi H, Tateishi T, et al. Growth factor combination for chondrogenic induction from human mesenchymal stem cell. *Biochem.Biophys.Res.Comm.* 2004;320:914-919.
- Ishibashi M, Ang SL, Shiota K, Nakanishi S, Kageyama R, Guillemot F. Targeted disruption of mammalian hairy and Enhancer of split homolog-1 (HES-1) leads to up-regulation of neural helix-loop-helix factors, premature neurogenesis, and severe neural tube defects. *Genes Dev.* 1995;9:3136-3148.
- Iso T, Kedes L, Hamamori Y. HES and HERP families: multiple effectors of the Notch signaling pathway. *J.Cell.Physiol.* 2003;194:237-255.
- Jack GS, Almeida FG, Zhang R, Alfonso ZC, Zuk PA, Rodriguez LV. Processed lipoaspirate cells for tissue engineering of the lower urinary tract: implications for the treatment of stress urinary incontinence and bladder reconstruction. *J.Urol.* 2005;174:2041-2045.
- Jakymiw A, Lian S, Eystathioy T, Li S, Satoh M, Hamel JC, et al. Disruption of GW bodies impairs mammalian RNA interference. *Nat.Cell Biol.* 2005;7:1267-1274.



- Jun ES, Lee TH, Cho HH, Suh SY, Jung JS. Expression of telomerase extends longevity and enhances differentiation in human adipose tissue-derived stromal cells. *Cell.Physiol.Biochem.* 2004;14:261-268.
- Kanellopoulou C, Muljo SA, Kung AL, Ganesan S, Drapkin R, Jenuwein T, et al. Dicer-deficient mouse embryonic stem cells are defective in differentiation and centromeric silencing. *Genes Dev.* 2005;19:489-501.
- Kang SK, Jun ES, Bae YC, Jung JS. Interactions between human adipose stromal cells and mouse neural stem cells in vitro. *Brain Res.Dev.Brain Res.* 2003a;145:141-149.
- Kang SK, Lee DH, Bae YC, Kim HK, Baik SY, Jung JS. Improvement of neurological deficits by intracerebral transplantation of human adipose tissue-derived stromal cells after cerebral ischemia in rats. *Exp.Neurol.* 2003b;183:355-366.
- Kang SK, Shin MJ, Jung JS, Kim YG, Kim CH. Autologous adipose tissue-derived stromal cells for treatment of spinal cord injury. *Stem Cells Dev.* 2006;15:583-594.
- Kato Y, Iwamoto M, Koike T, Suzuki F, Takano Y. Terminal differentiation and calcification in rabbit chondrocyte cultures grown in centrifuge tubes: regulation by transforming growth factor beta and serum factors. *Proc.Natl.Acad.Sci.U.S.A.* 1988;85:9552-9556.
- Ketting RF, Fischer SE, Bernstein E, Sijen T, Hannon GJ, Plasterk RH. Dicer functions in RNA interference and in synthesis of small RNA involved in developmental timing in *C. elegans*. *Genes Dev.* 2001;15:2654-2659.
- Khvorova A, Reynolds A, Jayasena SD. Functional siRNAs and miRNAs exhibit strand bias. *Cell* 2003;115:209-216.
- Kim DJ, Moon SH, Kim H, Kwon UH, Park MS, Han KJ, et al. Bone morphogenetic protein-2 facilitates expression of chondrogenic, not osteogenic, phenotype of human intervertebral disc cells. *Spine* 2003;28:2679-2684.

- Kim SK, Hebrok M. Intercellular signals regulating pancreas development and function. *Genes Dev.* 2001;15:111-127.
- Kim VN. MicroRNA precursors in motion: exportin-5 mediates their nuclear export. *Trends Cell Biol.* 2004;14:156-159.
- Klein-Nulend J, Louwrese RT, Heyligers IC, Wuisman PI, Semeins CM, Goei SW, et al. Osteogenic protein (OP-1, BMP-7) stimulates cartilage differentiation of human and goat perichondrium tissue in vitro. *J.Biomed.Mater.Res.* 1998;40:614-620.
- Klyushnenkova E, Mosca JD, Zernetkina V, Majumdar MK, Beggs KJ, Simonetti DW, et al. T cell responses to allogeneic human mesenchymal stem cells: immunogenicity, tolerance, and suppression. *J.Biomed.Sci.* 2005;12:47-57.
- Knippenberg M, Helder MN, Zandieh Doulabi B, Wuisman PI, Klein-Nulend J. Osteogenesis versus chondrogenesis by BMP-2 and BMP-7 in adipose stem cells. *Biochem.Biophys.Res.Commun.* 2006;342:902-908.
- Kokai LE, Rubin JP, Marra KG. The potential of adipose-derived adult stem cells as a source of neuronal progenitor cells. *Plast.Reconstr.Surg.* 2005;116:1453-1460.
- Krichevsky AM, Sonntag KC, Isacson O, Kosik KS. Specific microRNAs modulate embryonic stem cell-derived neurogenesis. *Stem Cells* 2006;24:857-864.
- Lagos-Quintana M, Rauhut R, Yalcin A, Meyer J, Lendeckel W, Tuschl T. Identification of tissue-specific microRNAs from mouse. *Curr.Biol.* 2002;12:735-739.
- Lai EC. Notch signaling: control of cell communication and cell fate. *Development* 2004;131:965-973.
- Le Blanc K, Rasmusson I, Sundberg B, Gotherstrom C, Hassan M, Uzunel M, et al. Treatment of severe acute graft-versus-host disease with third party haploidentical mesenchymal stem cells. *Lancet* 2004;363:1439-1441.



- Lee EJ, Gusev Y, Jiang J, Nuovo GJ, Lerner MR, Frankel WL, et al. Expression profiling identifies microRNA signature in pancreatic cancer. *Int.J.Cancer* 2007;120:1046-1054.
- Lee JA, Parrett BM, Conejero JA, Laser J, Chen J, Kogon AJ, et al. Biological alchemy: engineering bone and fat from fat-derived stem cells. *Ann.Plast.Surg.* 2003;50:610-617.
- Lee JH, Kemp DM. Human adipose-derived stem cells display myogenic potential and perturbed function in hypoxic conditions. *Biochem.Biophys.Res.Commun.* 2006;341:882-888.
- Lee RC, Feinbaum RL, Ambros V. The *C. elegans* heterochronic gene *lin-4* encodes small RNAs with antisense complementarity to *lin-14*. *Cell* 1993;75:843-854.
- Lee RH, Kim B, Choi I, Kim H, Choi HS, Suh K, et al. Characterization and expression analysis of mesenchymal stem cells from human bone marrow and adipose tissue. *Cell.Physiol.Biochem.* 2004;14:311-324.
- Lee WC, Rubin JP, Marra KG. Regulation of alpha-smooth muscle actin protein expression in adipose-derived stem cells. *Cells Tissues Organs* 2006;183:80-86.
- Lee Y, Ahn C, Han J, Choi H, Kim J, Yim J, et al. The nuclear RNase III Droscha initiates microRNA processing. *Nature* 2003;425:415-419.
- Lee Y, Kim M, Han J, Yeom KH, Lee S, Baek SH, et al. MicroRNA genes are transcribed by RNA polymerase II. *EMBO J.* 2004;23:4051-4060.
- Lendeckel S, Jodicke A, Christophis P, Heidinger K, Wolff J, Fraser JK, et al. Autologous stem cells (adipose) and fibrin glue used to treat widespread traumatic calvarial defects: case report. *J.Craniomaxillofac.Surg.* 2004;32:370-373.
- Lewis BP, Burge CB, Bartel DP. Conserved seed pairing, often flanked by adenosines, indicates that thousands of human genes are microRNA targets. *Cell* 2005;120:15-20.



- Li TF, Darowish M, Zuscik MJ, Chen D, Schwarz EM, Rosier RN, et al. Smad3-deficient chondrocytes have enhanced BMP signaling and accelerated differentiation. *J.Bone Miner.Res.* 2006;21:4-16.
- Li X, Schwarz EM, Zuscik MJ, Rosier RN, Ionescu AM, Puzas JE, et al. Retinoic acid stimulates chondrocyte differentiation and enhances bone morphogenetic protein effects through induction of Smad1 and Smad5. *Endocrinology* 2003;144:2514-2523.
- Lim LP, Glasner ME, Yekta S, Burge CB, Bartel DP. Vertebrate microRNA genes. *Science* 2003;299:1540.
- Lin Y, Chen X, Yan Z, Liu L, Tang W, Zheng X, et al. Multilineage differentiation of adipose-derived stromal cells from GFP transgenic mice. *Mol.Cell.Biochem.* 2006;285:69-78.
- Liu J, Carmell MA, Rivas FV, Marsden CG, Thomson JM, Song JJ, et al. Argonaute2 is the catalytic engine of mammalian RNAi. *Science* 2004;305:1437-1441.
- Liu J, Rivas FV, Wohlschlegel J, Yates JR,3rd, Parker R, Hannon GJ. A role for the P-body component GW182 in microRNA function. *Nat.Cell Biol.* 2005;7:1261-1266.
- Longobardi L, O'Rear L, Aakula S, Johnstone B, Shimer K, Chytil A, et al. Effect of IGF-I in the chondrogenesis of bone marrow mesenchymal stem cells in the presence or absence of TGF-beta signaling. *J.Bone Miner.Res.* 2006;21:626-636.
- Lu P, Blesch A, Tuszynski MH. Induction of bone marrow stromal cells to neurons: differentiation, transdifferentiation, or artifact? *J.Neurosci.Res.* 2004;77:174-191.
- Lund E, Guttinger S, Calado A, Dahlberg JE, Kutay U. Nuclear export of microRNA precursors. *Science* 2004;303:95-98.
- Lutolf S, Radtke F, Aguet M, Suter U, Taylor V. Notch1 is required for neuronal and glial differentiation in the cerebellum. *Development* 2002;129:373-385.

- Mackay AM, Beck SC, Murphy JM, Barry FP, Chichester CO, Pittenger MF. Chondrogenic differentiation of cultured human mesenchymal stem cells from marrow. *Tissue Eng.* 1998;4:415-428.
- Marshak DR, Gardner RL, Gottlieb D. *Stem Cell Biology.* : Cold Spring Harbor Laboratory Press, 2001.
- Massague J, Blain SW, Lo RS. TGFbeta signaling in growth control, cancer, and heritable disorders. *Cell* 2000;103:295-309.
- Massague J, Chen YG. Controlling TGF-beta signaling. *Genes Dev.* 2000;14:627-644.
- McIntosh K, Zvonic S, Garrett S, Mitchell JB, Floyd ZE, Hammill L, et al. The immunogenicity of human adipose-derived cells: temporal changes in vitro. *Stem Cells* 2006;24:1246-1253.
- Mehler MF, Mabie PC, Zhang D, Kessler JA. Bone morphogenetic proteins in the nervous system. *Trends Neurosci.* 1997;20:309-317.
- Mitchell JB, McIntosh K, Zvonic S, Garrett S, Floyd ZE, Kloster A, et al. Immunophenotype of human adipose-derived cells: temporal changes in stromal-associated and stem cell-associated markers. *Stem Cells* 2006;24:376-385.
- Miyahara Y, Nagaya N, Kataoka M, Yanagawa B, Tanaka K, Hao H, et al. Monolayered mesenchymal stem cells repair scarred myocardium after myocardial infarction. *Nat.Med.* 2006;12:459-465.
- Mizuno H, Hyakusoku H. Mesengenic potential and future clinical perspective of human processed lipoaspirate cells. *J.Nippon Med.Sch.* 2003;70:300-306.
- Mizuno H, Zuk PA, Zhu M, Lorenz HP, Benhaim P, Hedrick MH. Myogenic differentiation by human processed lipoaspirate cells. *Plast.Reconstr.Surg.* 2002;109:199-209; discussion 210-1.



- Murchison EP, Partridge JF, Tam OH, Cheloufi S, Hannon GJ. Characterization of Dicer-deficient murine embryonic stem cells. *Proc.Natl.Acad.Sci.U.S.A.* 2005;102:12135-12140.
- Naguibneva I, Ameyar-Zazoua M, Polesskaya A, Ait-Si-Ali S, Groisman R, Souidi M, et al. The microRNA miR-181 targets the homeobox protein Hox-A11 during mammalian myoblast differentiation. *Nat.Cell Biol.* 2006;8:278-284.
- Nakamura Y, Sakakibara S, Miyata T, Ogawa M, Shimazaki T, Weiss S, et al. The bHLH gene *hes1* as a repressor of the neuronal commitment of CNS stem cells. *J.Neurosci.* 2000;20:283-293.
- Nelson WJ, Nusse R. Convergence of Wnt, beta-catenin, and cadherin pathways. *Science* 2004;303:1483-1487.
- Nishihara A, Fujii M, Sampath TK, Miyazono K, Reddi AH. Bone morphogenetic protein signaling in articular chondrocyte differentiation. *Biochem.Biophys.Res.Comm.* 2003;301:617-622.
- O'Donoghue K, Fisk NM. Fetal stem cells. *Best Pract.Res.Clin.Obstet.Gynaecol.* 2004;18:853-875.
- Oedayrajsingh-Varma MJ, van Ham SM, Knippenberg M, Helder MN, Klein-Nulend J, Schouten TE, et al. Adipose tissue-derived mesenchymal stem cell yield and growth characteristics are affected by the tissue-harvesting procedure. *Cytotherapy* 2006;8:166-177.
- Ogawa R, Mizuno H, Watanabe A, Migita M, Shimada T, Hyakusoku H. Osteogenic and chondrogenic differentiation by adipose-derived stem cells harvested from GFP transgenic mice. *Biochem.Biophys.Res.Comm.* 2004;313:871-877.
- Paratore C, Sommer L. Stem Cells. In: Unsicker K, Krieglstein K, editors. *Cell Signaling and Growth Factors in Development* Weinheim: Wiley-VCH Verlag GmbH & Co.; 2006: 3-37.
- Patrick CW,Jr, Chauvin PB, Hogley J, Reece GP. Preadipocyte seeded PLGA scaffolds for adipose tissue engineering. *Tissue Eng.* 1999;5:139-151.



- Patrick CW,Jr, Zheng B, Johnston C, Reece GP. Long-term implantation of preadipocyte-seeded PLGA scaffolds. *Tissue Eng.* 2002;8:283-293.
- Pillai RS, Bhattacharyya SN, Artus CG, Zoller T, Cougot N, Basyuk E, et al. Inhibition of translational initiation by Let-7 MicroRNA in human cells. *Science* 2005;309:1573-1576.
- Pittenger MF, Mackay AM, Beck SC, Jaiswal RK, Douglas R, Mosca JD, et al. Multilineage potential of adult human mesenchymal stem cells. *Science* 1999;284:143-147.
- Planat-Benard V, Menard C, Andre M, Puceat M, Perez A, Garcia-Verdugo JM, et al. Spontaneous cardiomyocyte differentiation from adipose tissue stroma cells. *Circ.Res.* 2004a;94:223-229.
- Planat-Benard V, Silvestre JS, Cousin B, Andre M, Nibbelink M, Tamarat R, et al. Plasticity of human adipose lineage cells toward endothelial cells: physiological and therapeutic perspectives. *Circulation* 2004b;109:656-663.
- Puissant B, Barreau C, Bourin P, Clavel C, Corre J, Bousquet C, et al. Immunomodulatory effect of human adipose tissue-derived adult stem cells: comparison with bone marrow mesenchymal stem cells. *Br.J.Haematol.* 2005;129:118-129.
- Qi X, Li TG, Hao J, Hu J, Wang J, Simmons H, et al. BMP4 supports self-renewal of embryonic stem cells by inhibiting mitogen-activated protein kinase pathways. *Proc.Natl.Acad.Sci.U.S.A.* 2004;101:6027-6032.
- Rao PK, Kumar RM, Farkhondeh M, Baskerville S, Lodish HF. Myogenic factors that regulate expression of muscle-specific microRNAs. *Proc.Natl.Acad.Sci.U.S.A.* 2006;103:8721-8726.
- Reinhart BJ, Slack FJ, Basson M, Pasquinelli AE, Bettinger JC, Rougvie AE, et al. The 21-nucleotide let-7 RNA regulates developmental timing in *Caenorhabditis elegans*. *Nature* 2000;403:901-906.

- Reissmann E, Ernsberger U, Francis-West PH, Rueger D, Brickell PM, Rohrer H. Involvement of bone morphogenetic protein-4 and bone morphogenetic protein-7 in the differentiation of the adrenergic phenotype in developing sympathetic neurons. *Development* 1996;122:2079-2088.
- Reya T, Duncan AW, Ailles L, Domen J, Scherer DC, Willert K, et al. A role for Wnt signalling in self-renewal of haematopoietic stem cells. *Nature* 2003;423:409-414.
- Ringden O, Uzunel M, Rasmusson I, Remberger M, Sundberg B, Lonnies H, et al. Mesenchymal stem cells for treatment of therapy-resistant graft-versus-host disease. *Transplantation* 2006;81:1390-1397.
- Rodriguez AM, Elabd C, Amri EZ, Ailhaud G, Dani C. The human adipose tissue is a source of multipotent stem cells. *Biochimie* 2005a;87:125-128.
- Rodriguez AM, Pisani D, Dechesne CA, Turc-Carel C, Kurzenne JY, Wdziekonski B, et al. Transplantation of a multipotent cell population from human adipose tissue induces dystrophin expression in the immunocompetent mdx mouse. *J.Exp.Med.* 2005b;201:1397-1405.
- Rodriguez LV, Alfonso Z, Zhang R, Leung J, Wu B, Ignarro LJ. Clonogenic multipotent stem cells in human adipose tissue differentiate into functional smooth muscle cells. *Proc.Natl.Acad.Sci.U.S.A.* 2006;103:12167-12172.
- Rupnick MA, Panigrahy D, Zhang CY, Dallabrida SM, Lowell BB, Langer R, et al. Adipose tissue mass can be regulated through the vasculature. *Proc.Natl.Acad.Sci.U.S.A.* 2002;99:10730-10735.
- Ryan DG, Oliveira-Fernandes M, Lavker RM. MicroRNAs of the mammalian eye display distinct and overlapping tissue specificity. *Mol.Vis.* 2006;12:1175-1184.
- Ryden M, Dicker A, Gotherstrom C, Astrom G, Tammik C, Arner P, et al. Functional characterization of human mesenchymal stem cell-derived adipocytes. *Biochem.Biophys.Res.Comm.* 2003;311:391-397.



- Safford KM, Hicok KC, Safford SD, Halvorsen YD, Wilkison WO, Gimble JM, et al. Neurogenic differentiation of murine and human adipose-derived stromal cells. *Biochem.Biophys.Res.Commun.* 2002;294:371-379.
- Safford KM, Safford SD, Gimble JM, Shetty AK, Rice HE. Characterization of neuronal/glial differentiation of murine adipose-derived adult stromal cells. *Exp.Neurol.* 2004;187:319-328.
- Sakaguchi Y, Sekiya I, Yagishita K, Muneta T. Comparison of human stem cells derived from various mesenchymal tissues: superiority of synovium as a cell source. *Arthritis Rheum.* 2005;52:2521-2529.
- Sato N, Meijer L, Skaltsounis L, Greengard P, Brivanlou AH. Maintenance of pluripotency in human and mouse embryonic stem cells through activation of Wnt signaling by a pharmacological GSK-3-specific inhibitor. *Nat.Med.* 2004;10:55-63.
- Sato N, Sanjuan IM, Heke M, Uchida M, Naef F, Brivanlou AH. Molecular signature of human embryonic stem cells and its comparison with the mouse. *Dev.Biol.* 2003;260:404-413.
- Schaffler A, Buchler C. Concise review: adipose tissue-derived stromal cells--basic and clinical implications for novel cell-based therapies. *Stem Cells* 2007;25:818-827.
- Schneider C, Wicht H, Enderich J, Wegner M, Rohrer H. Bone morphogenetic proteins are required in vivo for the generation of sympathetic neurons. *Neuron* 1999;24:861-870.
- Schratt GM, Tuebing F, Nigh EA, Kane CG, Sabatini ME, Kiebler M, et al. A brain-specific microRNA regulates dendritic spine development. *Nature* 2006;439:283-289.
- Schwarz DS, Hutvagner G, Du T, Xu Z, Aronin N, Zamore PD. Asymmetry in the assembly of the RNAi enzyme complex. *Cell* 2003;115:199-208.
- Sell S. *Stem Cells Handbook*. : Humana Press, 2004.



- Sempere LF, Freemantle S, Pitha-Rowe I, Moss E, Dmitrovsky E, Ambros V. Expression profiling of mammalian microRNAs uncovers a subset of brain-expressed microRNAs with possible roles in murine and human neuronal differentiation. *Genome Biol.* 2004;5:R13.
- Sen A, Lea-Currie YR, Sujkowska D, Franklin DM, Wilkison WO, Halvorsen YD, et al. Adipogenic potential of human adipose derived stromal cells from multiple donors is heterogeneous. *J.Cell.Biochem.* 2001;81:312-319.
- Seo MJ, Suh SY, Bae YC, Jung JS. Differentiation of human adipose stromal cells into hepatic lineage in vitro and in vivo. *Biochem.Biophys.Res.Commun.* 2005;328:258-264.
- Serra R, Johnson M, Filvaroff EH, LaBorde J, Sheehan DM, Derynck R, et al. Expression of a truncated, kinase-defective TGF-beta type II receptor in mouse skeletal tissue promotes terminal chondrocyte differentiation and osteoarthritis. *J.Cell Biol.* 1997;139:541-552.
- Shah NM, Groves AK, Anderson DJ. Alternative neural crest cell fates are instructively promoted by TGFbeta superfamily members. *Cell* 1996;85:331-343.
- Shea CM, Edgar CM, Einhorn TA, Gerstenfeld LC. BMP treatment of C3H10T1/2 mesenchymal stem cells induces both chondrogenesis and osteogenesis. *J.Cell.Biochem.* 2003;90:1112-1127.
- Shi Y, Massague J. Mechanisms of TGF-beta signaling from cell membrane to the nucleus. *Cell* 2003;113:685-700.
- Shi YY, Nacamuli RP, Salim A, Longaker MT. The osteogenic potential of adipose-derived mesenchymal cells is maintained with aging. *Plast.Reconstr.Surg.* 2005;116:1686-1696.
- Smirnova L, Grafe A, Seiler A, Schumacher S, Nitsch R, Wulczyn FG. Regulation of miRNA expression during neural cell specification. *Eur.J.Neurosci.* 2005;21:1469-1477.

- Solchaga LA, Penick K, Porter JD, Goldberg VM, Caplan AI, Welter JF. FGF-2 enhances the mitotic and chondrogenic potentials of human adult bone marrow-derived mesenchymal stem cells. *J.Cell.Physiol.* 2005;203:398-409.
- Stevens MM, Marini RP, Martin I, Langer R, Prasad Shastri V. FGF-2 enhances TGF-beta1-induced periosteal chondrogenesis. *J.Orthop.Res.* 2004;22:1114-1119.
- Strauss WM, Chen C, Lee CT, Ridzon D. Nonrestrictive developmental regulation of microRNA gene expression. *Mamm.Genome* 2006;17:833-840.
- Strem BM, Hicok KC, Zhu M, Wulur I, Alfonso Z, Schreiber RE, et al. Multipotential differentiation of adipose tissue-derived stem cells. *Keio J.Med.* 2005a;54:132-141.
- Strem BM, Zhu M, Alfonso Z, Daniels EJ, Schreiber R, Beygui R, et al. Expression of cardiomyocytic markers on adipose tissue-derived cells in a murine model of acute myocardial injury. *Cytotherapy* 2005b;7:282-291.
- Suh MR, Lee Y, Kim JY, Kim SK, Moon SH, Lee JY, et al. Human embryonic stem cells express a unique set of microRNAs. *Dev.Biol.* 2004;270:488-498.
- Suzuki F. Effects of various growth factors on a chondrocyte differentiation model. *Adv.Exp.Med.Biol.* 1992;324:101-106.
- Tang F, Hajkova P, Barton SC, Lao K, Surani MA. MicroRNA expression profiling of single whole embryonic stem cells. *Nucleic Acids Res.* 2006;34:e9.
- Timper K, Seboek D, Eberhardt M, Linscheid P, Christ-Crain M, Keller U, et al. Human adipose tissue-derived mesenchymal stem cells differentiate into insulin, somatostatin, and glucagon expressing cells. *Biochem.Biophys.Res.Commun.* 2006;341:1135-1140.
- Tondreau T, Lagneaux L, Dejeneffe M, Massy M, Mortier C, Delforge A, et al. Bone marrow-derived mesenchymal stem cells already express specific neural proteins before any differentiation. *Differentiation* 2004;72:319-326.



- Tuddenham L, Wheeler G, Ntounia-Fousara S, Waters J, Hajihosseini MK, Clark I, et al. The cartilage specific microRNA-140 targets histone deacetylase 4 in mouse cells. *FEBS Lett.* 2006;580:4214-4217.
- Van Harmelen V, Rohrig K, Hauner H. Comparison of proliferation and differentiation capacity of human adipocyte precursor cells from the omental and subcutaneous adipose tissue depot of obese subjects. *Metabolism* 2004;53:632-637.
- von Heimburg D, Zachariah S, Heschel I, Kuhling H, Schoof H, Hafemann B, et al. Human preadipocytes seeded on freeze-dried collagen scaffolds investigated in vitro and in vivo. *Biomaterials* 2001a;22:429-438.
- von Heimburg D, Zachariah S, Low A, Pallua N. Influence of different biodegradable carriers on the in vivo behavior of human adipose precursor cells. *Plast.Reconstr.Surg.* 2001b;108:411-20; discussion 421-2.
- Wagner W, Wein F, Seckinger A, Frankhauser M, Wirkner U, Krause U, et al. Comparative characteristics of mesenchymal stem cells from human bone marrow, adipose tissue, and umbilical cord blood. *Exp.Hematol.* 2005;33:1402-1416.
- Wei Y, Hu Y, Lv R, Li D. Regulation of adipose-derived adult stem cells differentiating into chondrocytes with the use of rhBMP-2. *Cytherapy* 2006;8:570-579.
- Weisberg SP, McCann D, Desai M, Rosenbaum M, Leibel RL, Ferrante AW, Jr. Obesity is associated with macrophage accumulation in adipose tissue. *J.Clin.Invest.* 2003;112:1796-1808.
- Wienholds E, Kloosterman WP, Miska E, Alvarez-Saavedra E, Berezikov E, de Bruijn E, et al. MicroRNA expression in zebrafish embryonic development. *Science* 2005;309:310-311.
- Wightman B, Ha I, Ruvkun G. Posttranscriptional regulation of the heterochronic gene *lin-14* by *lin-4* mediates temporal pattern formation in *C. elegans*. *Cell* 1993;75:855-862.



- Woodbury D, Schwarz EJ, Prockop DJ, Black IB. Adult rat and human bone marrow stromal cells differentiate into neurons. *J.Neurosci.Res.* 2000;61:364-370.
- Wozney JM, Rosen V, Celeste AJ, Mitsock LM, Whitters MJ, Kriz RW, et al. Novel regulators of bone formation: molecular clones and activities. *Science* 1988;242:1528-1534.
- Wu L, Fan J, Belasco JG. MicroRNAs direct rapid deadenylation of mRNA. *Proc.Natl.Acad.Sci.U.S.A.* 2006;103:4034-4039.
- Yanez R, Lamana ML, Garcia-Castro J, Colmenero I, Ramirez M, Bueren JA. Adipose tissue-derived mesenchymal stem cells have in vivo immunosuppressive properties applicable for the control of the graft-versus-host disease. *Stem Cells* 2006;24:2582-2591.
- Yang LY, Liu XM, Sun B, Hui GZ, Fei J, Guo LH. Adipose tissue-derived stromal cells express neuronal phenotypes. *Chin.Med.J.(Engl)* 2004;117:425-429.
- Yekta S, Shih IH, Bartel DP. MicroRNA-directed cleavage of HOXB8 mRNA. *Science* 2004;304:594-596.
- Yi R, O'Carroll D, Pasolli HA, Zhang Z, Dietrich FS, Tarakhovsky A, et al. Morphogenesis in skin is governed by discrete sets of differentially expressed microRNAs. *Nat.Genet.* 2006;38:356-362.
- Yi R, Qin Y, Macara IG, Cullen BR. Exportin-5 mediates the nuclear export of pre-microRNAs and short hairpin RNAs. *Genes Dev.* 2003;17:3011-3016.
- Ying QL, Nichols J, Chambers I, Smith A. BMP induction of Id proteins suppresses differentiation and sustains embryonic stem cell self-renewal in collaboration with STAT3. *Cell* 2003;115:281-292.
- Zhao Y, Samal E, Srivastava D. Serum response factor regulates a muscle-specific microRNA that targets Hand2 during cardiogenesis. *Nature* 2005;436:214-220.
- Zuk PA, Zhu M, Ashjian P, De Ugarte DA, Huang JI, Mizuno H, et al. Human adipose tissue is a source of multipotent stem cells. *Mol.Biol.Cell* 2002;13:4279-4295.

Zuk PA, Zhu M, Mizuno H, Huang J, Futrell JW, Katz AJ, et al. Multilineage cells from human adipose tissue: implications for cell-based therapies. *Tissue Eng.* 2001;7:211-228.

Zwijssen A, Verschueren K, Huylebroeck D. New intracellular components of bone morphogenetic protein/Smad signaling cascades. *FEBS Lett.* 2003;546:133-139.





CUHK Libraries



004461348